

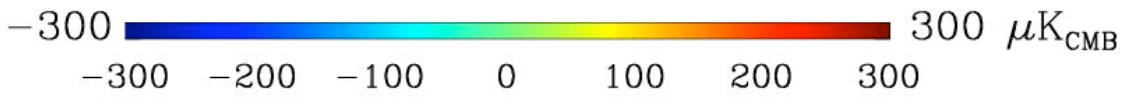
*From BOOMERanG
to B-Pol*

P. de Bernardis
Dipartimento di Fisica
La Sapienza, Roma

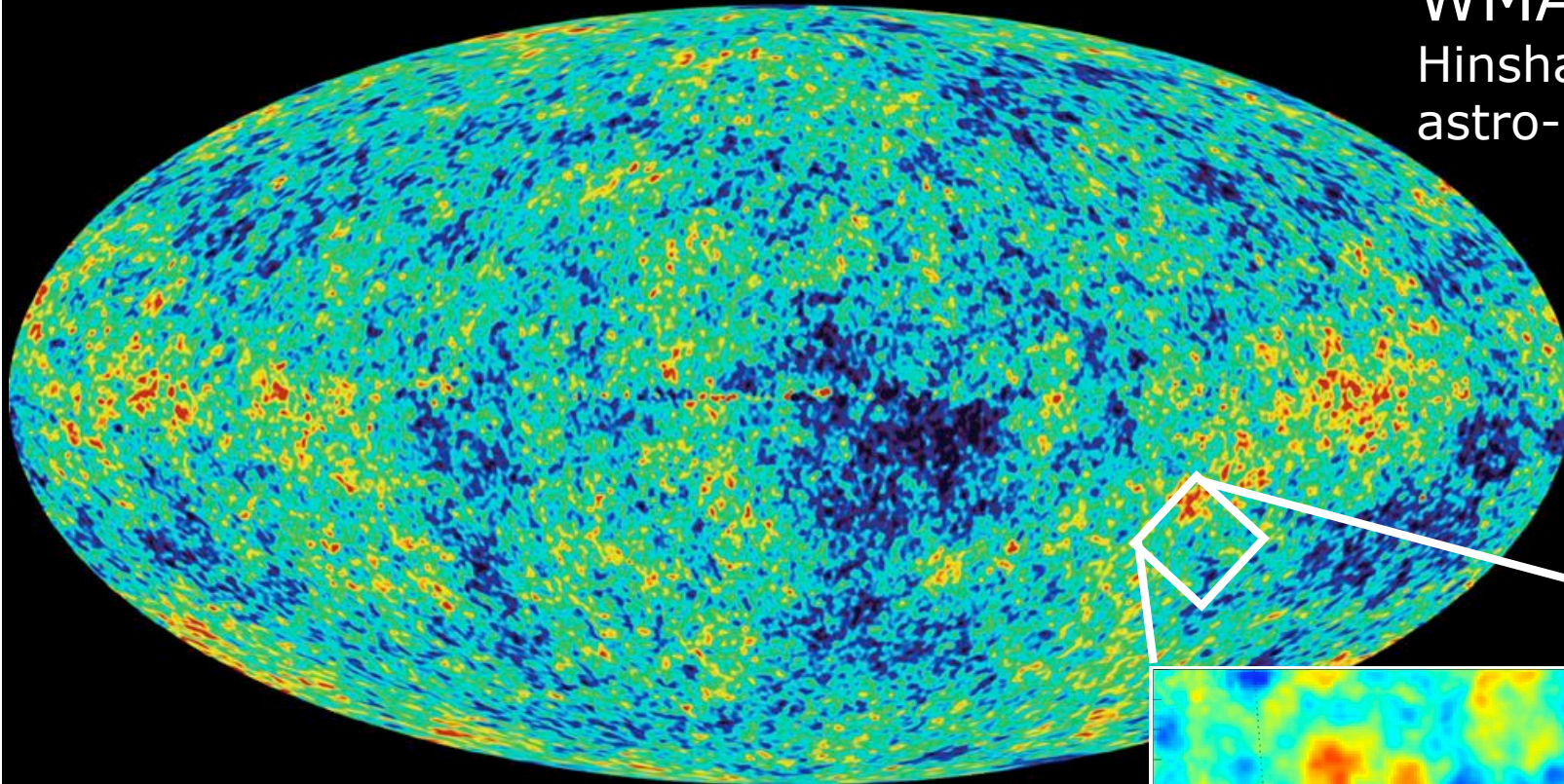
A Century of Cosmology
Venezia, S.Servolo 31/08/2007

contents

- CMB experiments: state of the art
 - Anisotropy
 - Polarization
- Open problems : how to attack them with CMB
- Enabling technologies
- High angular resolution CMB anisotropy
- The spectrum of CMB anisotropy
- The polarization of the CMB

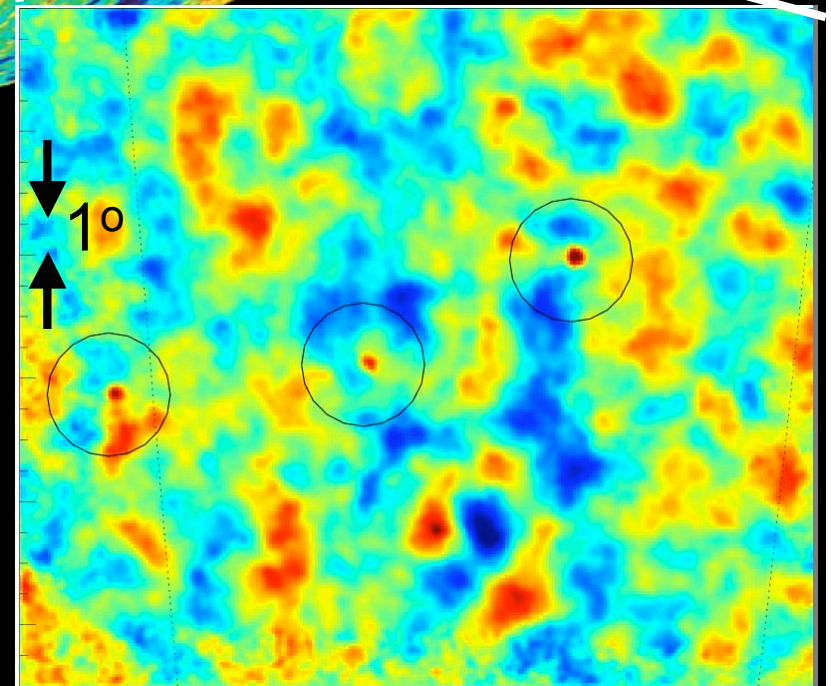


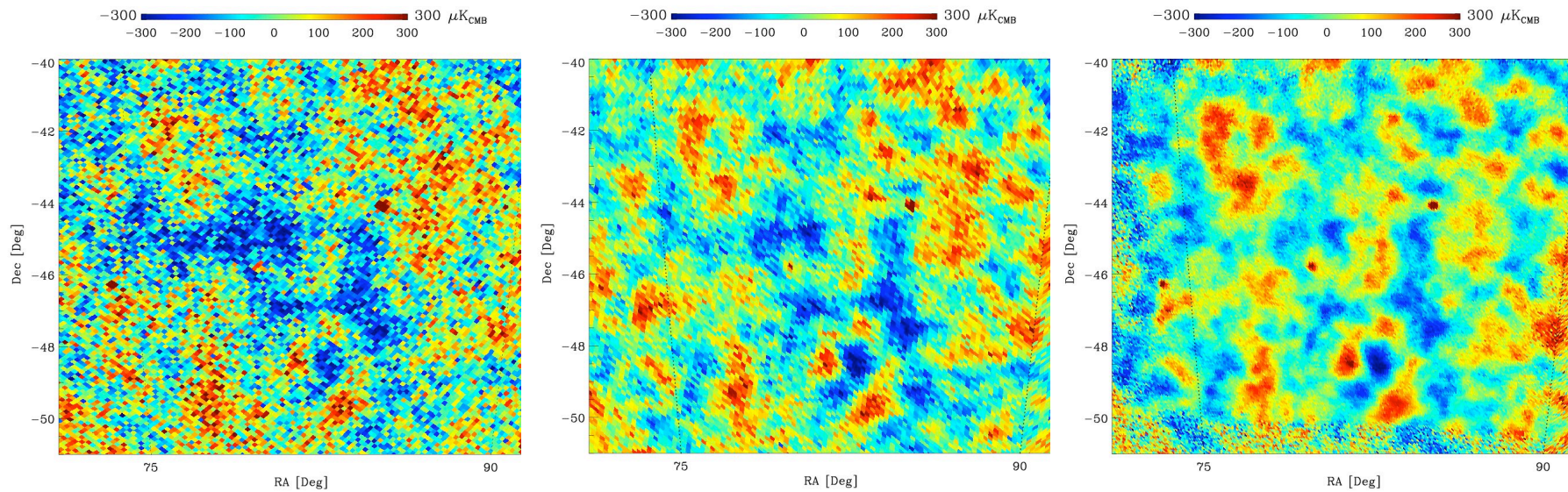
WMAP
Hinshaw et al. 2006
astro-ph/0603451



Detailed Views of the
Recombination Epoch
($z=1088$, 13.7 Gyrs ago)

BOOMERanG
Masi et al. 2005
astro-ph/0507509





WMAP 3 years
23-94 GHz

BOOMERanG-98
145 GHz

BOOMERanG-03
145 GHz

The consistency of the maps from three *independent* experiments, working at very different frequencies and with very different measurement methods, is the best evidence that the faint structure observed

- *is not due to instrumental artifacts*
- *has exactly the spectrum of CMB anisotropy, so it is not due to foreground emission*
- The comparison also shows the *extreme sensitivity of cryogenic bolometers* operated at balloon altitude (the B03 map is the result of 5 days of observation)

- This means that we have a reliable snapshot of density inhomogeneities at recombination, i.e. of the early conditions of the process of structure formation.
- Also, through observations of the irrotational component of the linear polarization of the CMB, we start to have significant information about the velocity fields at recombination.

Angular power spectrum:

C_l

$$\Delta T(\theta, \varphi) = \sum_{\ell, m} a_{\ell m} Y_{\ell}^m(\theta, \varphi)$$

$$c_{\ell} = \langle a_{\ell m}^2 \rangle$$

Cosmological
Parameters: $\Omega_o, \Omega_b h^2,$
 $n, \Omega_{\Lambda}, H_o, A, \tau, \dots$

The current adiabatic
inflationary scenario

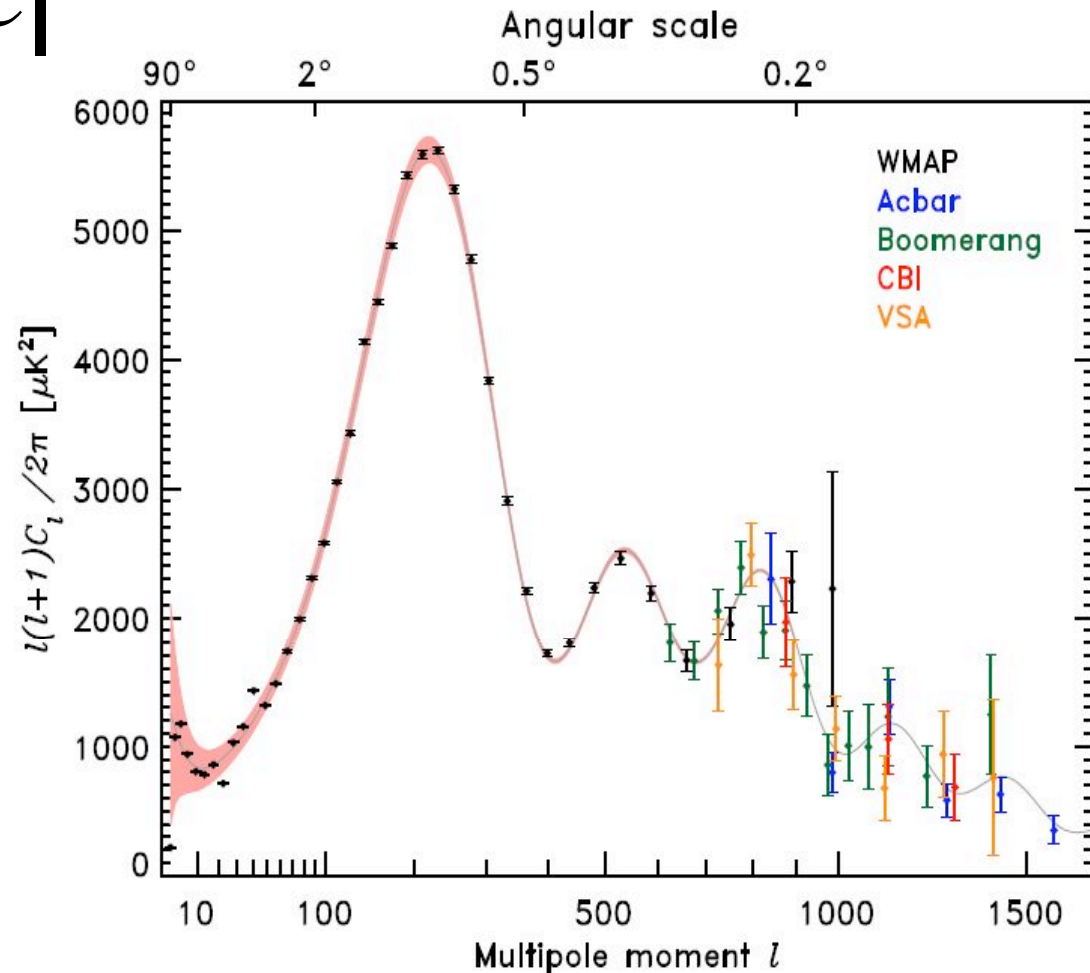
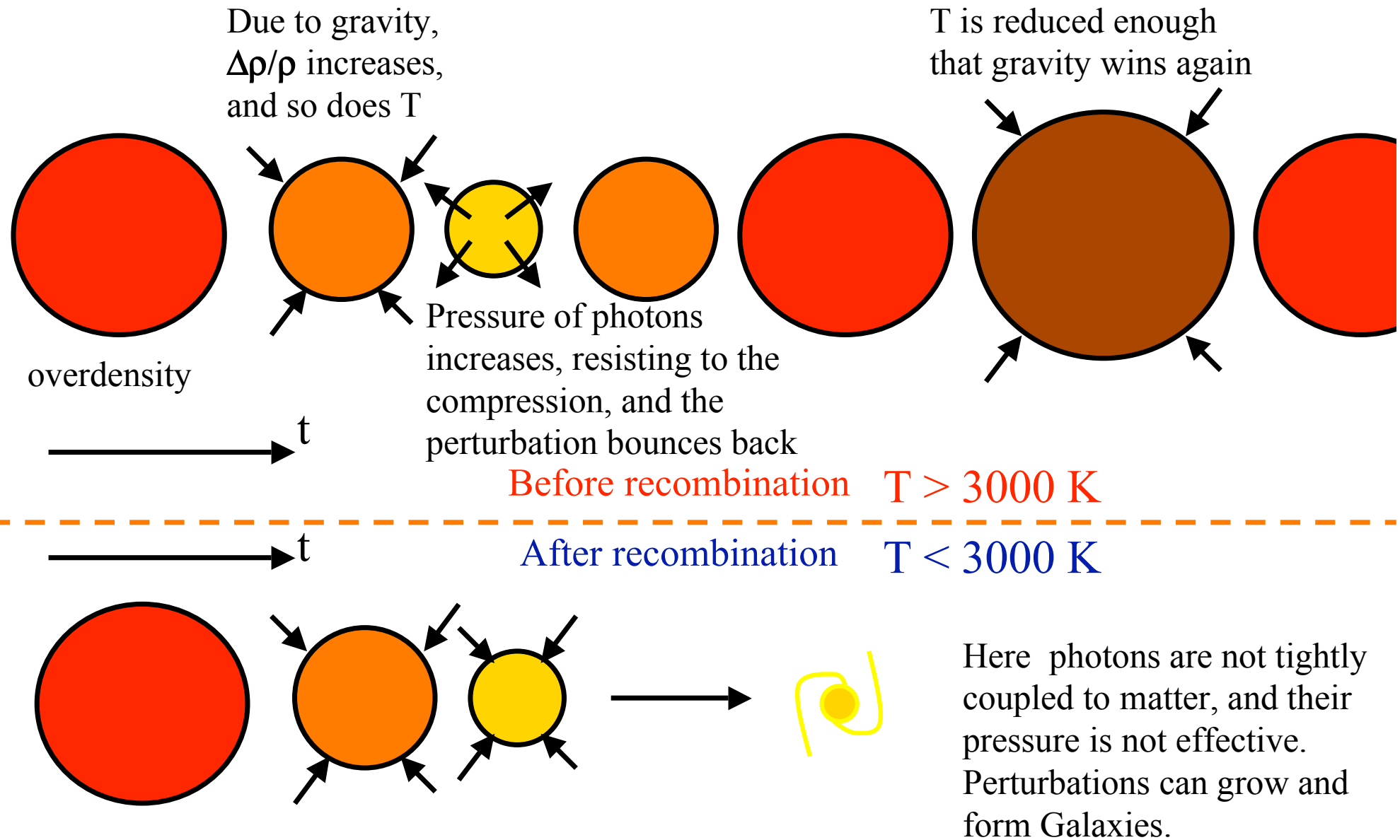


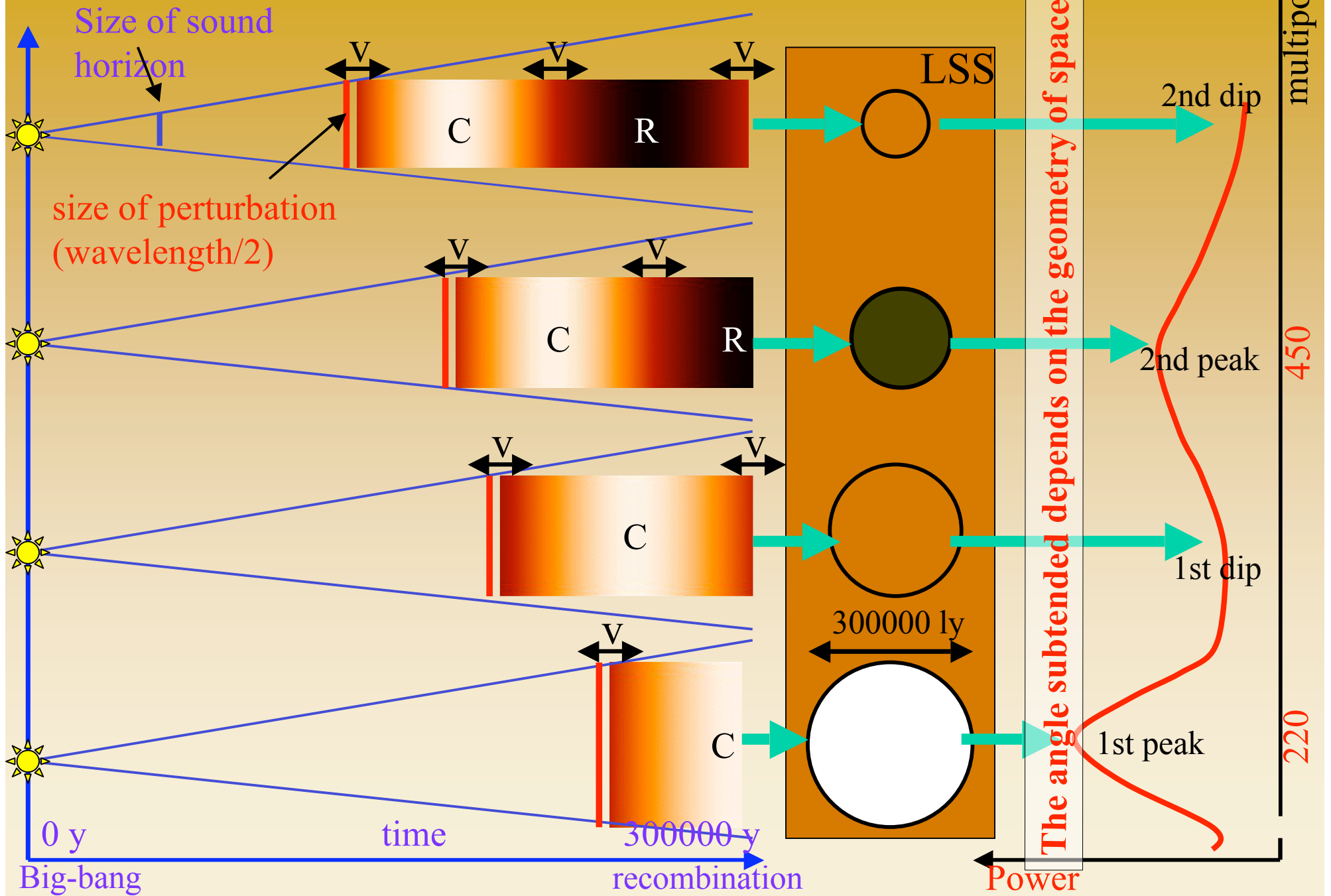
Fig. 18.— The WMAP three-year power spectrum (in black) compared to other recent measurements of the CMB angular power spectrum, including Boomerang (Jones et al. 2005), Acbar (Kuo et al. 2004), CBI (Readhead et al. 2004), and VSA (Dickinson et al. 2004). For clarity, the $l < 600$ data from Boomerang and VSA are omitted; as the measurements are consistent with WMAP, but with lower weight. These data impressively confirm the turnover in the 3rd acoustic peak and probe the onset of Silk damping. With improved sensitivity on sub-degree scales, the WMAP data are becoming an increasingly important calibration source for high-resolution experiments.

Density perturbations ($\Delta\rho/\rho$) were **oscillating** in the primeval plasma (as a result of the opposite effects of gravity and photon pressure).



After recombination, density perturbation can **grow** and create the hierarchy of structures we see in the nearby Universe.

In the primeval plasma, photons/baryons density perturbations start to oscillate only when the sound horizon becomes larger than their linear size. Small wavelength perturbations oscillate faster than large ones.



Angular power spectrum:

C_l

$$\Delta T(\theta, \varphi) = \sum_{\ell, m} a_{\ell m} Y_{\ell}^m(\theta, \varphi)$$

$$c_{\ell} = \langle a_{\ell m}^2 \rangle$$

Cosmological
Parameters: $\Omega_o, \Omega_b h^2,$
 $n, \Omega_{\Lambda}, H_o, A, \tau, \dots$

The current adiabatic
inflationary scenario

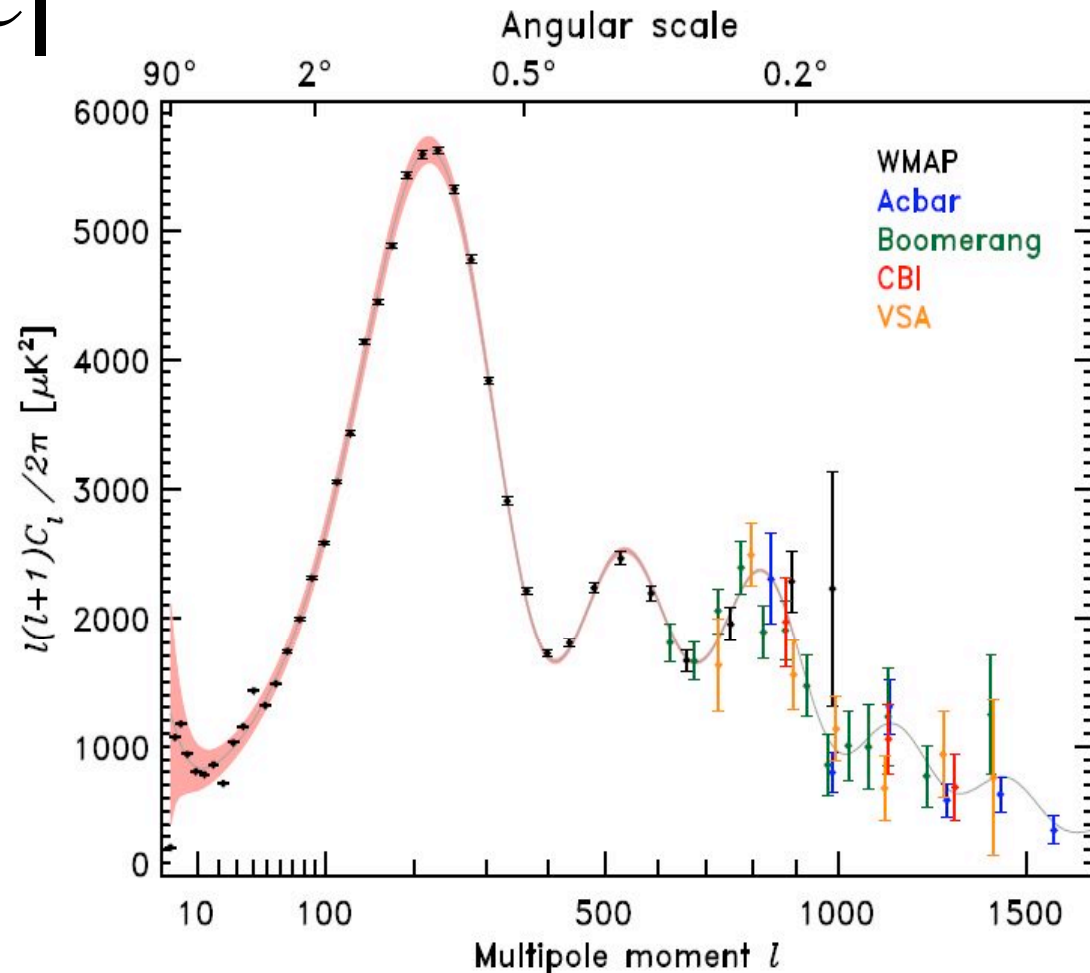
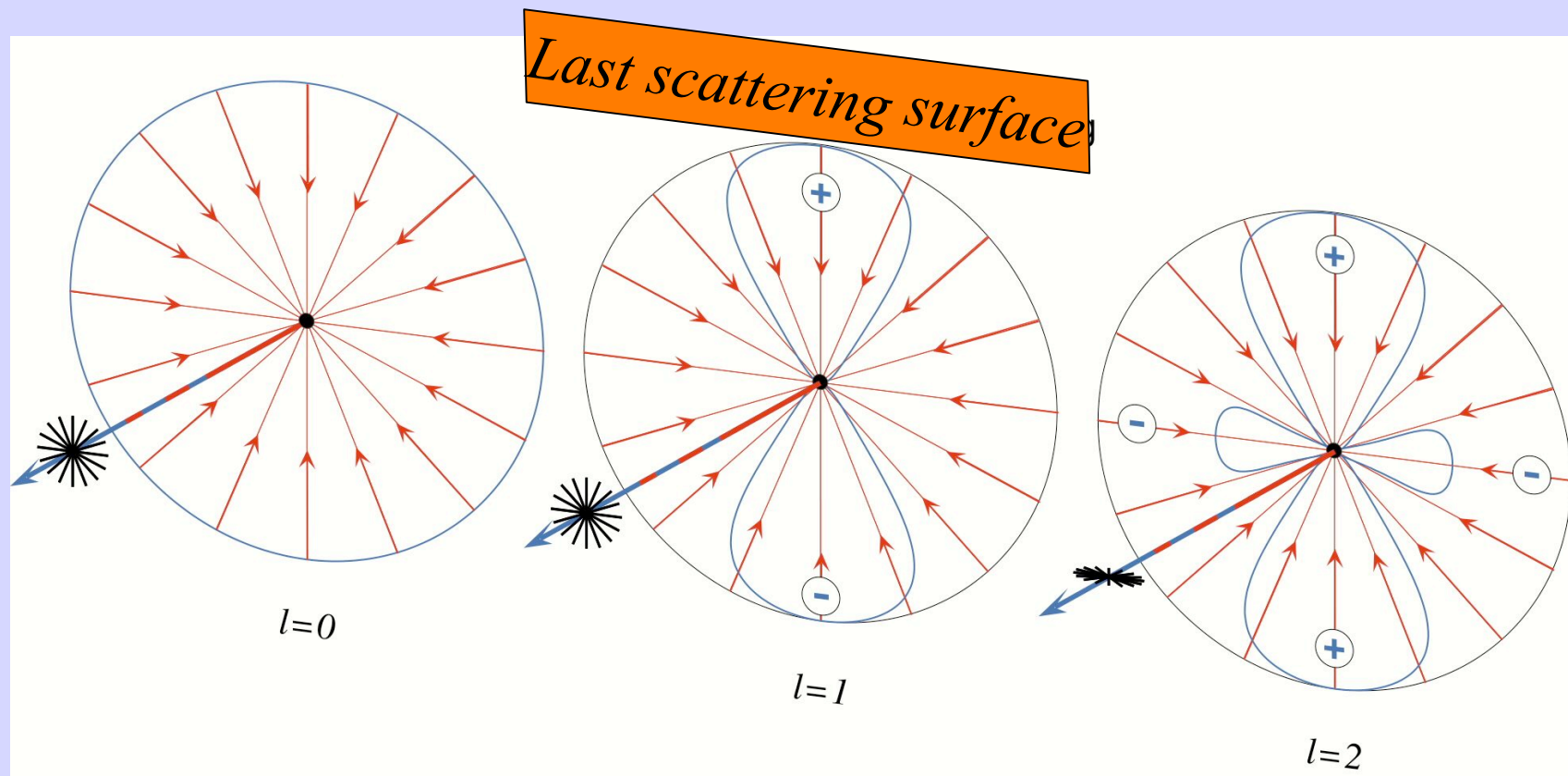
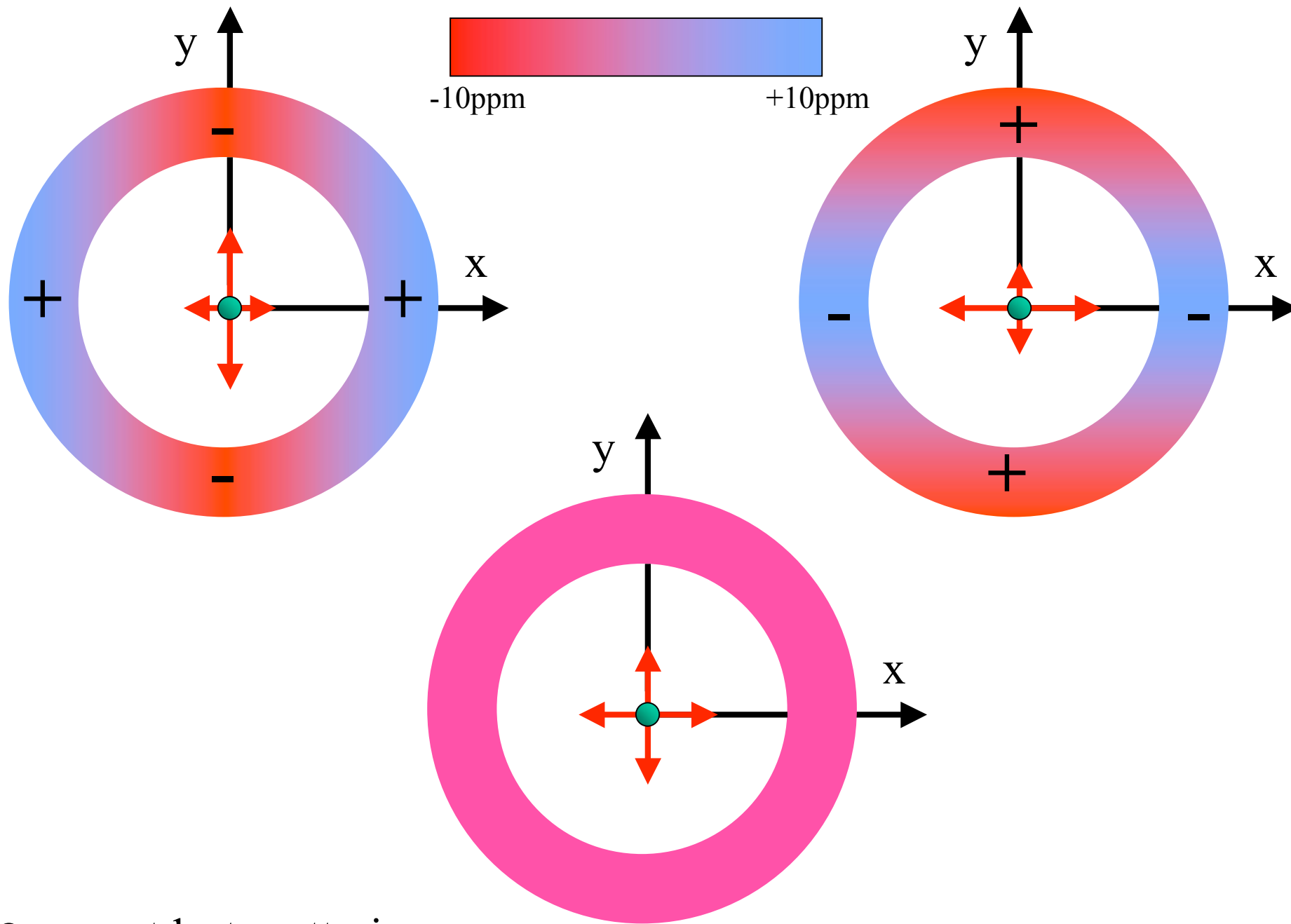


Fig. 18.— The WMAP three-year power spectrum (in black) compared to other recent measurements of the CMB angular power spectrum, including Boomerang (Jones et al. 2005), Acbar (Kuo et al. 2004), CBI (Readhead et al. 2004), and VSA (Dickinson et al. 2004). For clarity, the $l < 600$ data from Boomerang and VSA are omitted; as the measurements are consistent with WMAP, but with lower weight. These data impressively confirm the turnover in the 3rd acoustic peak and probe the onset of Silk damping. With improved sensitivity on sub-degree scales, the WMAP data are becoming an increasingly important calibration source for high-resolution experiments.

CMB polarization

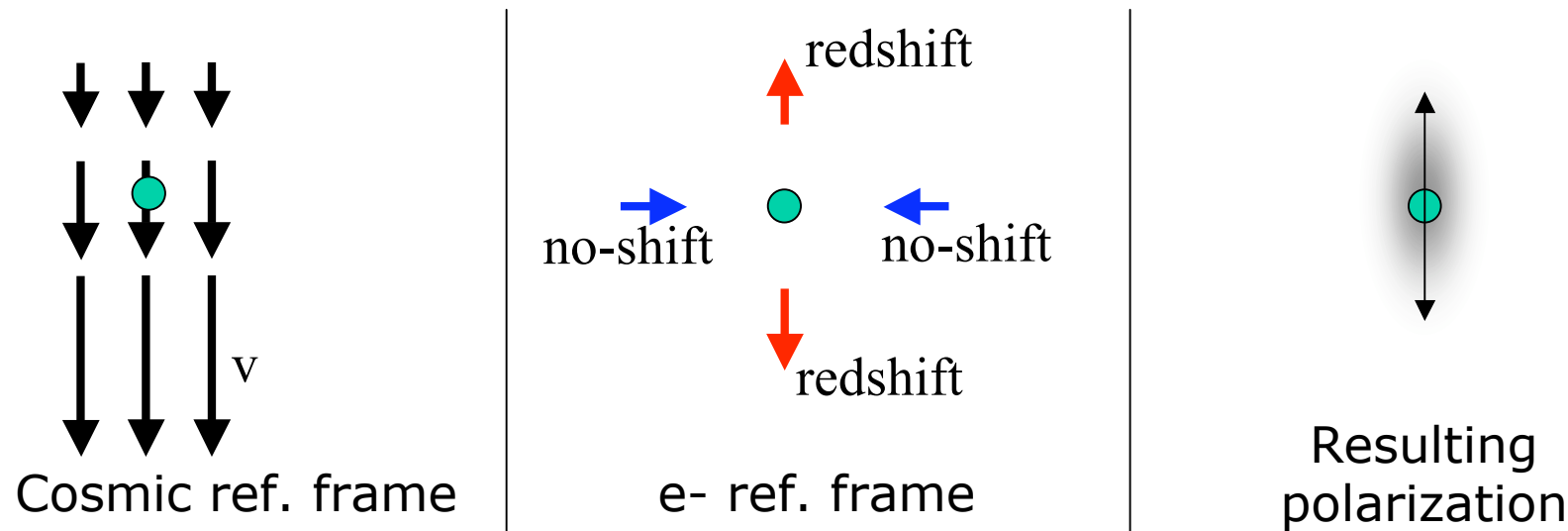
- CMB radiation is Thomson scattered at recombination.
- If the local distribution of incoming radiation in the rest frame of the electron has a *quadrupole moment*, the scattered radiation acquires some degree of linear polarization.





● = e⁻ at last scattering

- There are two sources of quadrupole anisotropy at the last scattering:
- **1-Velocity gradients** in the cosmic fluid at recombination produce a **quadrupole** in the rest-frame of the scattering electron.



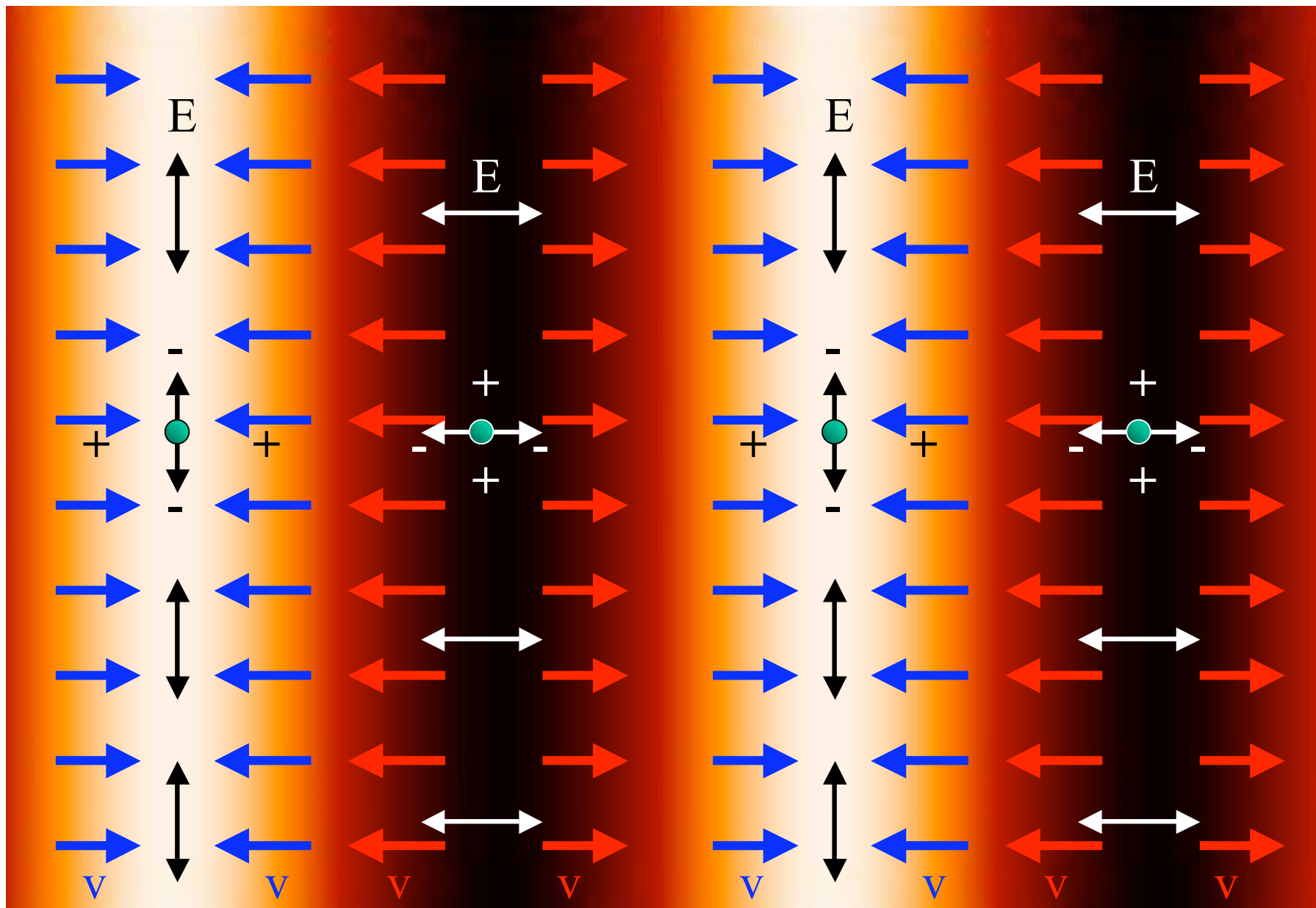
- This component of the CMB polarization field is called **E** component, or **gradient component**.
- We expect correlations between the CMB anisotropy (T) and the E-modes of the polarization field.

Overdensity

Underdensity

Overdensity

Underdensity

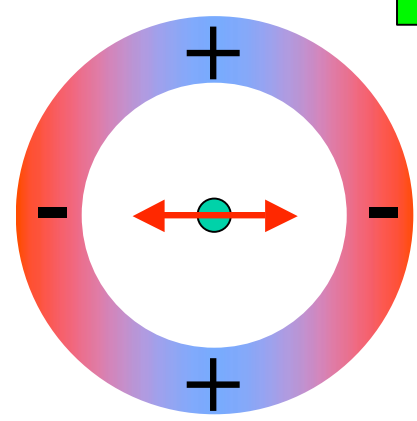
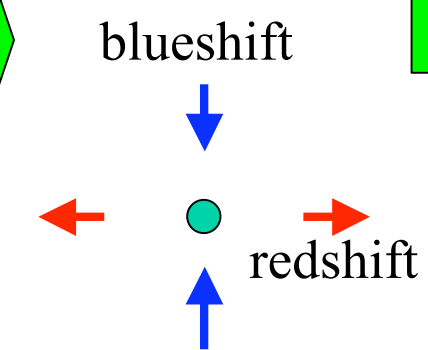
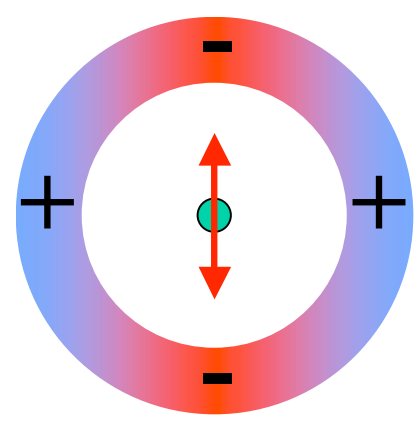
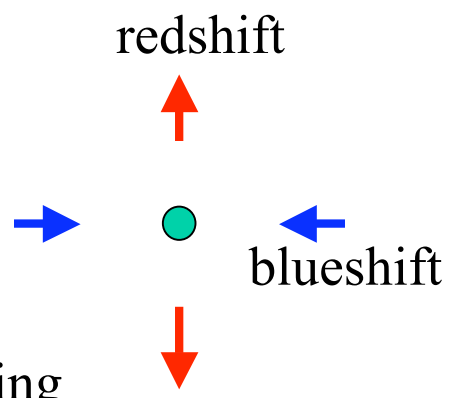
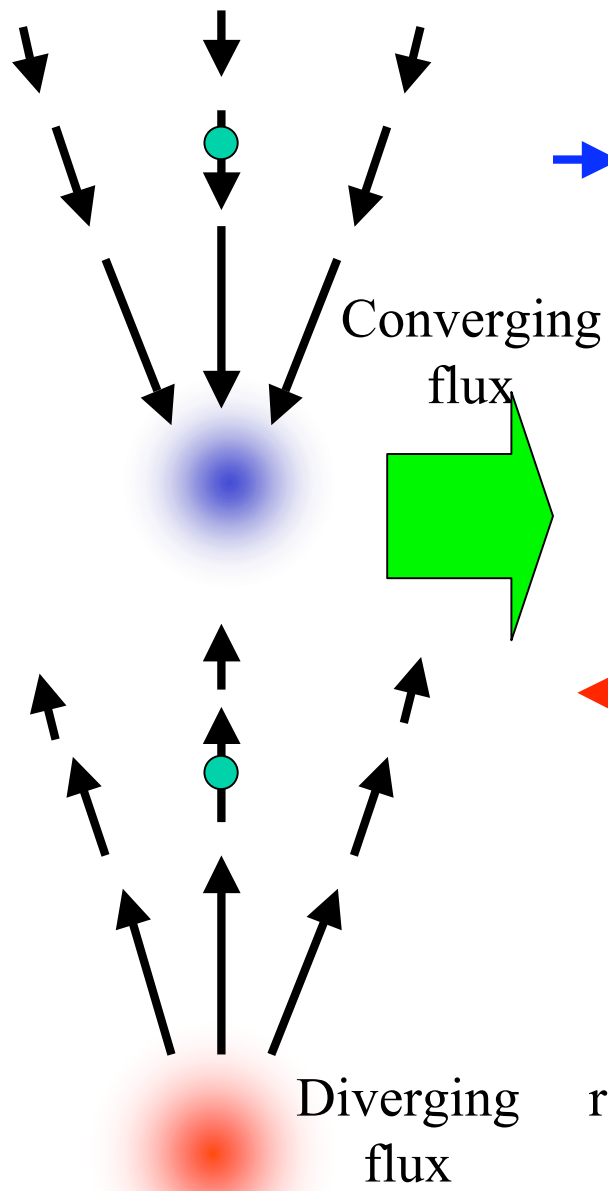


E-modes in the polarization pattern

Velocity fields
at recombination

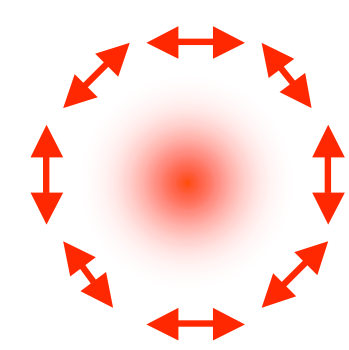
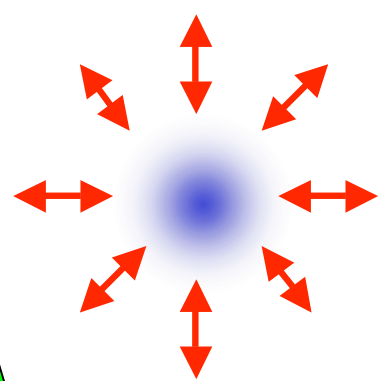


resulting
CMB polarization
field (E-modes)



Same flux as
seen in the
electron
reference frame

Quadrupole anisotropy
due to Doppler effect



- E-modes are irrotational
- E modes are related to velocities, while T is related mainly to density
- We expect a power spectrum of the E-modes, $\langle EE \rangle$, with maxima and minima in quadrature with the anisotropy power spectrum $\langle \overline{TT} \rangle$.

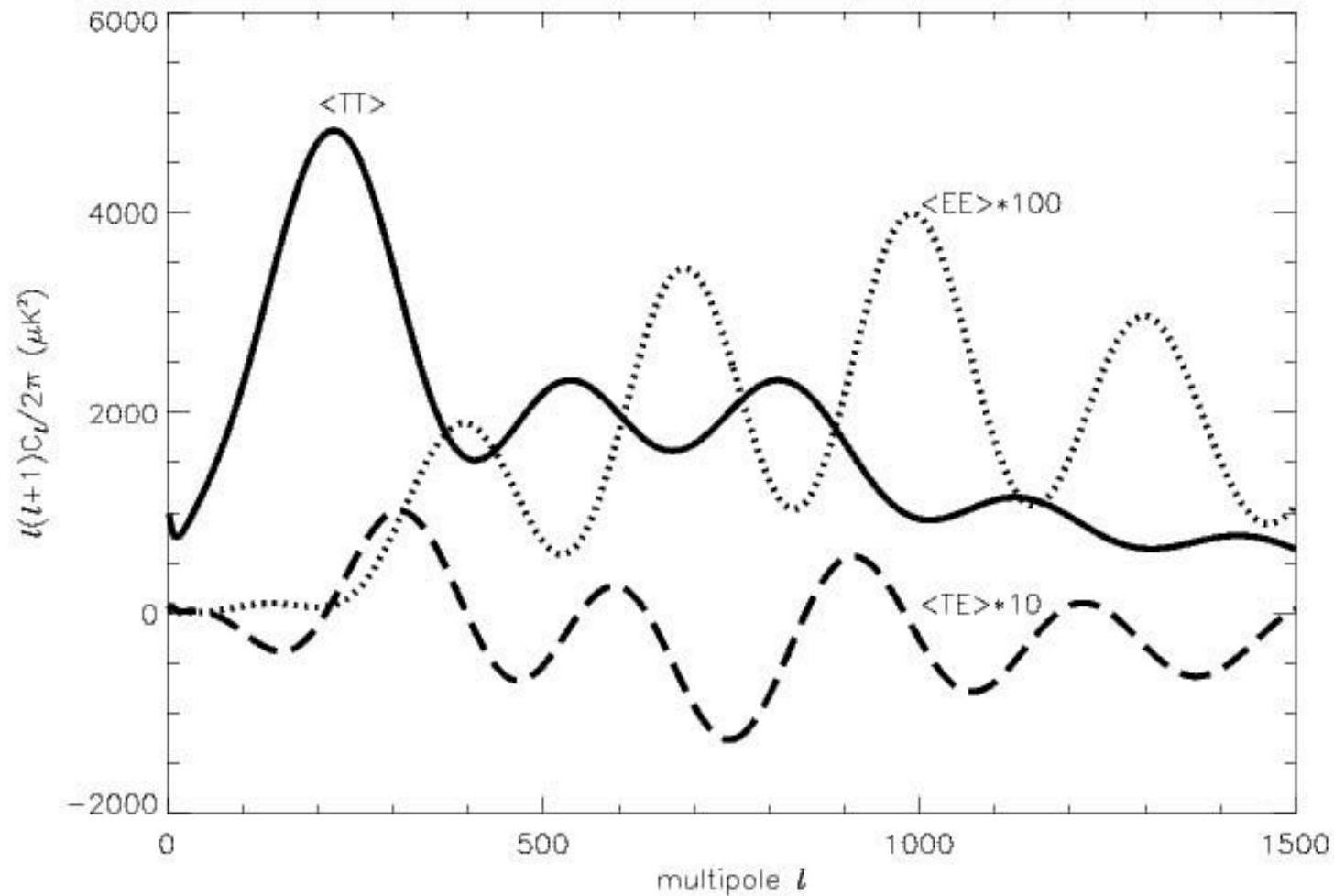


Figure 1.7: Estimated power spectra for the cosmological parameters: $\Omega_b = 0.05$, $\Omega_{cdm} = 0.3$, $\Omega_\Lambda = 0.65$, $\Omega_\nu = 0$, $H_0 = 65$ km/s/Mpc, $\tau = 0.17$. The temperature power spectrum, $\langle TT \rangle = C_\ell^T$, the E -modes power spectrum $\langle EE \rangle = C_\ell^E$ multiplied by a factor 100 to make it visible and the cross power spectrum between temperature and polarization, $\langle TE \rangle = C_\ell^{TE}$ multiplied by a factor 10. The spectra are computed using the publicly available code CMBFAST (<http://www.cmbfast.org>),

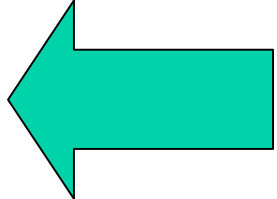
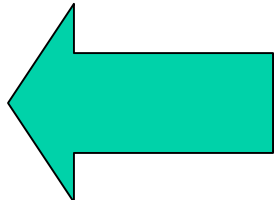
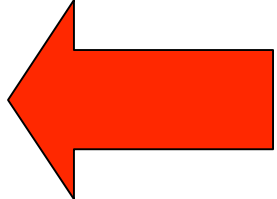
Interest of detecting E-modes (1):

- In all the cosmological parameters analysis an *adiabatic* type of fluctuations is assumed (because simple and predicted by the simplest inflation models)
- If **other types of fluctuations** are considered (for example isocurvature ones) the determination of cosmological parameters becomes much less precise.
- Precision can be recovered by studying independent observables, like the **polarization** of the CMB.
- See e.g. Bucher et al., astro-ph/0012141

Interest of detecting E-modes (2)

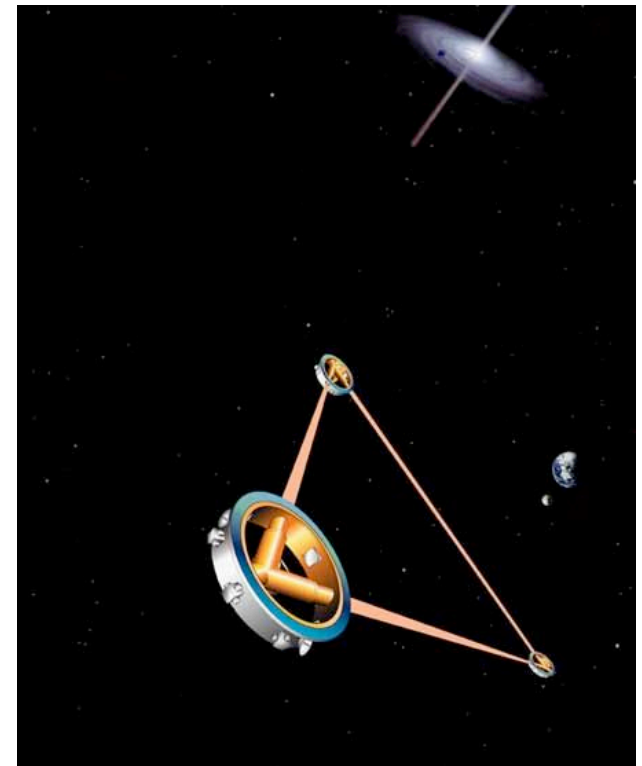
- The universe gets reionized when the first stars form.
- The **polarization** of the CMB at **large angular scales** is heavily affected by reionization.
- It is a way to measure the redshift of reionization, between $z=5$ and 20, complementary to work based on the Gunn-Peterson effect (see e.g. Becker et al. (2001) and Djorgovski et al. (2001).)

If inflation really happened...

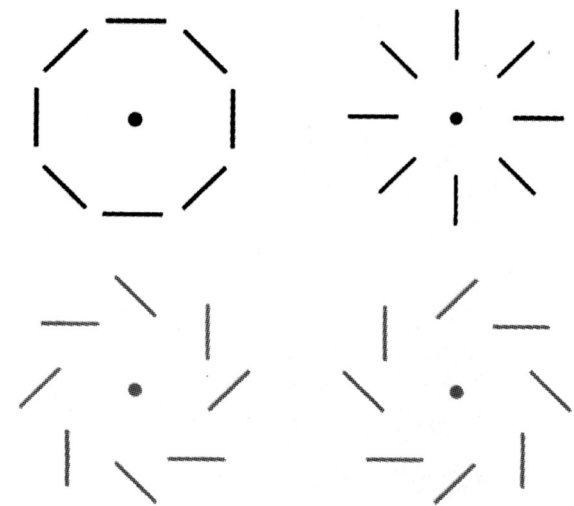
- It stretched geometry of space to nearly Euclidean  OK
- It produced a nearly scale invariant spectrum of density fluctuations  OK
- It produced a stochastic background of gravitational waves, i.e. another source of quadrupole anisotropy at recombination.  ?

Quadrupole from P.G.W.

- The background is so faint that even LISA will not be able to measure it.
- Tensor perturbations also produce quadrupole anisotropy. They generate irrotational (E-modes) **and rotational (B-modes) components** in the CMB polarization field.
- Since B-modes are not produced by scalar fluctuations, they represent a signature of inflation.



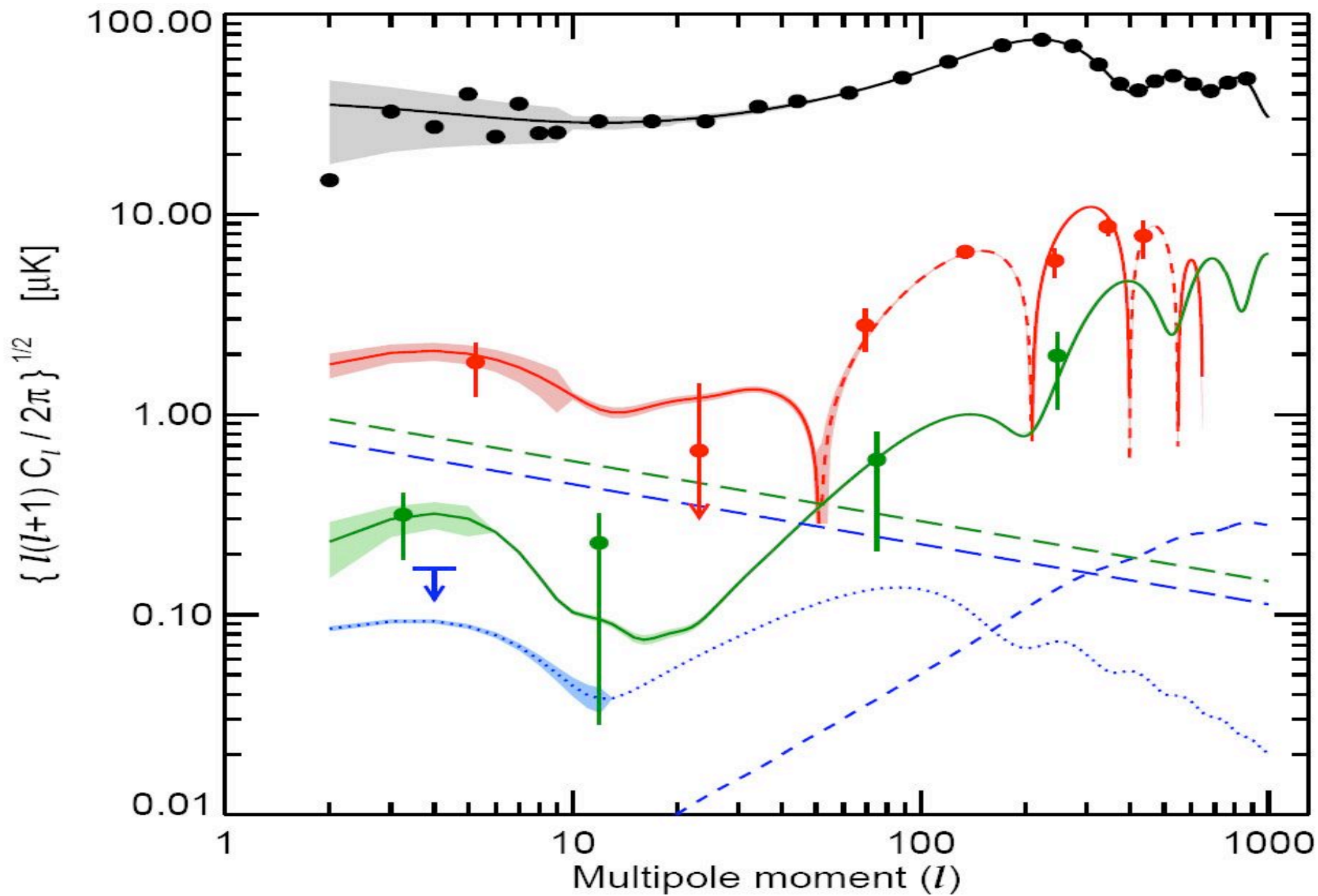
E-modes



B-modes

The signal is extremely weak (<100 nK !!!)

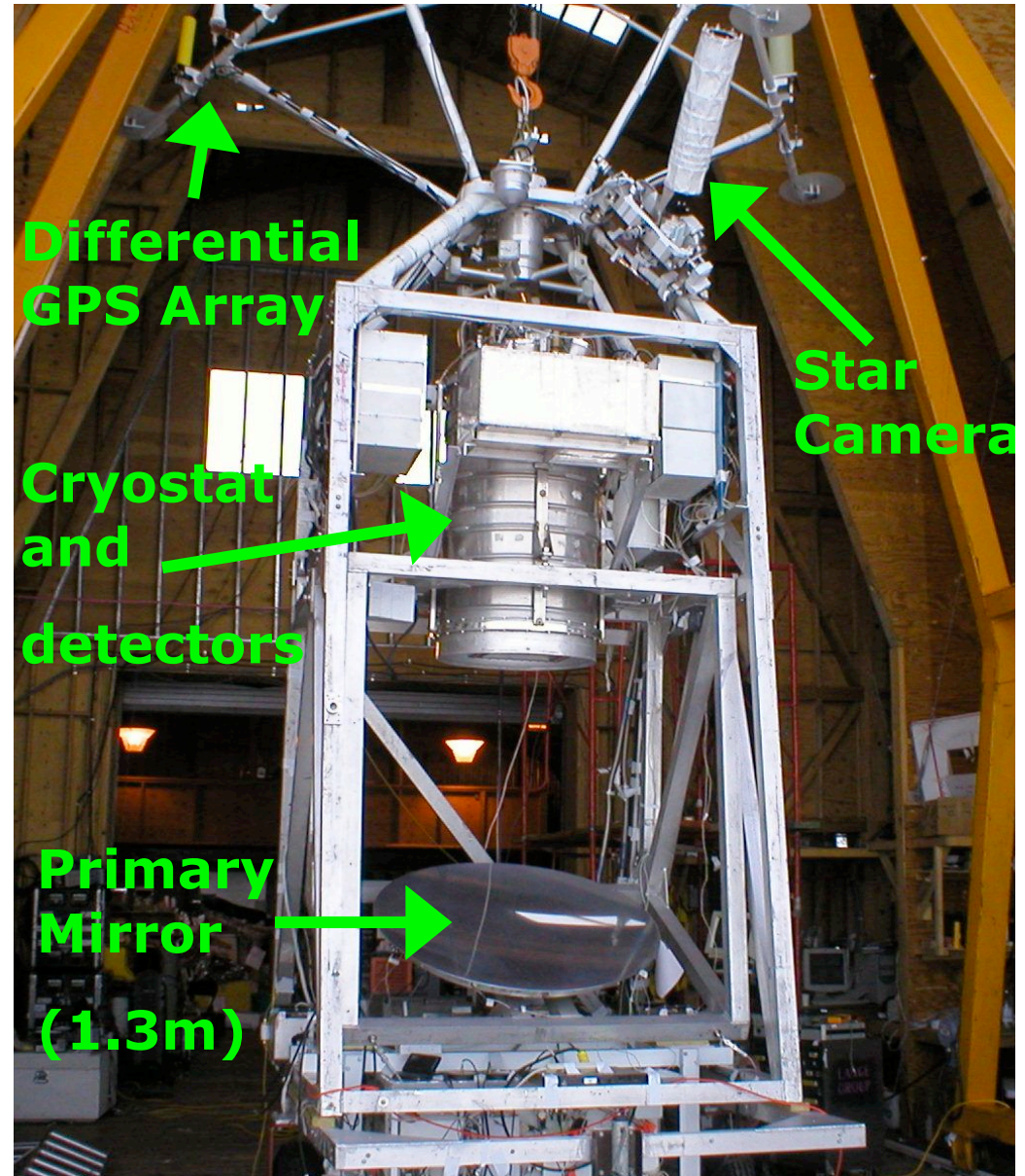
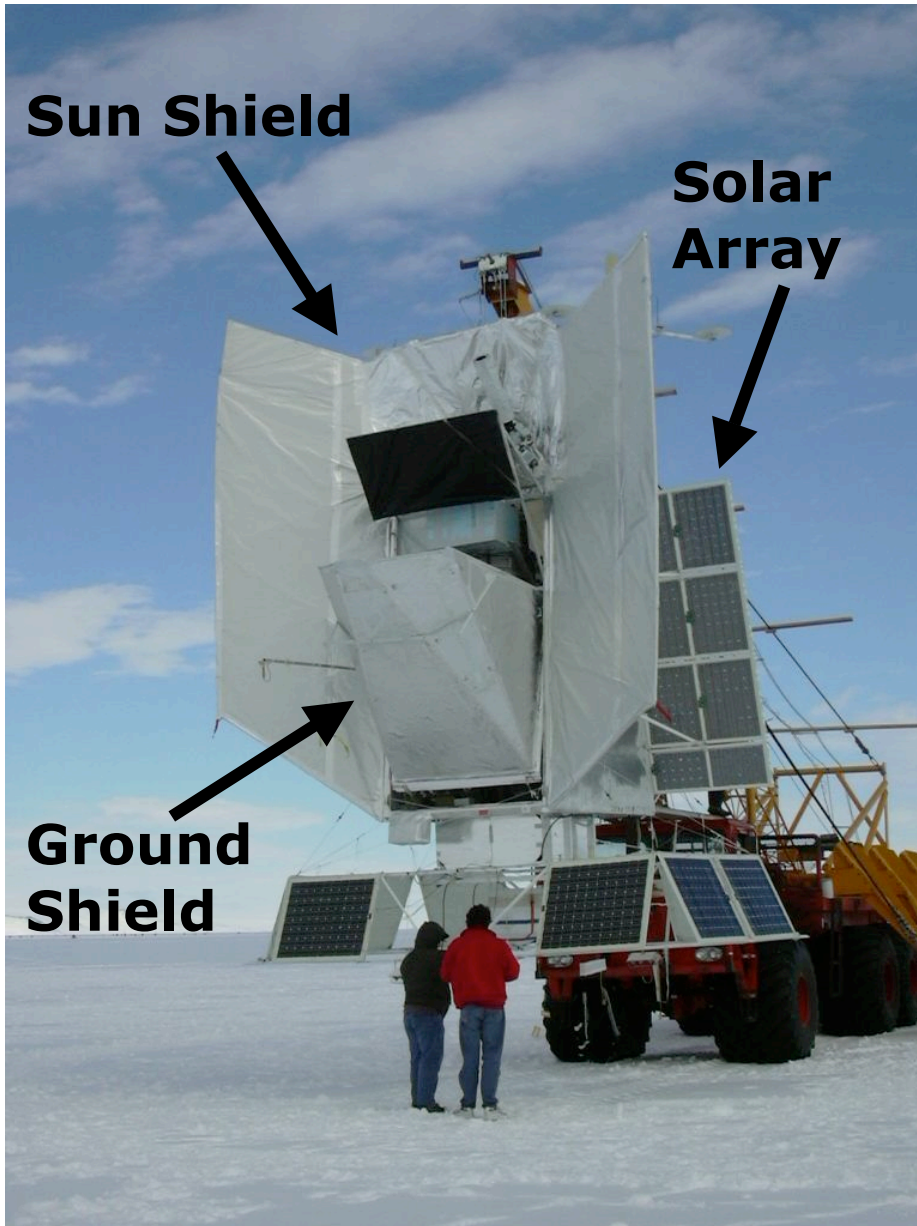
- Nobody really knows how to detect this.
 - Pathfinder experiments are needed
- Whatever smart, ambitious experiment we design to detect the B-modes:
 - It needs to be extremely sensitive
 - It needs an extremely careful control of systematic effects
 - It needs careful control of foregrounds
 - It will need **independent experiments with orthogonal systematics.**
- **There is still a long way to go: ...**



- Page et al., 2006, WMAP 3 years

- CMB polarization was first detected by DASI and then by several other experiments:

the BOOMERanG balloon-borne telescope

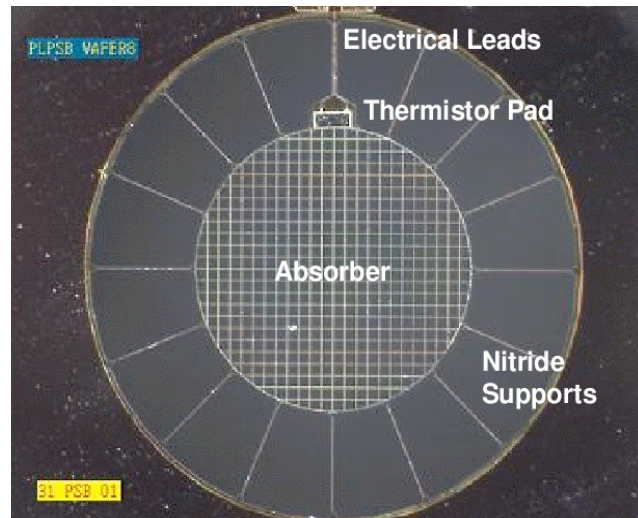
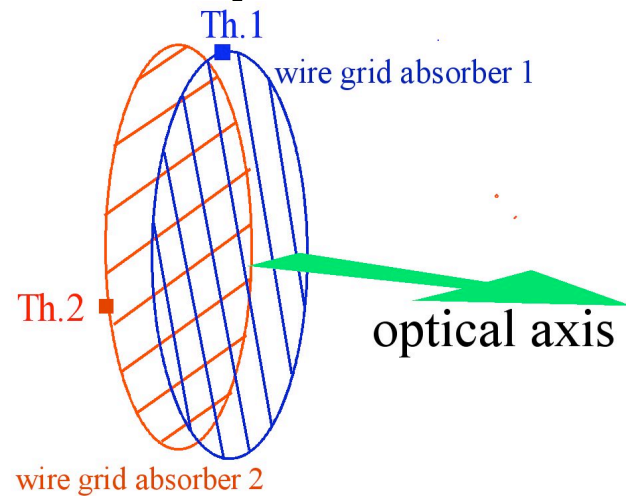
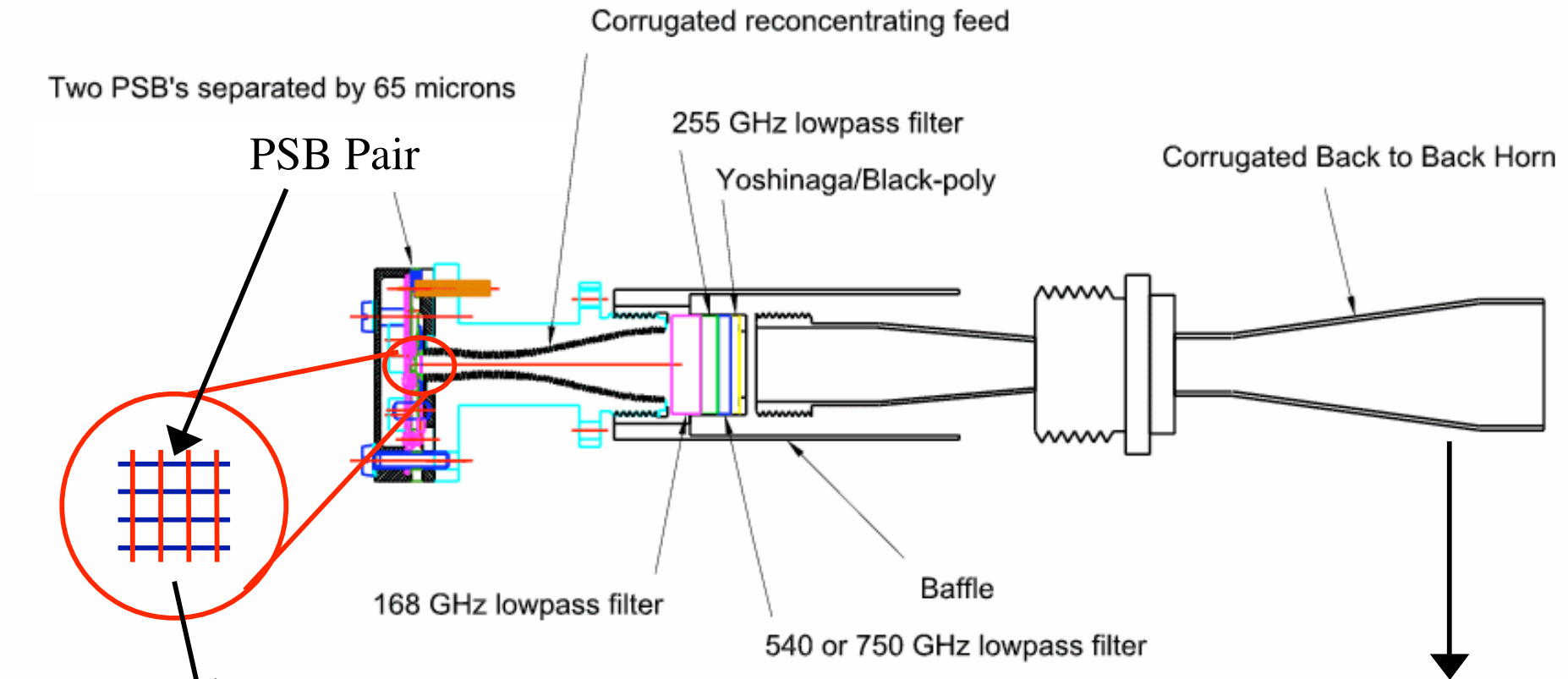


B03 Sensitive at 145, 245, 345 GHz

- The focal plane : all you see is cooled at 270 mK



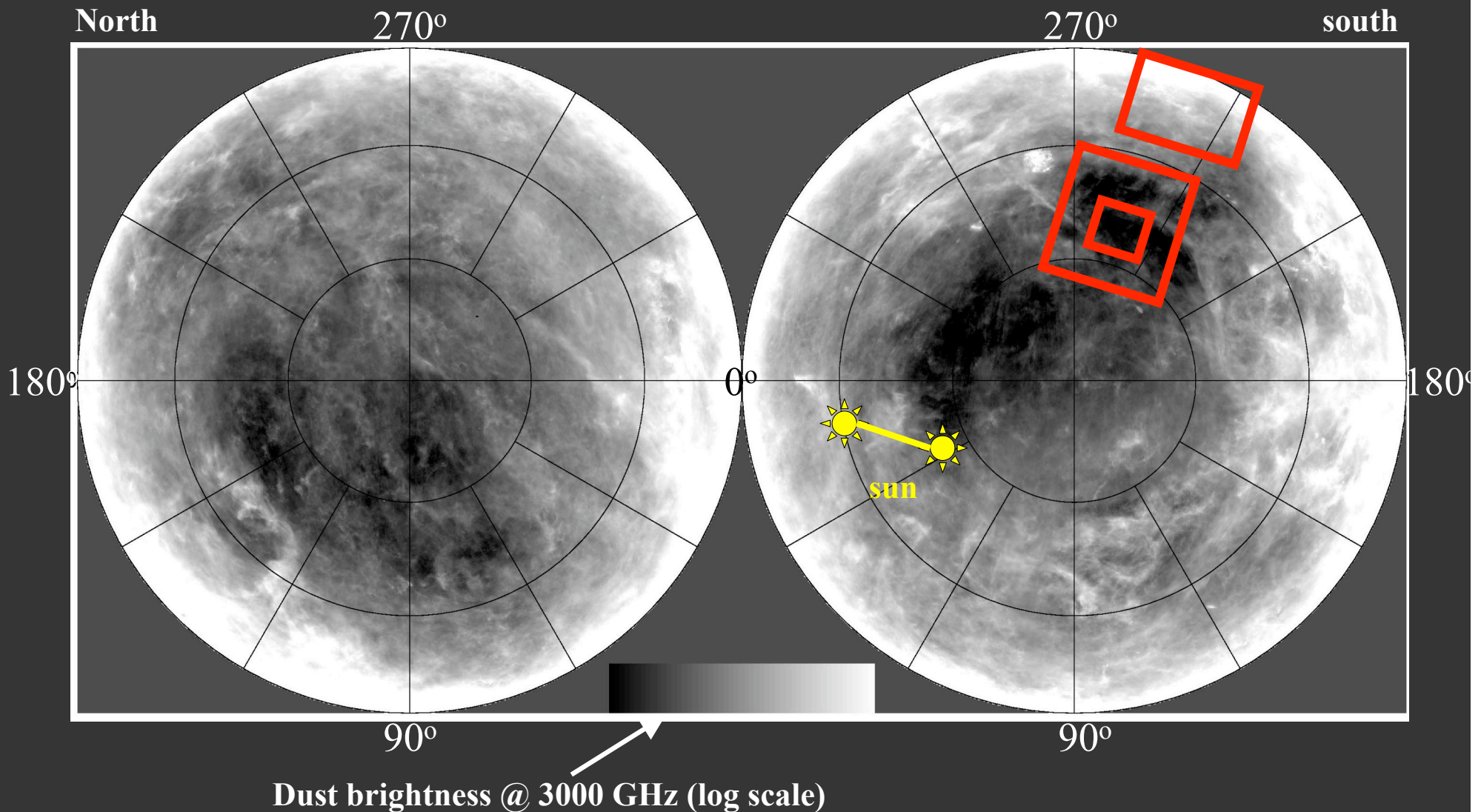
PSB devices & feed optics (Caltech + JPL)



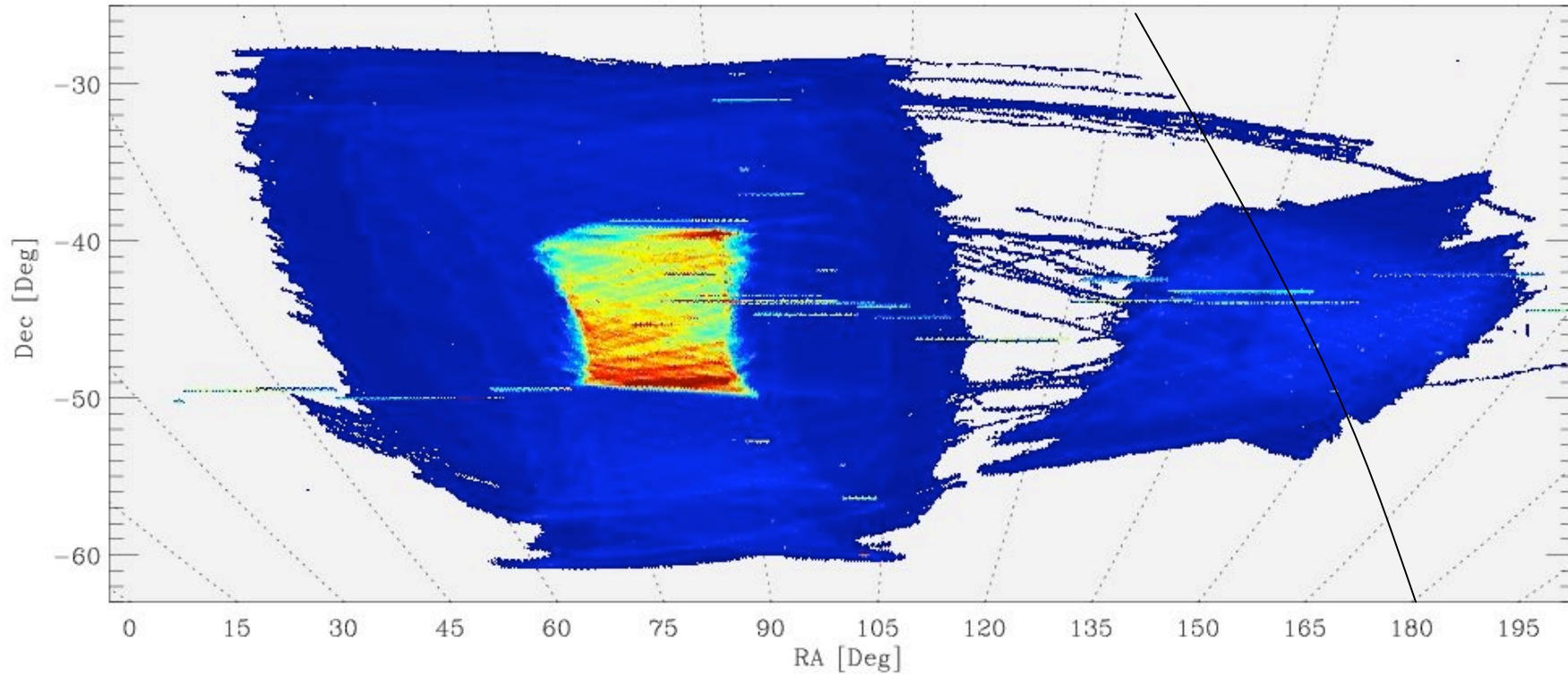


06/01/2003

We have selected one of the lowest dust regions in the sky, which is opposite to the sun during the Antarctic summer



Survey Strategy

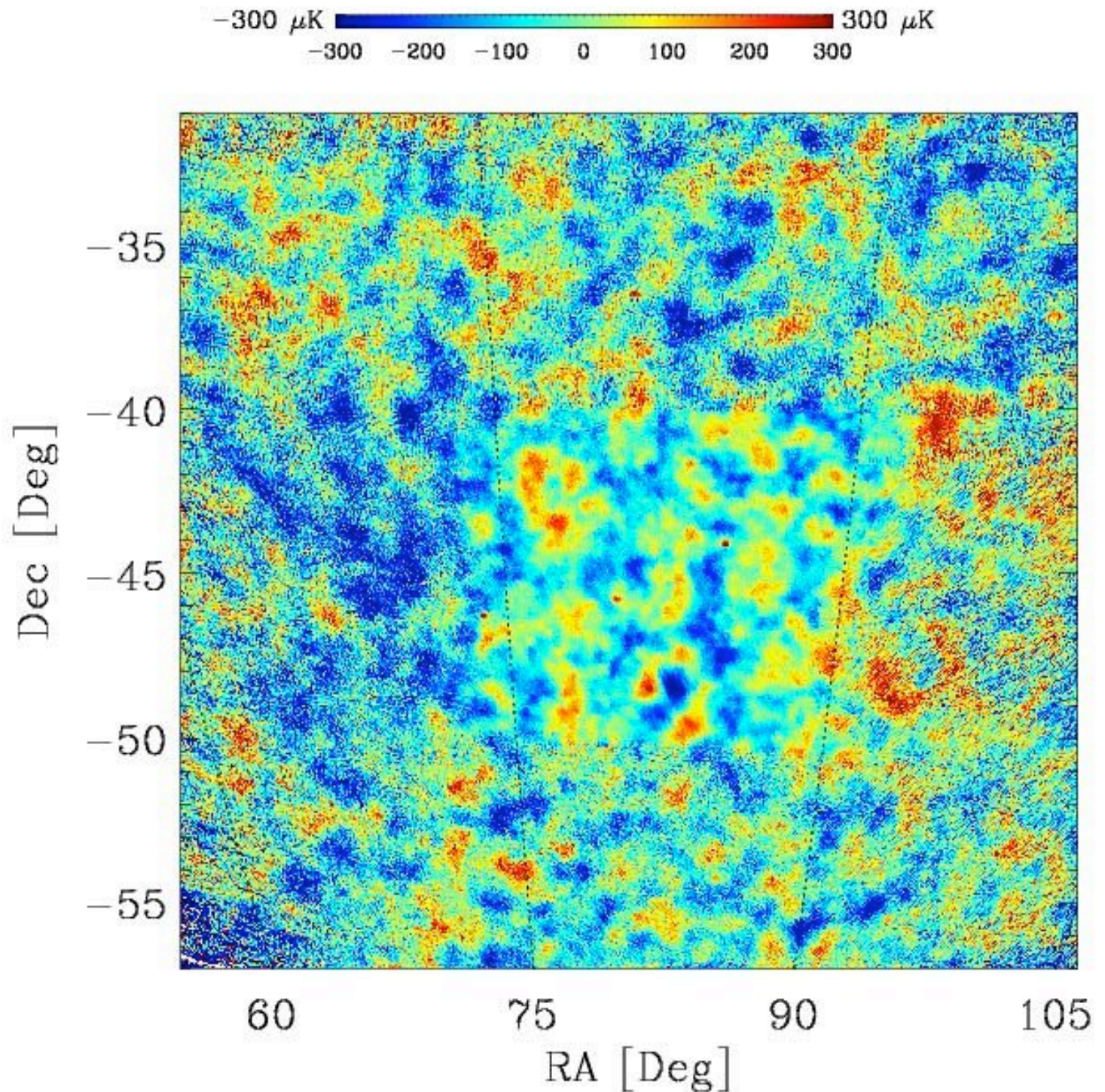


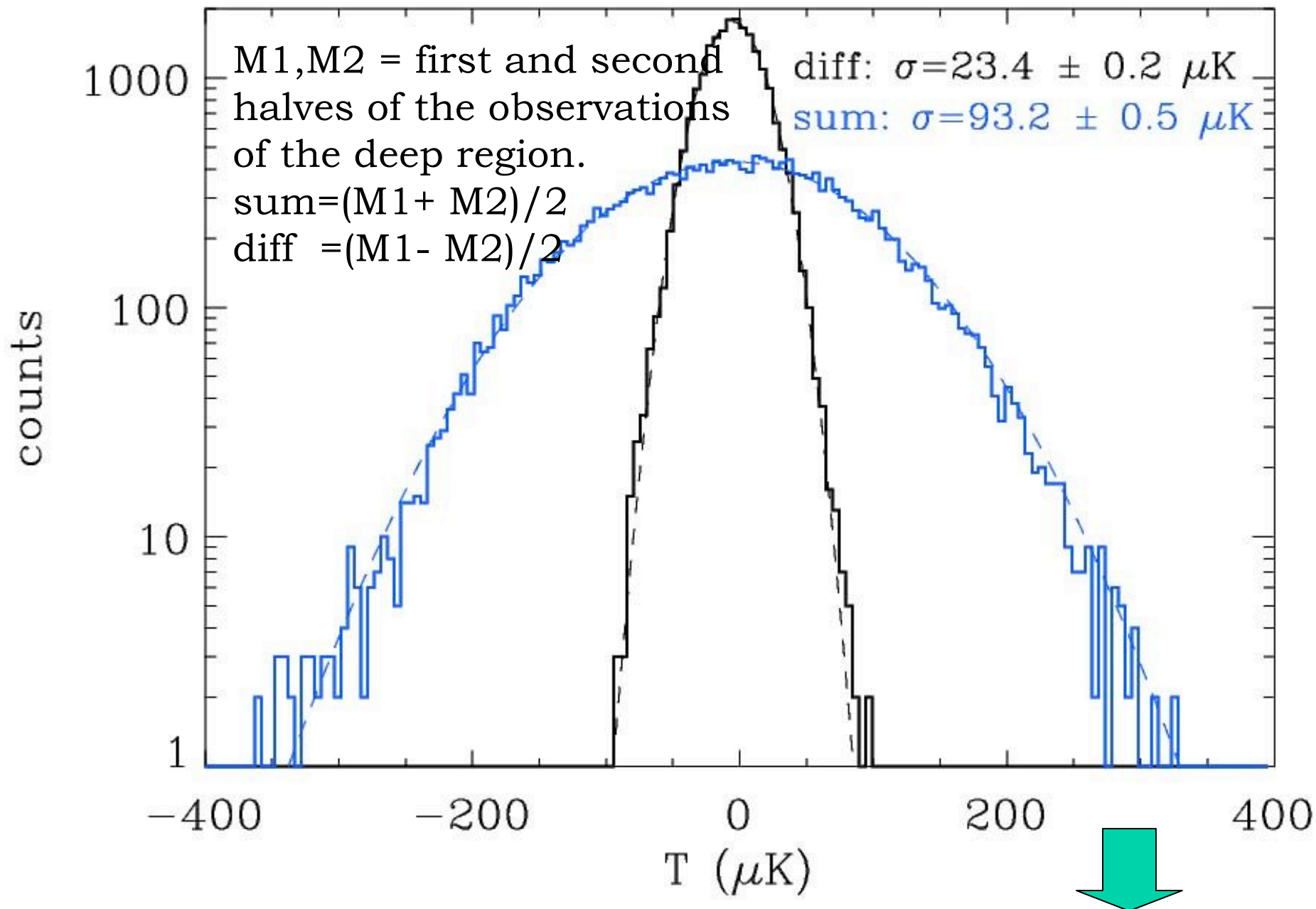
Region	Size (sq deg)	Goal	Time per 7' pixel (for each detector)
Deep CMB	115	$\langle EE \rangle$	60 sec
Shallow CMB	1130	$\langle TE \rangle$ and $\langle TT \rangle$	3.3 sec
Galactic Plane	390	Polarized Foregrounds	4.7 sec

145 GHz T map

(Masi et al.,
2005)

the deepest
CMB map
ever



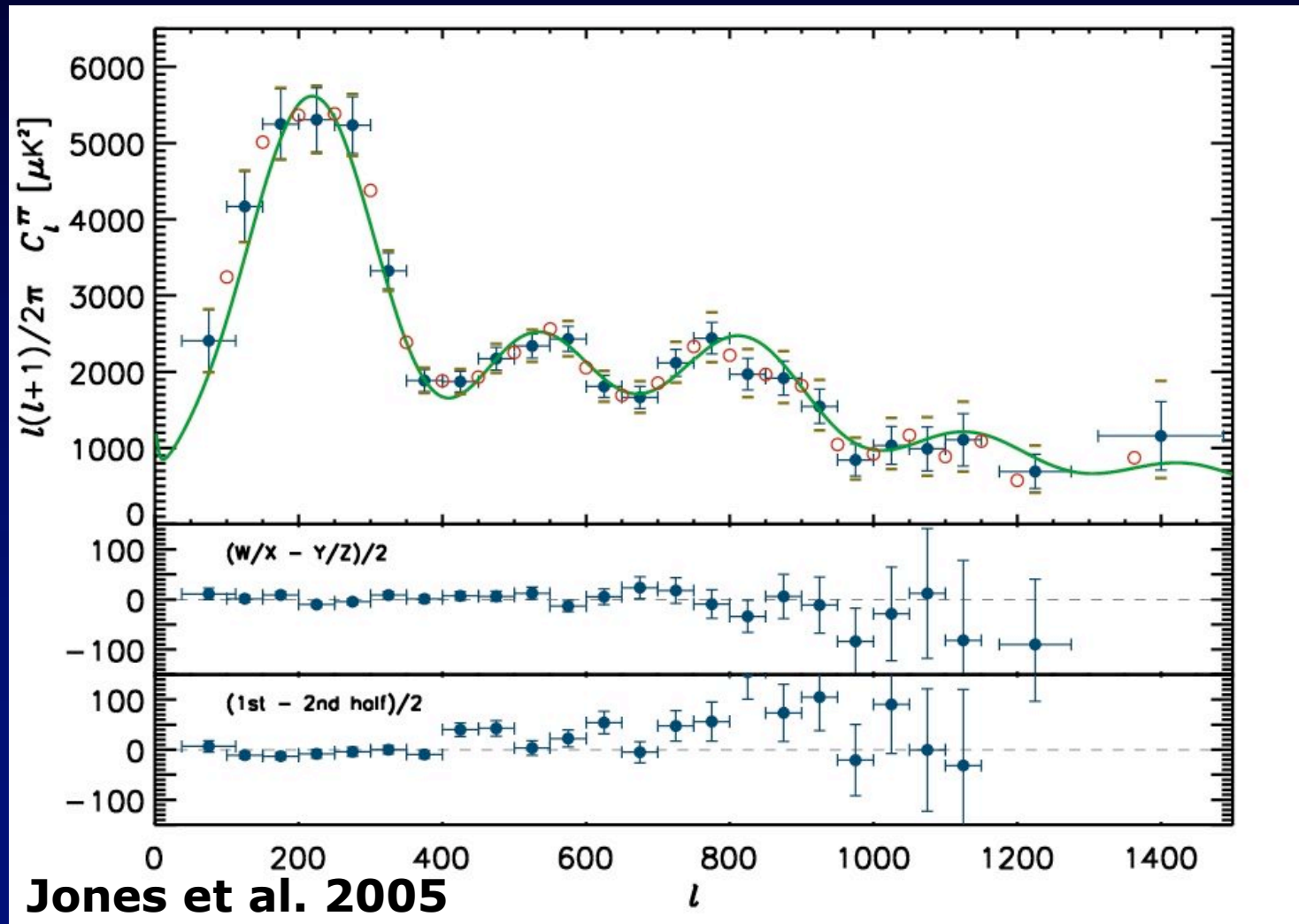


- In the deep survey the S/N is high.
- The fluctuations are gaussian.

$$\Delta T_{\text{rms}} = (90.2 \pm 2.3) \mu\text{K}$$

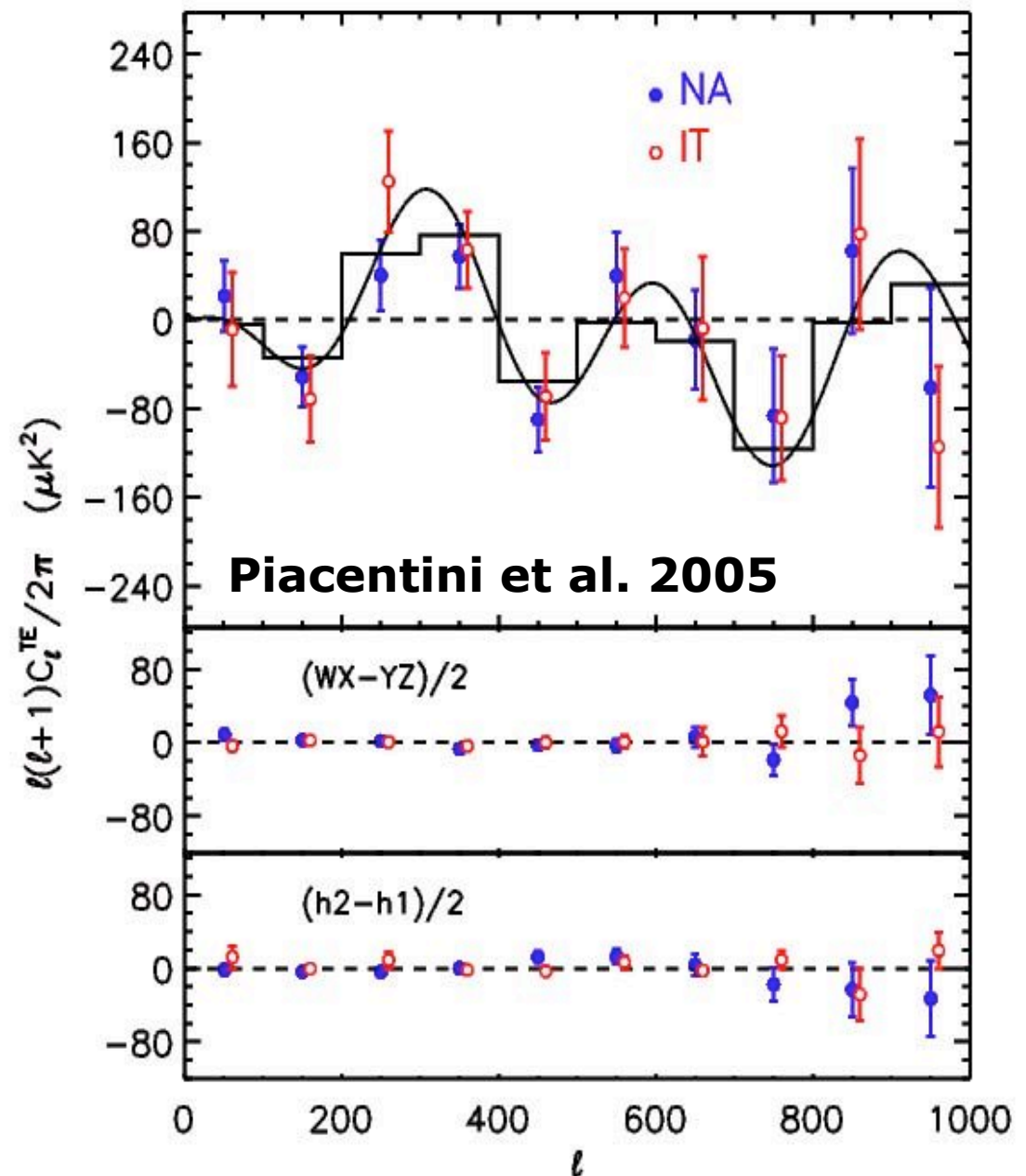
B03 TT Power Spectrum

- Detection of anisotropy signals all the way up to $l=1500$
- Time and detector jackknife tests OK
- Systematic effects negligible wrt noise & cosmic variance



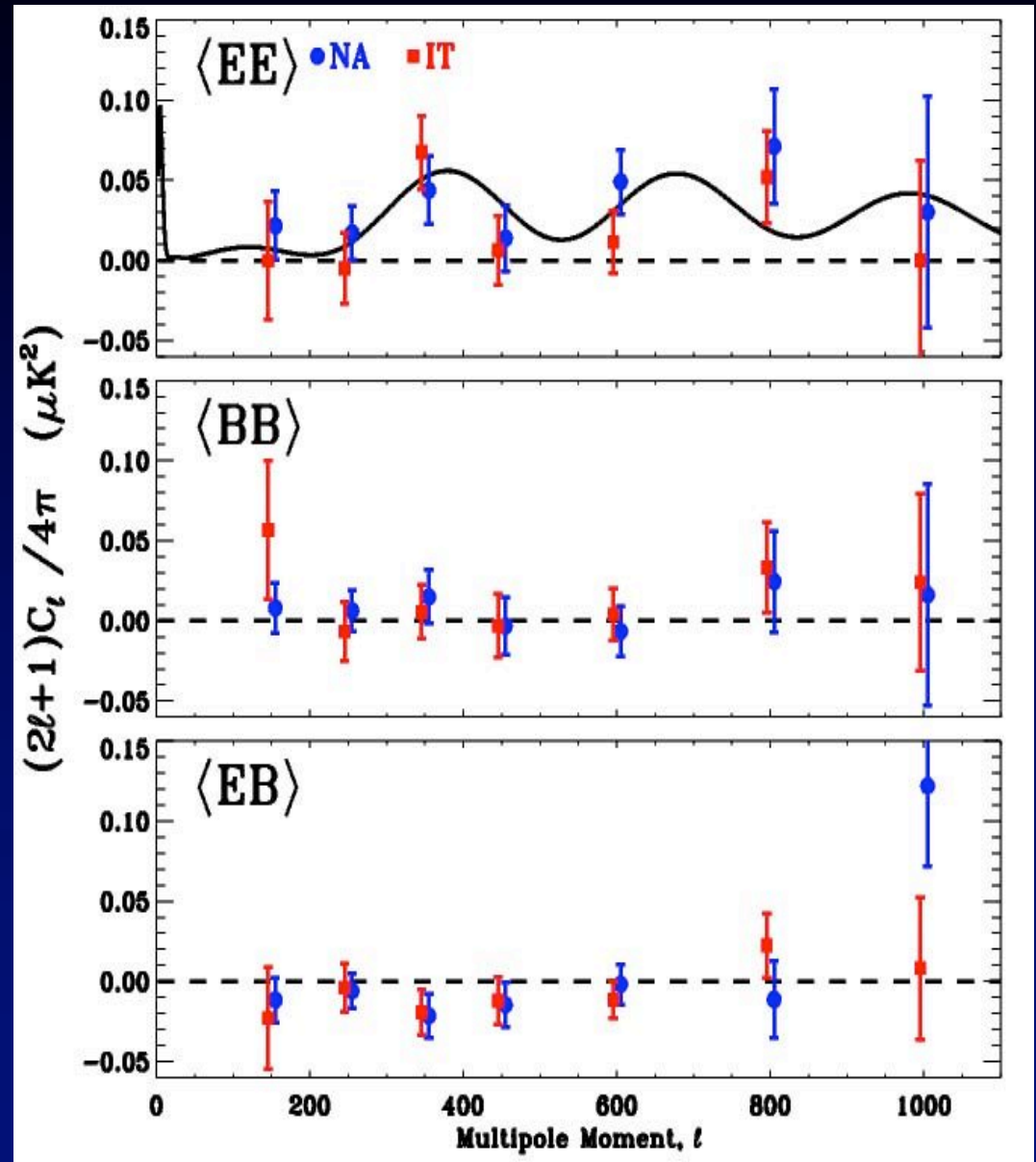
TE from BOOMERanG 03 (140 GHz)

- Small signal, but detection evident (3.5σ)
- NA and IT results consistent
- Error bars dominated by cosmic variance
- Time and detectors jackknife OK, i.e. systematics negligible
- Data consistent with TT best fit model

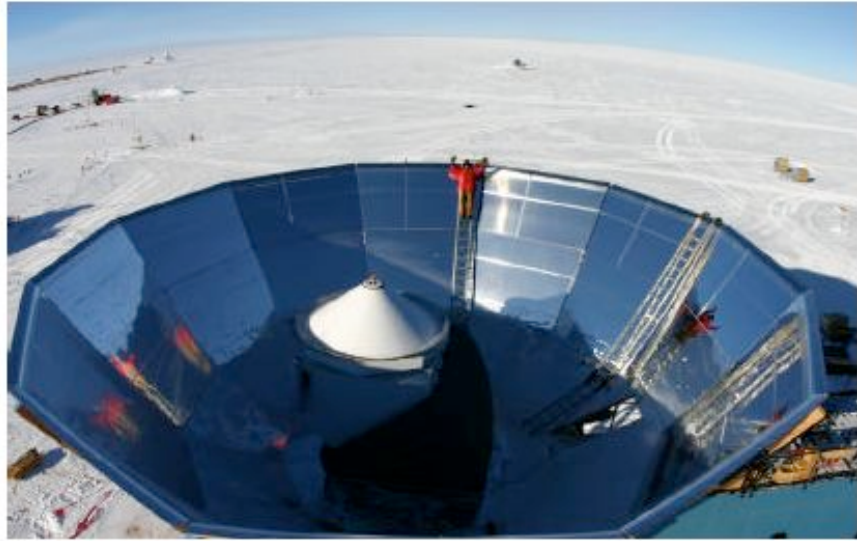


EE from BOOMERanG-03 (140 GHz)

- Signal extremely small, but detection evident for EE (non zero at 4.8σ).
- No detection for BB nor for EB
- Time and detectors jackknife OK, i.e. systematics negligible
- Data consistent with Λ CDM best fit model
- Error bars dominated by detector noise.



QUAD



The QUaD Collaboration

- Stanford University
- U. of Wales, Cardiff
- Caltech
- JPL
- U. of Chicago
- N.U.I Maynooth
- U. of Edinburgh
- Collège de France



QUAD: astro-ph/0705.2359

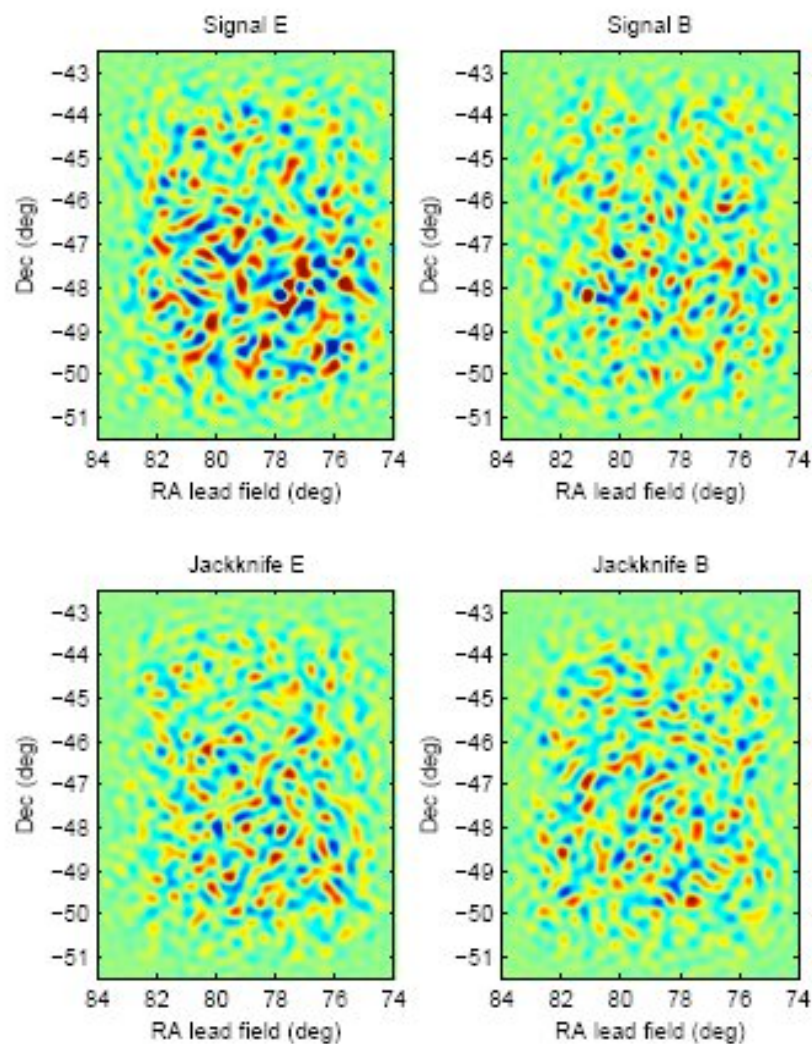
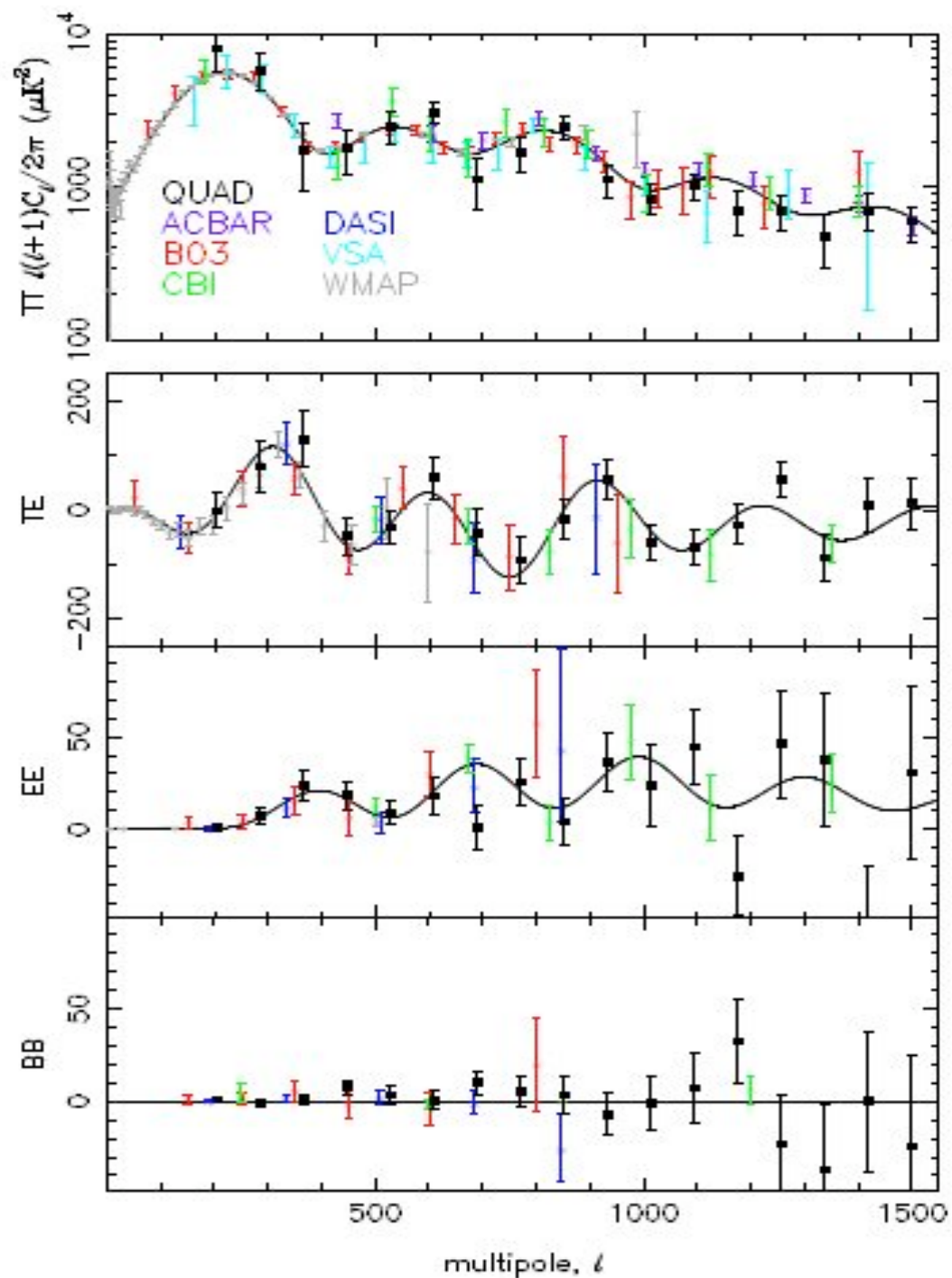
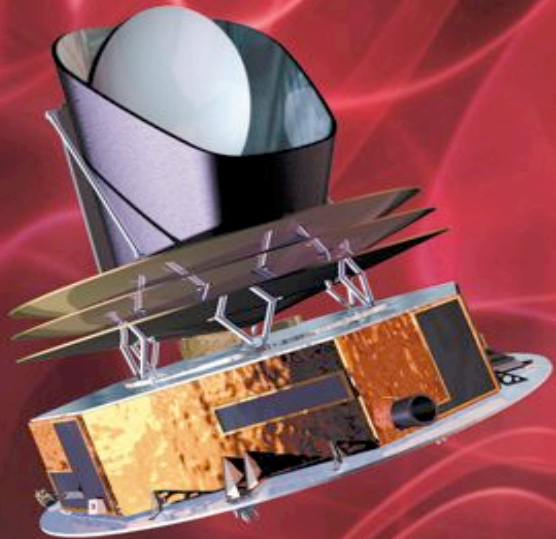


FIG. 1.— QUaD first season field differenced polarization maps decomposed into E and B -modes, and filtered to include only the angular scale range $200 < \ell < 1000$. The top row shows the result for signal (non-jackknife) maps, while the bottom row is for the “deck” jackknife (see text). This plot shows 150 GHz maps and the color scale is $\pm 30 \mu\text{K}^2$ in all cases.



Polarization summary

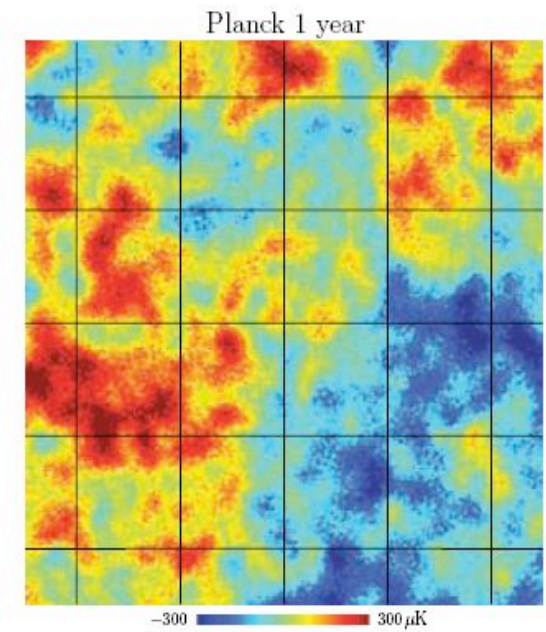
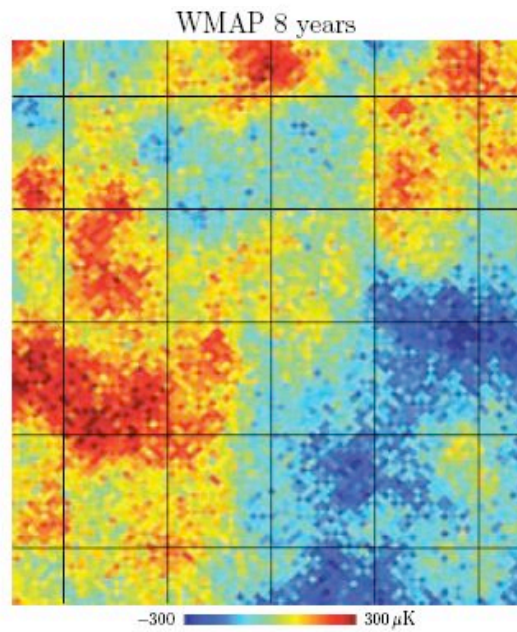
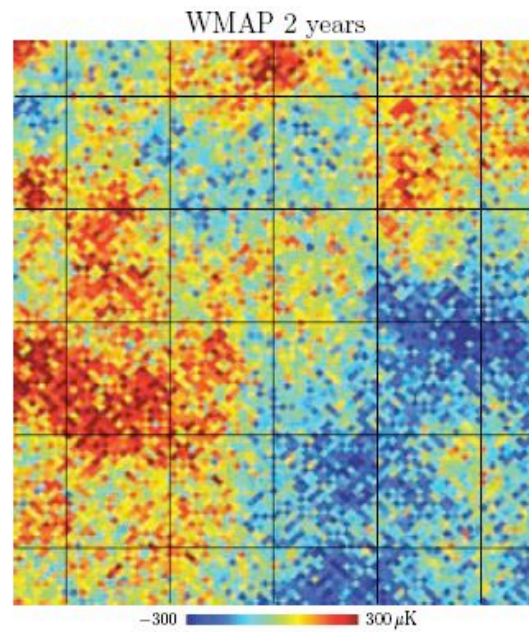
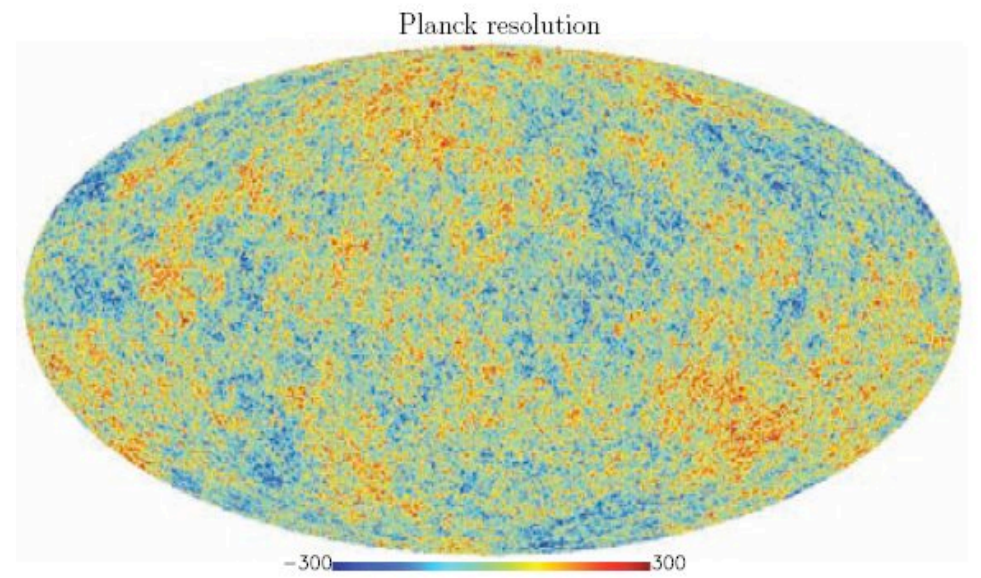
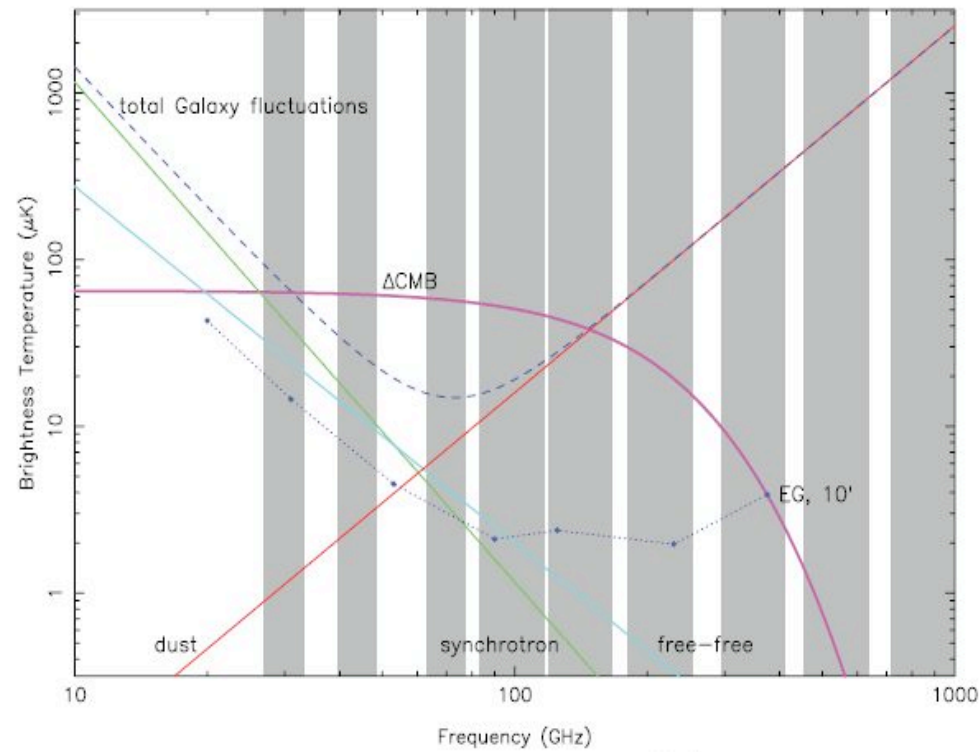
- CMB polarization is really there (several consistent detections by independent experiments)
- The measured amplitude of the E-modes is consistent with the expectation from the model best-fitting CMB anisotropy data.
- The accuracy is not great yet, and the polarization data do not add much to our knowledge of cosmological parameters.
- Main exception: the optical depth of reionization.
- B-modes not detected yet.



PLANCK

Looking back to the dawn of time
Un regard vers l'aube du temps

<http://sci.esa.int/planck>



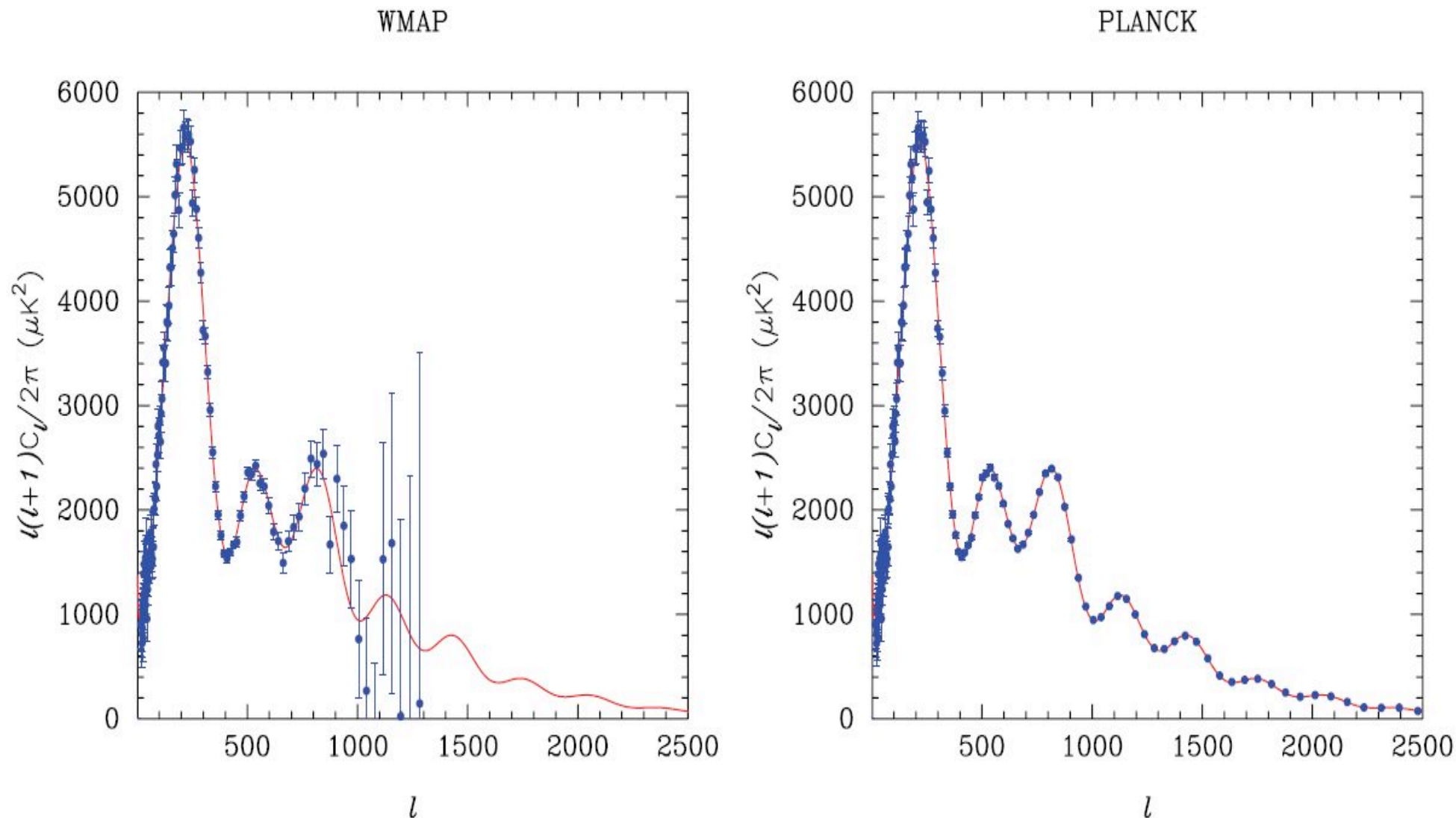


FIG 2.8.—The left panel shows a realisation of the CMB power spectrum of the concordance Λ CDM model (red line) after 4 years of *WMAP* observations. The right panel shows the same realisation observed with the sensitivity and angular resolution of *Planck*.

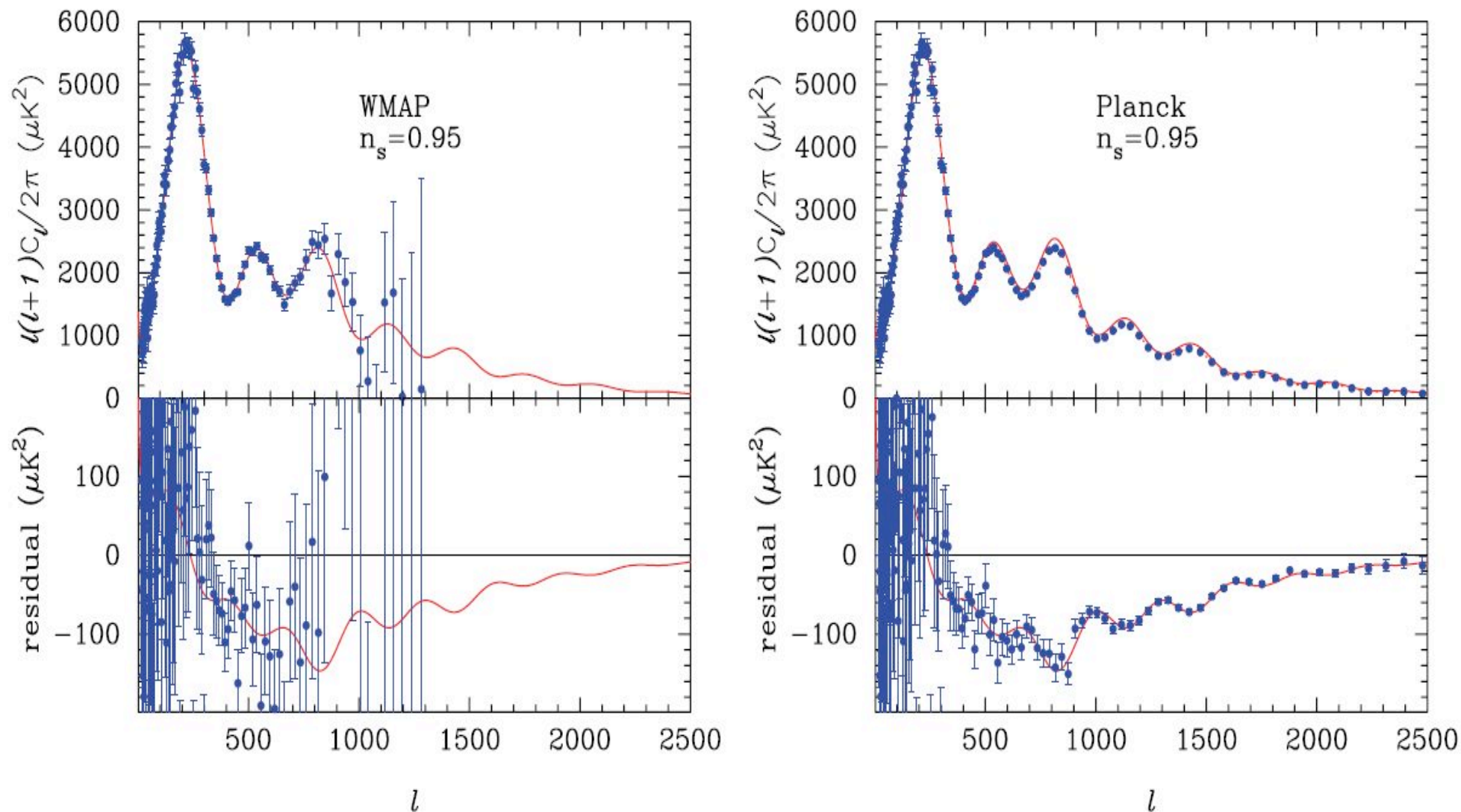
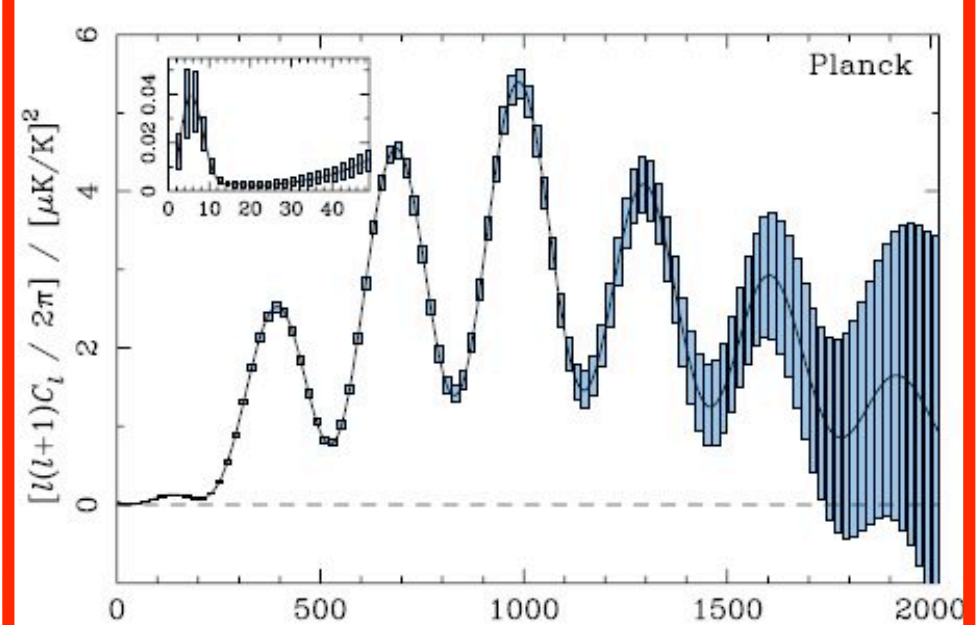
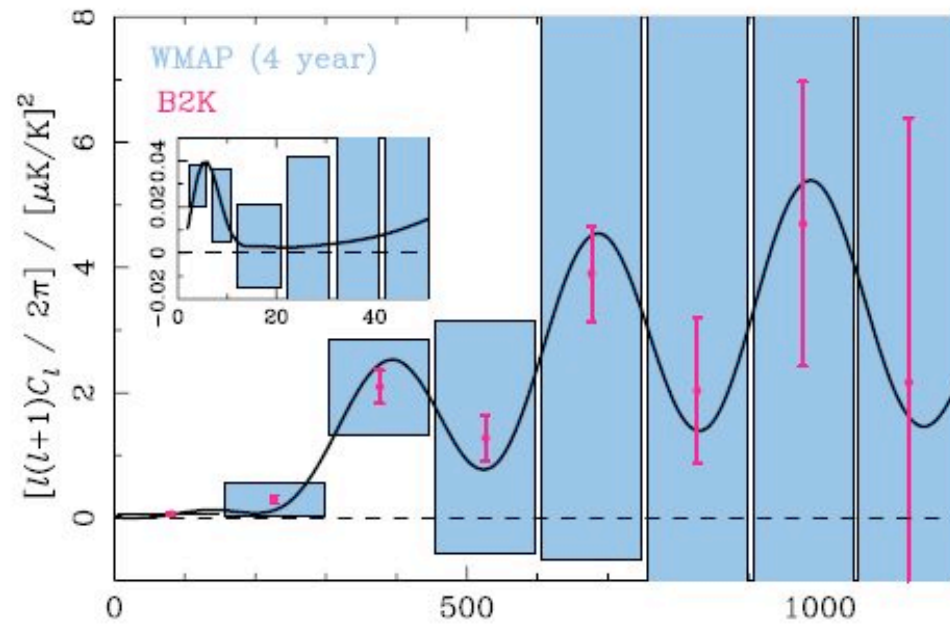
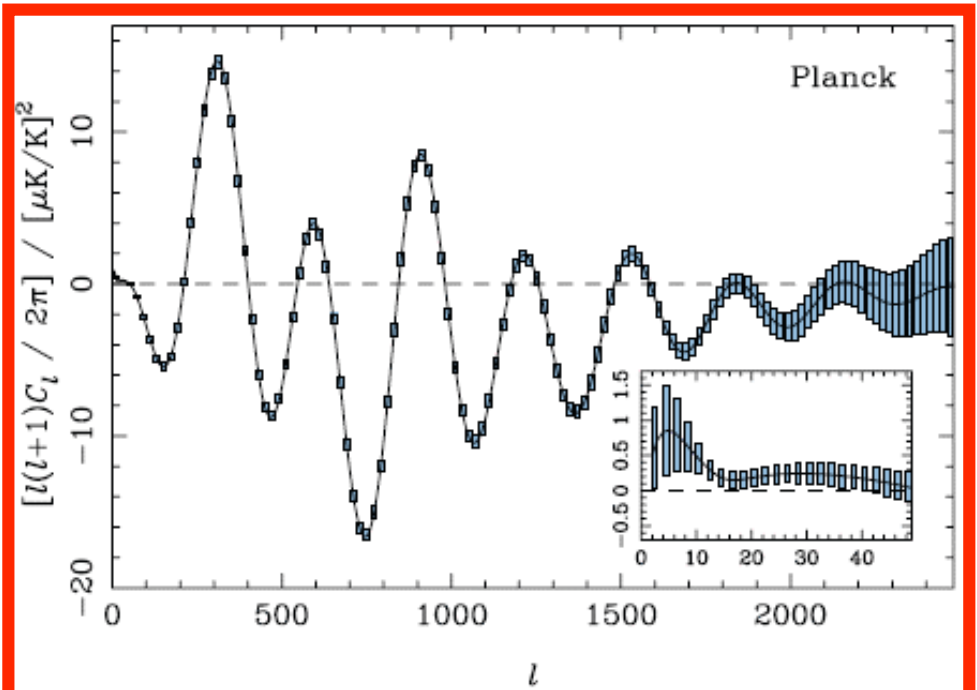
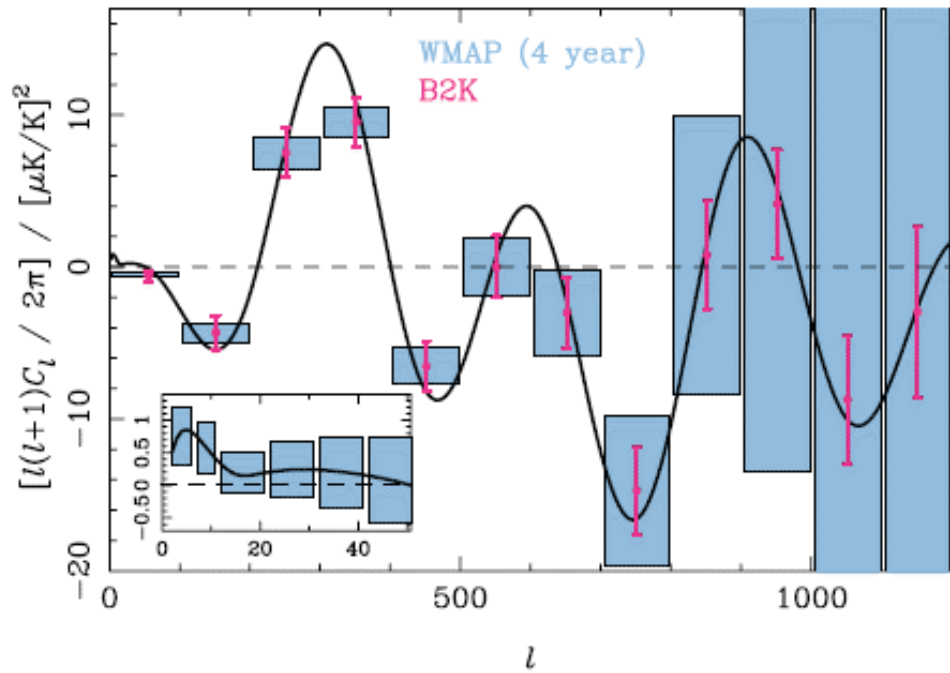
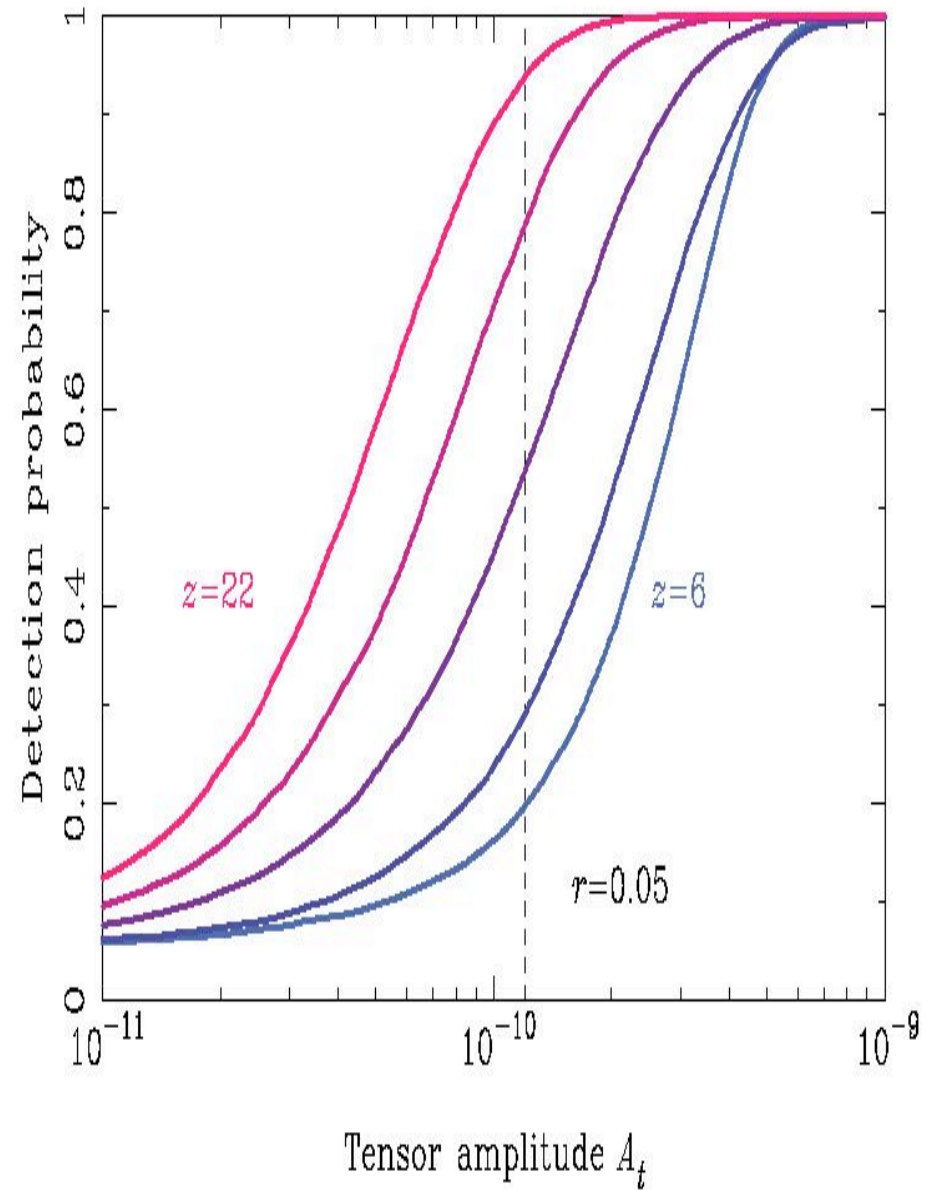
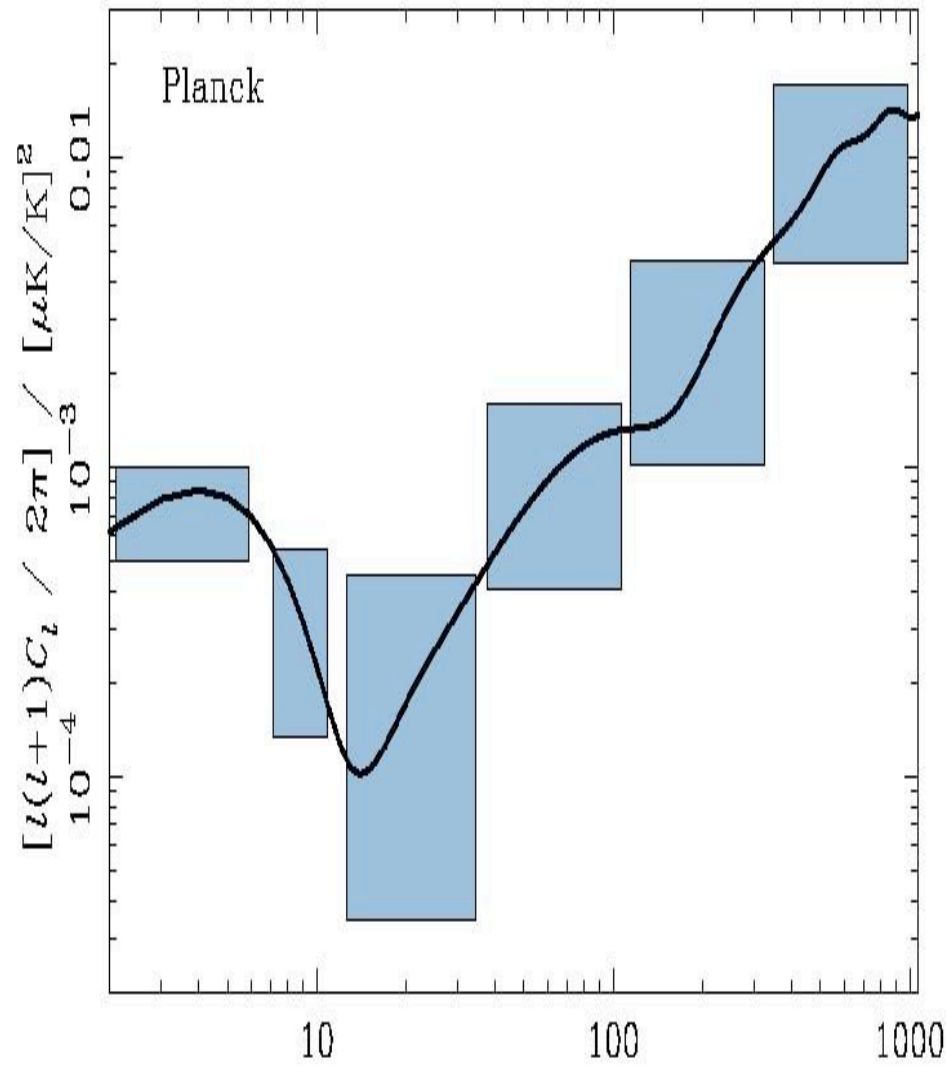


FIG 2.11.—The solid lines in the upper panels of these figures show the power spectrum of the concordance Λ CDM model with an exactly scale invariant power spectrum, $n_s = 1$. The points, on the other hand, have been generated from a model with $n_s = 0.95$ but otherwise identical parameters. The lower panels show the residuals between the points and the $n_s = 1$ model, and the solid lines show the theoretical expectation for these residuals. The left and right plots show simulations for *WMAP* and *Planck*, respectively.



E-modes, as will be observed by Planck



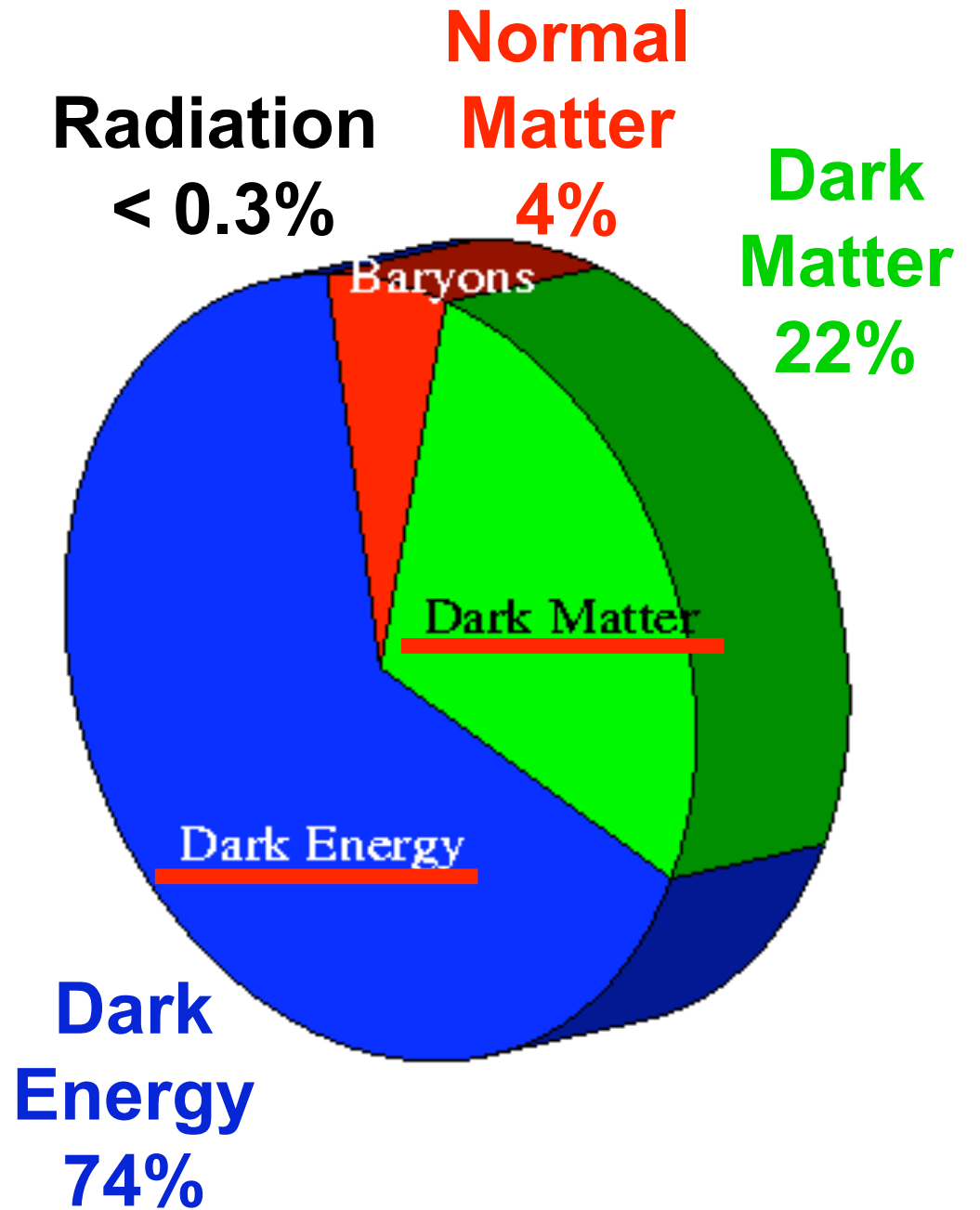
B-modes, as might be observed by Planck

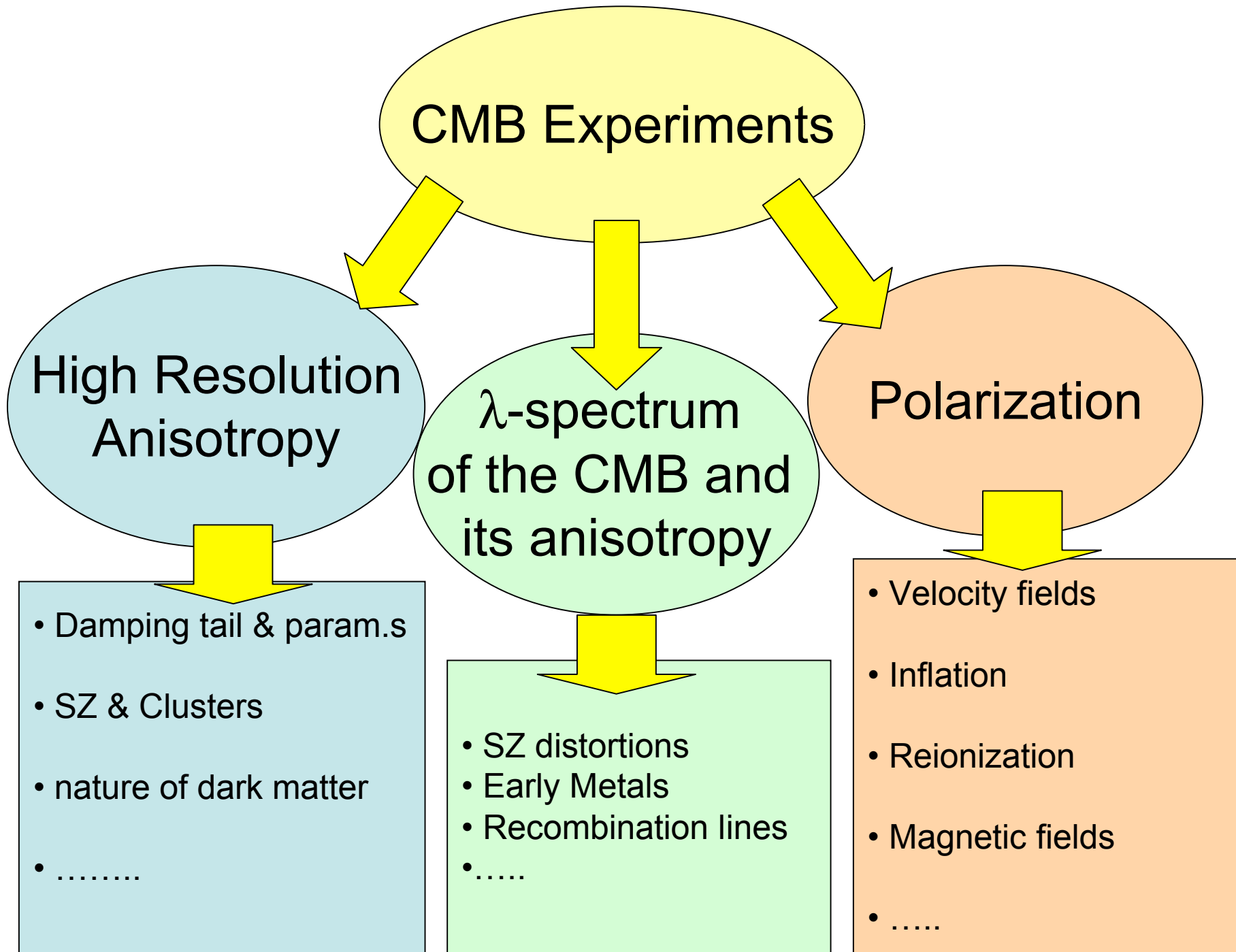
contents

- CMB experiments: state of the art
- Open problems : how to attack them with CMB
- Enabling technologies
- High angular resolution CMB anisotropy
- The spectrum of CMB anisotropy
- The polarization of CMB

- Given all this,
 - Which are the big questions ?
 - Where are we going with new CMB experiments / techniques to answer these questions ?

INFLATION





contents

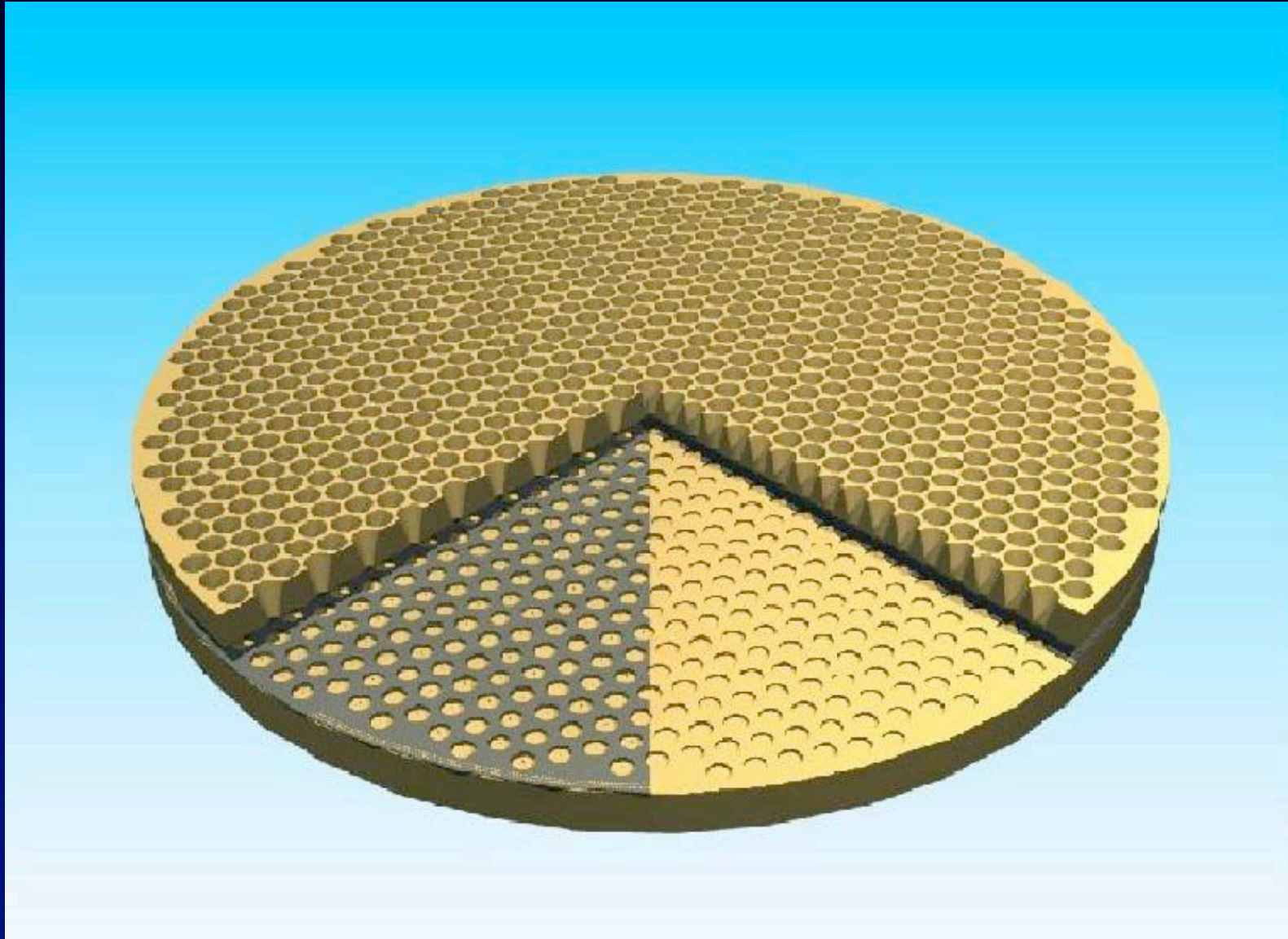
- CMB experiments: state of the art
- Open problems : how to attack them with CMB
- Enabling technologies
- High angular resolution CMB anisotropy
- The spectrum of CMB anisotropy
- The polarization of CMB

Improvement in sensitivity

- Anisotropy signals: $80 \mu\text{K rms}$
- E-Polarization: $3 \mu\text{K rms}$
- B-Polarization: $< 0.1 \mu\text{K rms}$
- Recombination lines $< 0.05 \mu\text{K}$
- CMB anisotropy detectors are close to be limited by the photon noise of the CMB (e.g. the bolometers in the CMB channels of Planck-HFI will be in CMB BLIP)
- In these conditions, the only way to improve the efficiency of an experiment, is to multiply the number of detectors in the focal plane, to improve the mapping speed.
-  need for large format arrays

Large Bolometer Arrays

- > 1000 TES bolometers for the South Pole Telescope devoted to SZ (Adrian Lee, Berkeley)

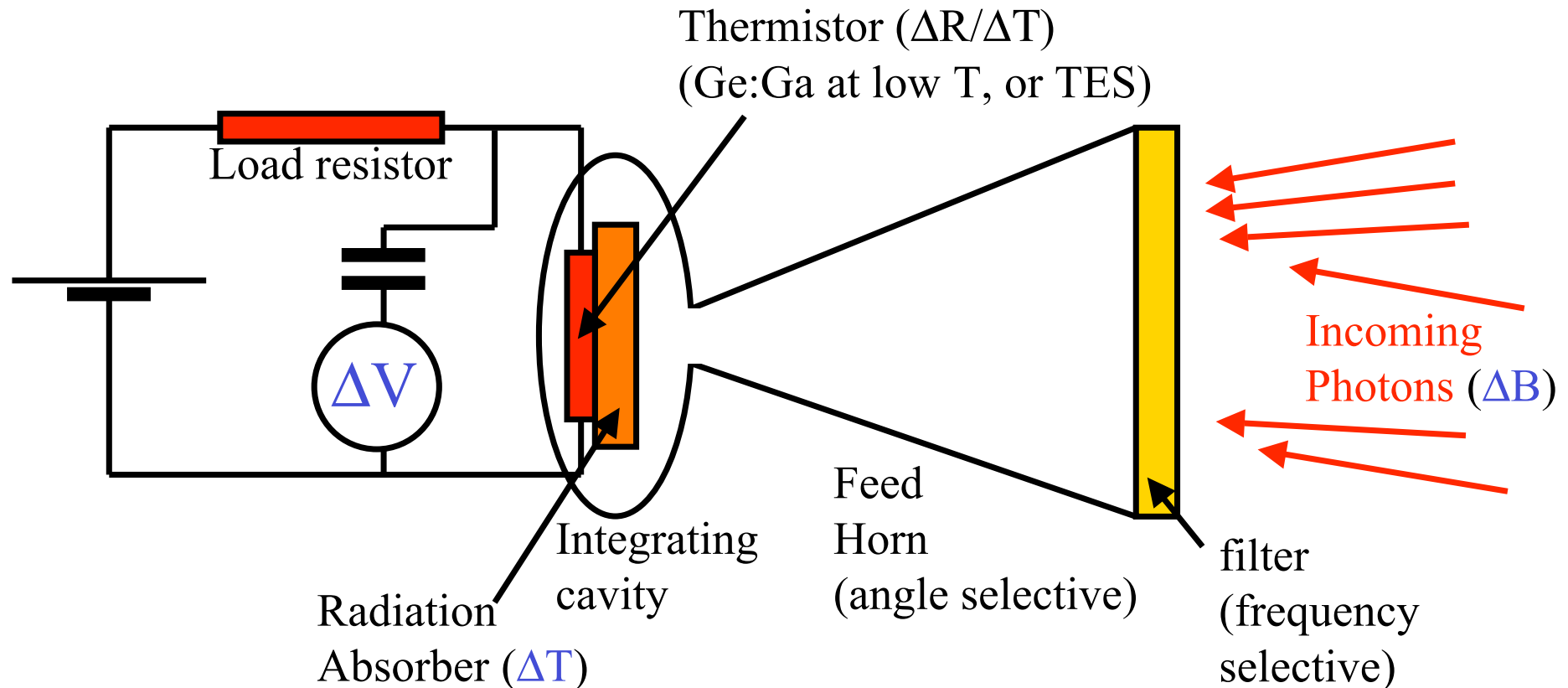


Competing technologies

- CMB brightness peak: 159 GHz
 - High frequency for coherent detectors
(antenna + amplifier + rectifier) work at 20 K
 - Low frequency for thermal detectors
(absorber + thermistor) work at 0.3-0.1 K
- Search for a **scalable** technology (replicate the sensor in an array with several thousand elements) a big step forward with respect to current technology.
- Radiometers on-a-chip (MMICs, hear about QUIET)
- TES (transition edge superconductor sensors)
- KIDs (kinetic inductance detectors)
- CEBs (cold electrons bolometers)

Cryogenic Bolometers

- The most sensitive broad band detectors for FIR & mm-waves.



- Fundamental noise sources are Johnson noise in the thermistor ($\langle \Delta V^2 \rangle = 4kTR\Delta f$), temperature fluctuations in the thermistor ($\langle \Delta W^2 \rangle = 4kGT^2\Delta f$), background radiation noise (T_{bkg}^5) need to reduce the temperature of the detector and the radiative background.

Cryogenic Bolometers

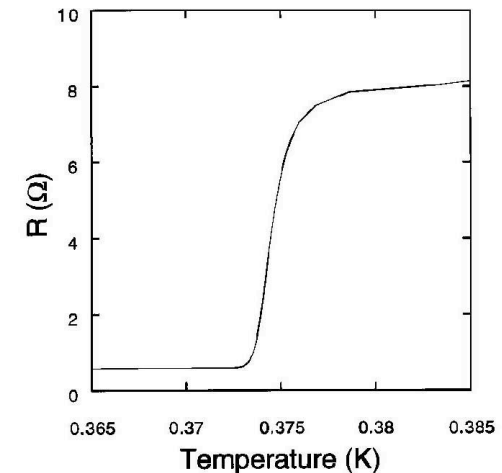
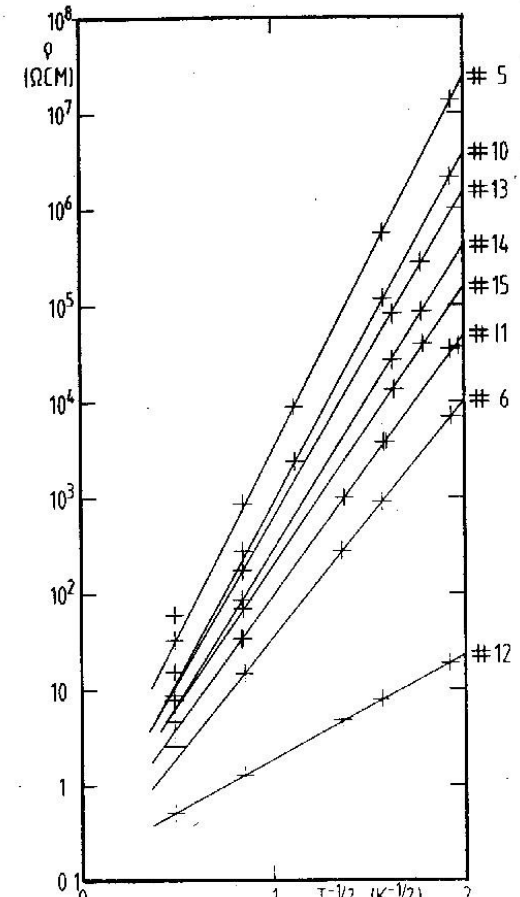
$$\alpha = \frac{1}{R(T)} \frac{dR(T)}{dT}$$

$$\mathfrak{R} = \frac{i\alpha R}{G_{eff} \sqrt{1 + \tau^2 \omega^2}}$$

- A large α is important for high responsivity.

- Ge thermistors: $\frac{\alpha}{T} \approx -10K^{-1}$

- Superconducting transition edge thermistors: $\frac{\alpha}{T} \approx 1000K^{-1}$



Spider-Web Bolometers

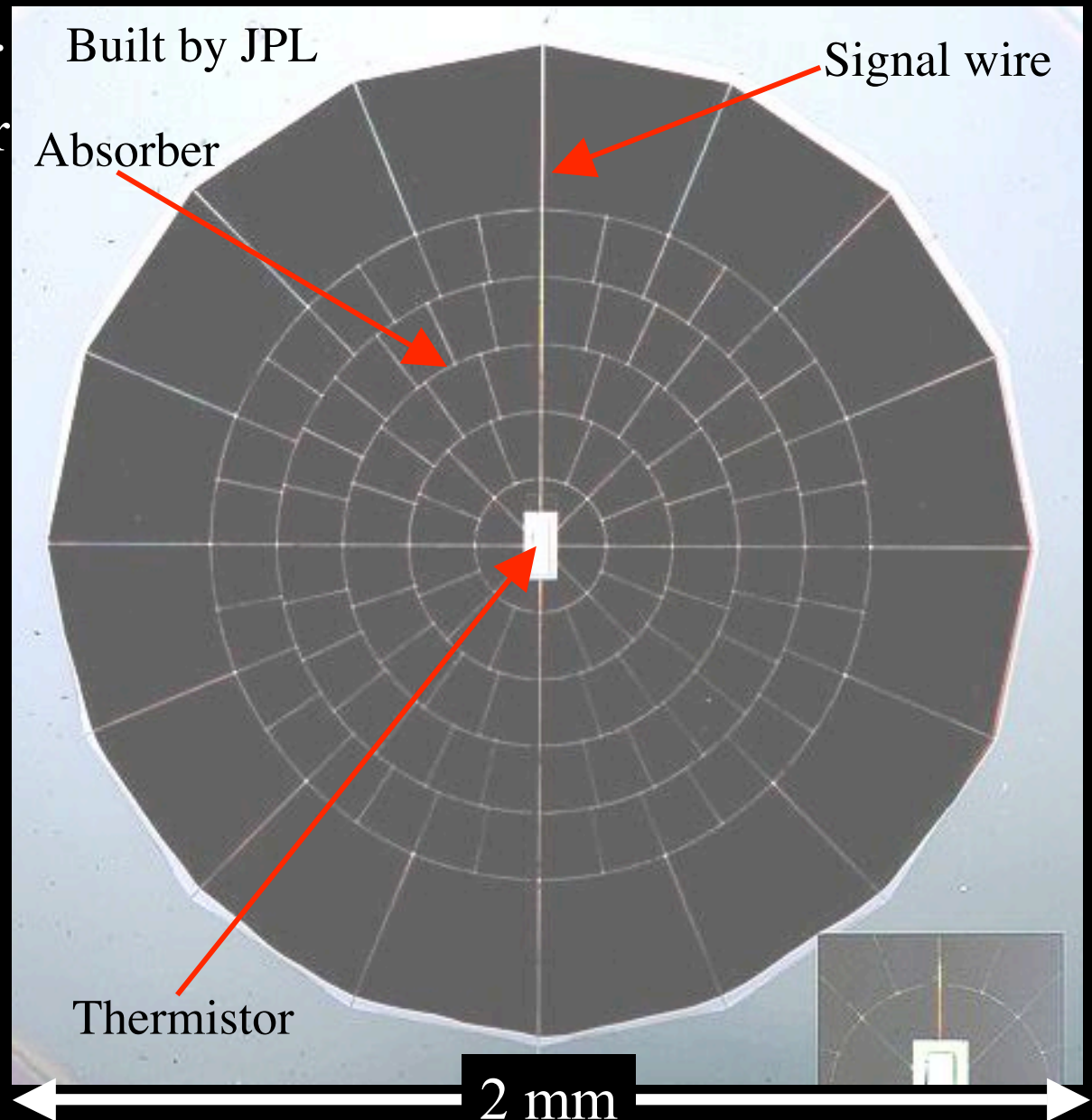
- The absorber is micro machined as a web of metallized Si_3N_4 wires, $2\ \mu\text{m}$ thick, with $0.1\ \text{mm}$ pitch.

- This is a good absorber for mm-wave photons and features a very low cross section for cosmic rays. Also, the heat capacity is reduced by a large factor with respect to the solid absorber.

- NEP $\sim 2 \cdot 10^{-17}\ \text{W}/\text{Hz}^{0.5}$ is achieved @0.3K

- $150\ \mu\text{K}_{\text{CMB}}$ in 1 s

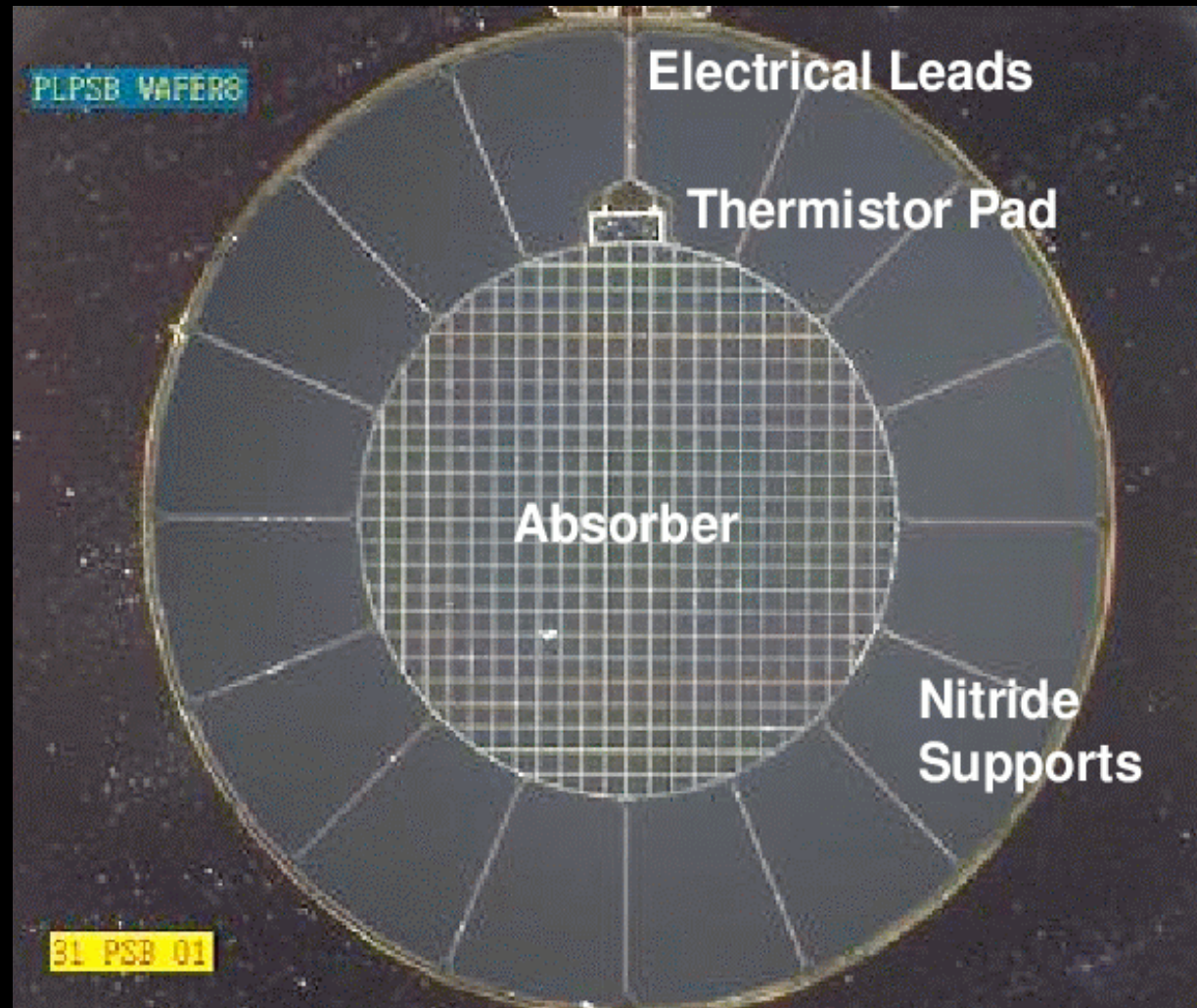
- Mauskopf *et al.* Appl.Opt. **36**, 765-771, (1997)



Polarization-sensitive version

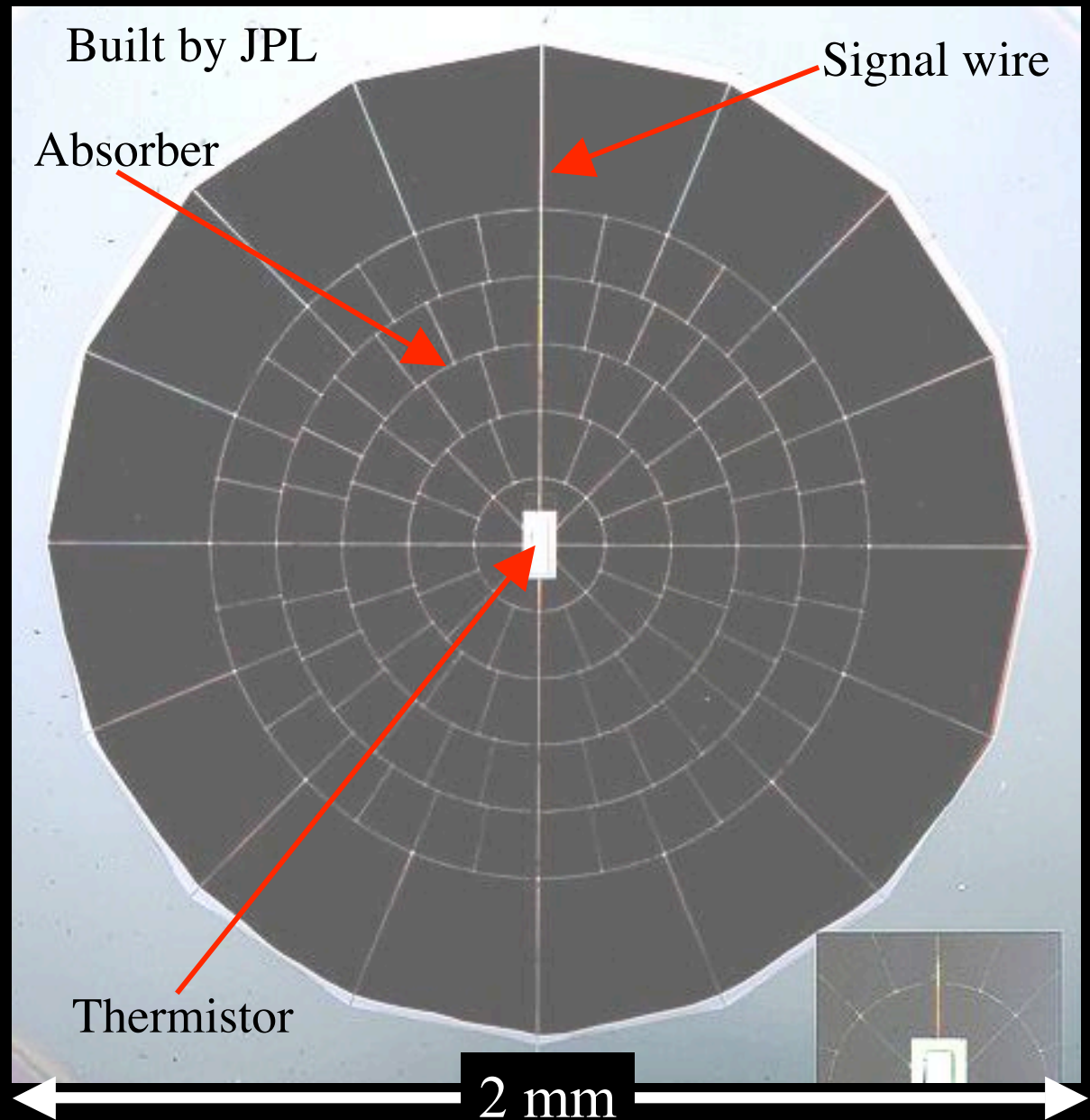
3 μm thick
wire grids,
Separated by
60 μm , in the
same groove
of a circular
corrugated
waveguide

Planck-HFI



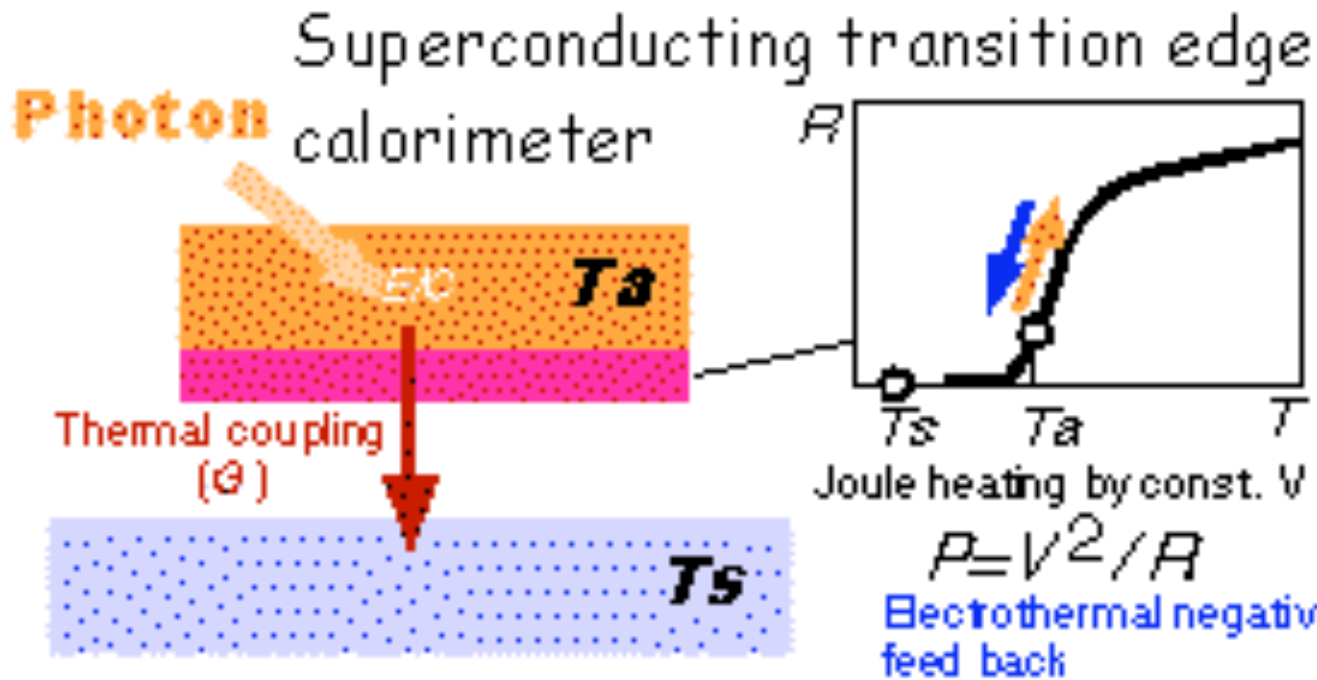
Spider-Web Bolometers

- Used in BOOMERanG, MAXIMA, ARCHEOPS, ACBAR, Planck-HFI, ...
- and, in array form, in BOLOCAM (140 pixels)
- This is a composite system: the thermistor (Ge) is glued on the absorber (Si).
- Assembly basically by hand (and critical). Yield around 70% (see e.g. BOLOCAM).
- Not suitable for thousands of elements.

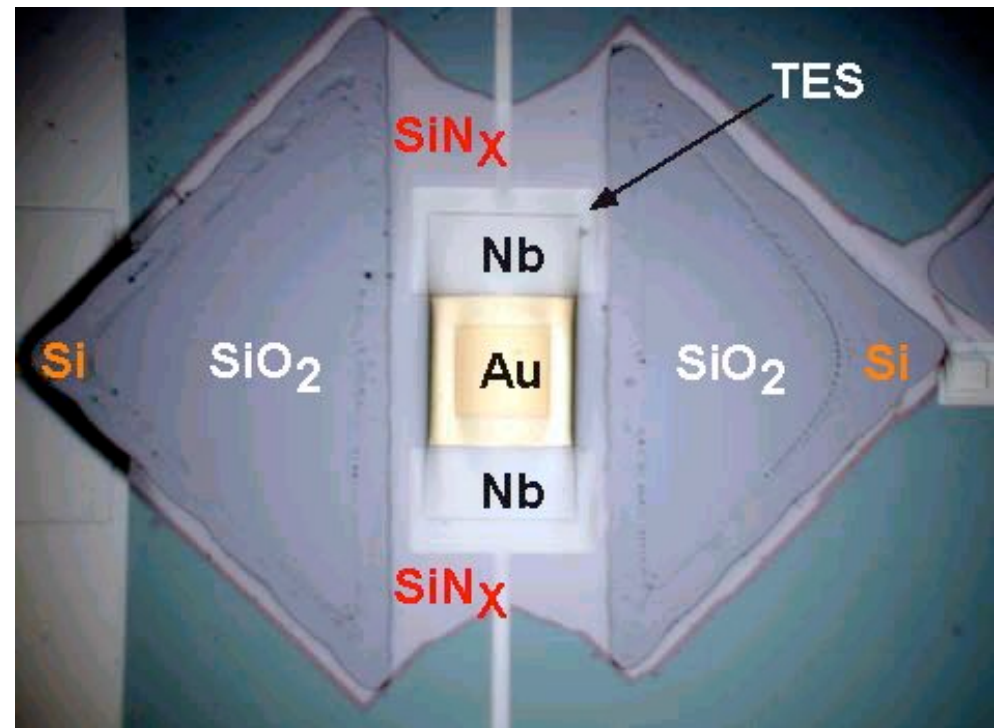
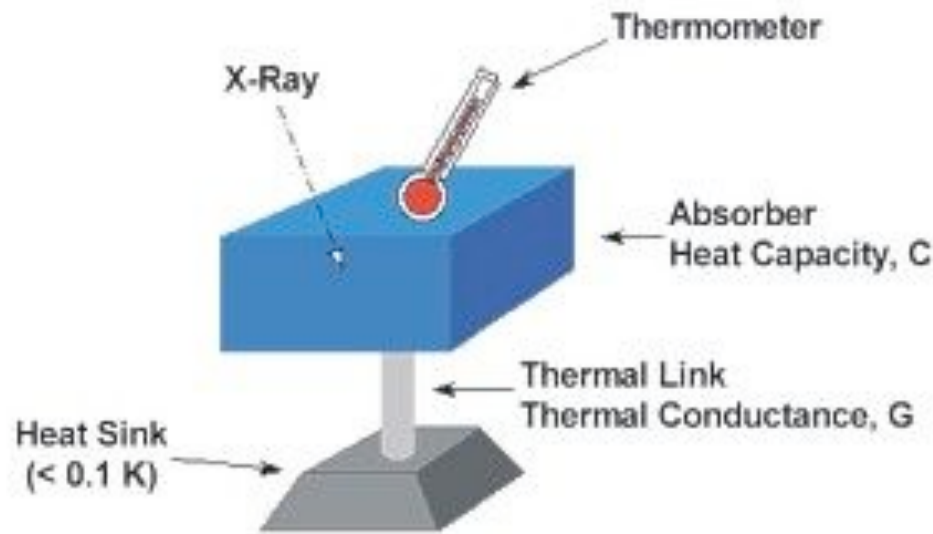


Transition Edge Sensors

- TES can be evaporated on the Si substrate.
- This makes automated construction possible, even if through a very complex process (9-10 masks, and very different materials: Si, Si Nitride, Au, Nb, ...)
- Low impedance of the TES implies
 - Low microphonics
 - Voltage-biased autocalibrated detectors (responsivity $1/V$ in the extreme electrothermal feedback limit EETFL)
 - Improvement in time constant (in EETFL)
- but requires
 - Low impedance amplifier (SQUID amperometer almost ideal)
 - Extremely careful magnetic shielding



Baseline detectors for CMB missions and for X-ray spectroscopy missions



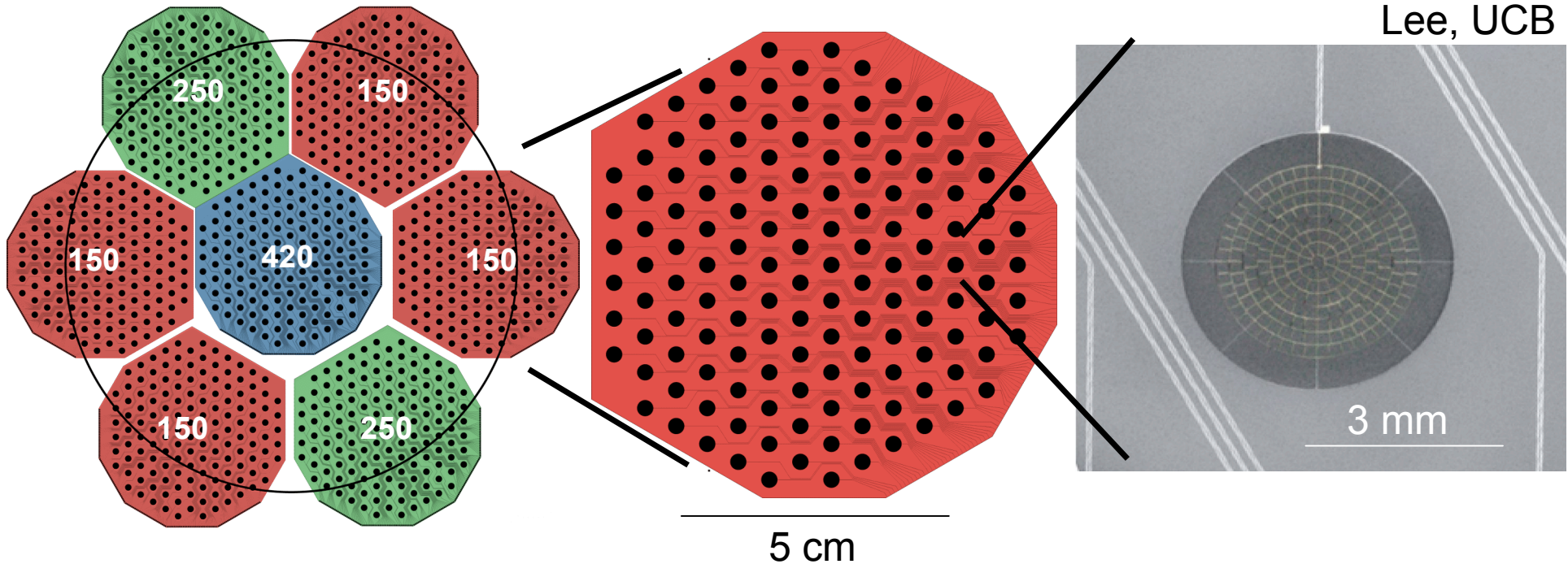


EBEX Focal Plane

738 element array

141 element hexagon

Single TES

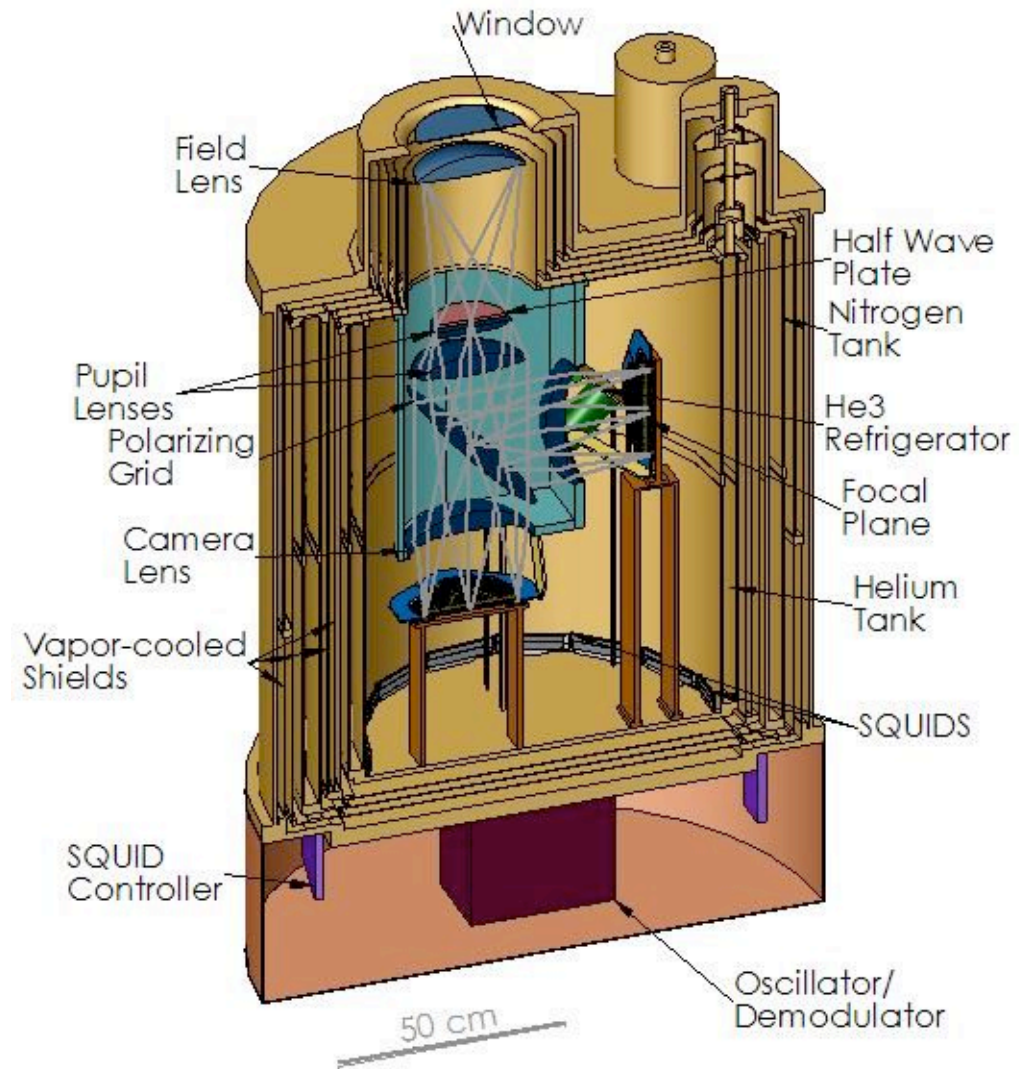
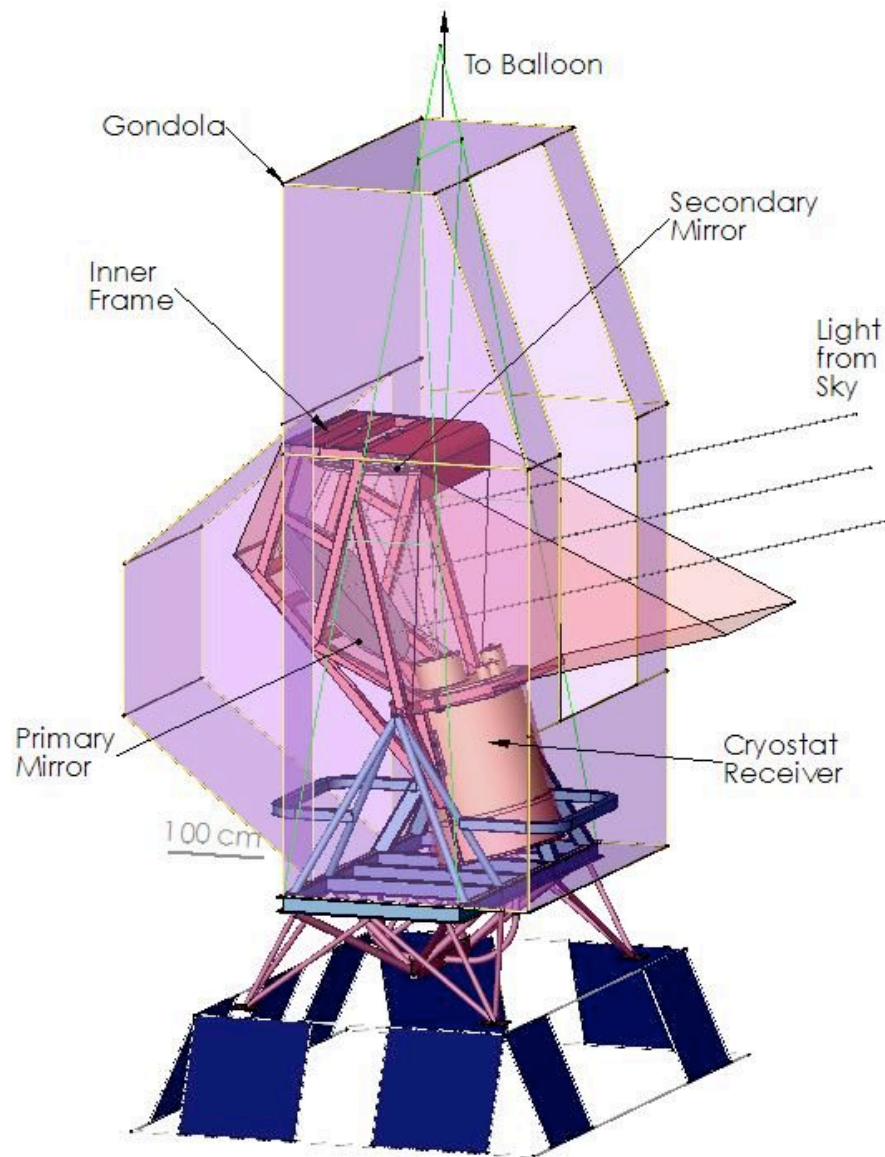


- Total of 1476 detectors
- Maintained at 0.27 K
- 3 frequency bands/focal plane

- $G=15-30$ pWatt/K
- $NEP = 1.4e-17$ (150 GHz)
- $NEQ = 156 \mu K * rt(sec)$ (150 GHz)
- $\tau = 3$ msec,



EBEX Design



Slide: Hanany

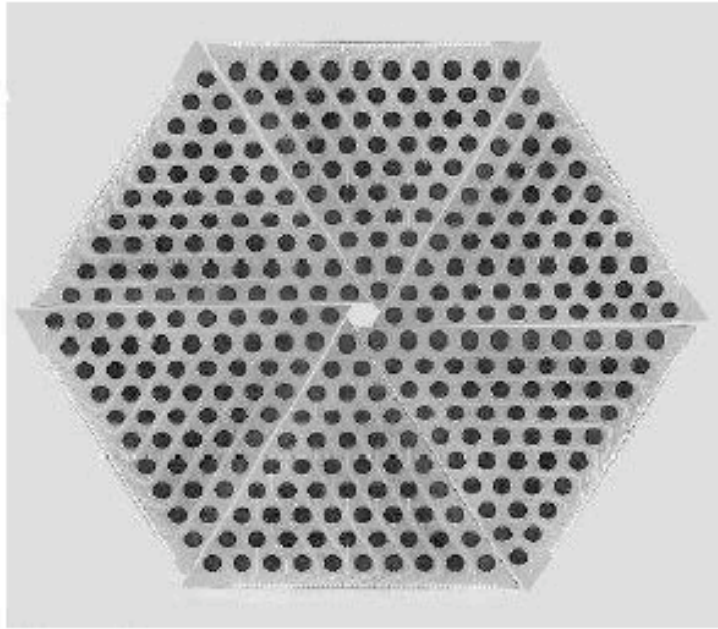


Figure 4. Montage image of a single 55-element TES spider bolometer wedge to show how an array of six identical wedges would look. The complete prototype array will have 330 bolometers and be 12 cm in diameter.

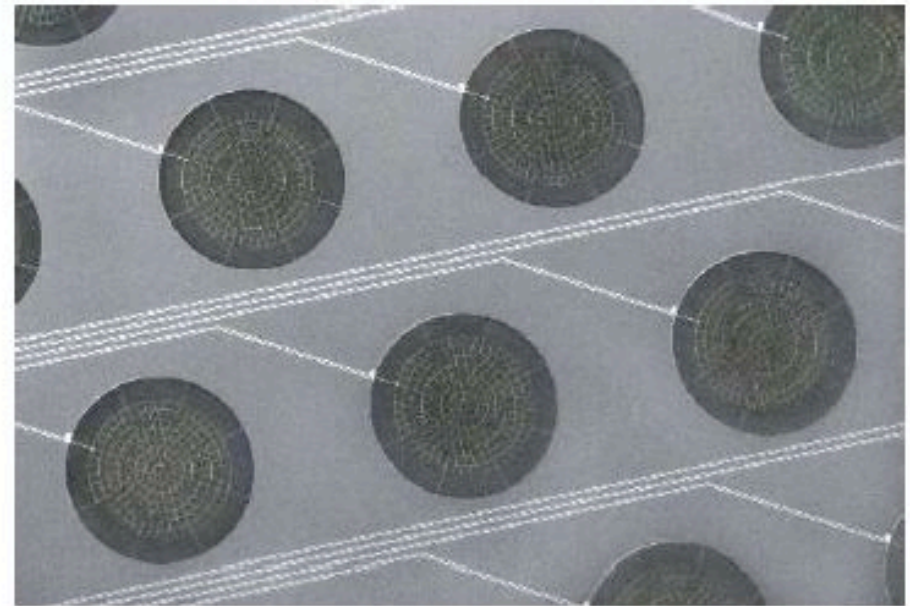
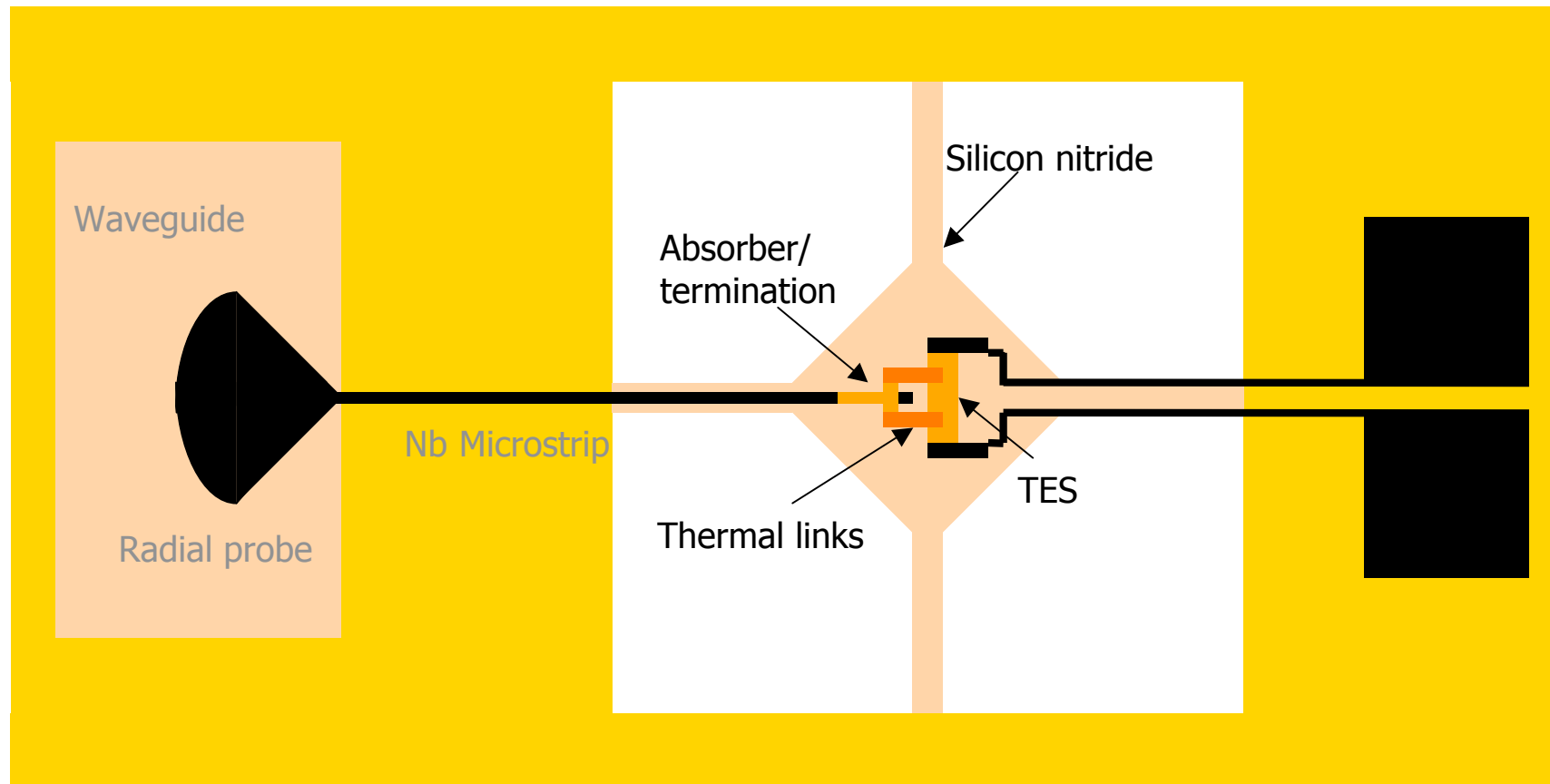


Figure 5. Close up of a 55 element bolometer wedge. The sensors are constructed with an Al/Ti proximity effect sandwich. Webs are metalized with gold for microwave absorption. Suspended spider-web absorbers are fabricated from 1 μm thick silicon nitride. The membrane is released from the front side using a gaseous xenon difluoride etch. Bolometers are 5 mm diameter with 0.5 mm long legs. Wiring layer is superconducting aluminum. This array was fabricated in the U.C. Berkeley microfabrication facility.

ν_0 (GHz)	$\Delta\nu$ (GHz)	T	P_o (pW)	G (pW/K)	NET _{RJ} ($\mu\text{K}\sqrt{\text{s}}$)	NET _{CMB} ($\mu\text{K}\sqrt{\text{s}}$)	θ_{fwhm} (arcmin)	NEFD (mJy $\sqrt{\text{s}}$)
95	24	0.964	8.1	2×10^{-10}	221	278	1.58	14.6
150	38	0.982	10.8	2×10^{-10}	150	259	1.00	9.9
219	35	0.969	11.0	2×10^{-10}	184	551	0.69	12.2
274	67	0.950	24.5	4×10^{-10}	159	774	0.56	10.5

PROTOTYPE SINGLE PIXEL - 150 GHz (Mauskopf)

Schematic:



Similar to JPL design, Hunt, et al., 2002 but with waveguide coupled antenna

- TES arrays are being prepared for

<ul style="list-style-type: none">– South Pole Telescope– APEX (Atacama)– ACT (Atacama)– IRAM 30m dish (Pico Veleta)– PolarBear (White Mountain)	Large Dishes
<ul style="list-style-type: none">– EBEX– SPIDER– OLIMPO	Balloons

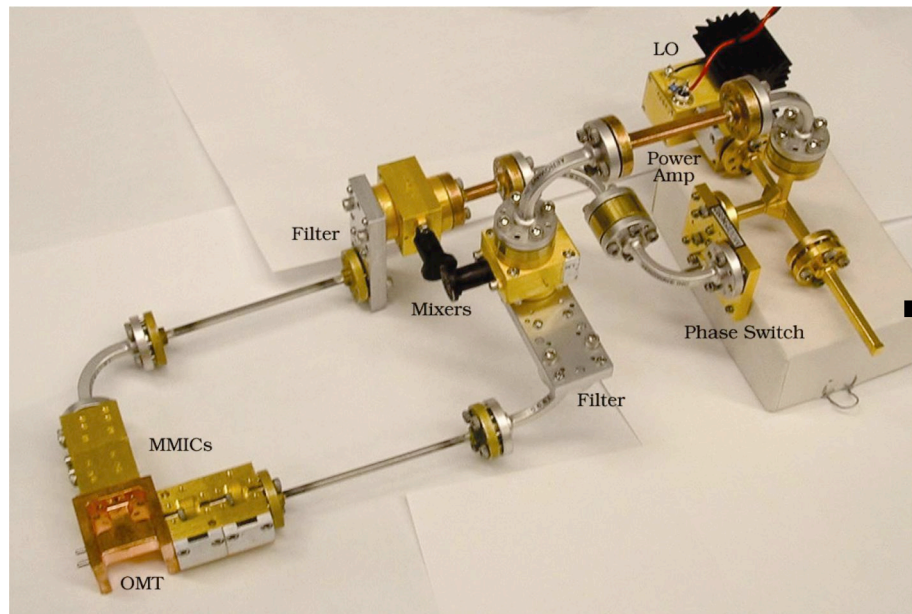
–

- The readout system for TESs requires SQUIDs and is very complex.

- KIDs (see e.g. Zmuidzinas, Caltech) represent a good alternative because are intrinsically multiplexable
- Cold electron bolometers (e.g. Kuzmin, Chalmers) represent a good alternative because the readout system is much simpler

Breakthrough in MMIC Packaging makes arrays of coherent receiver possible

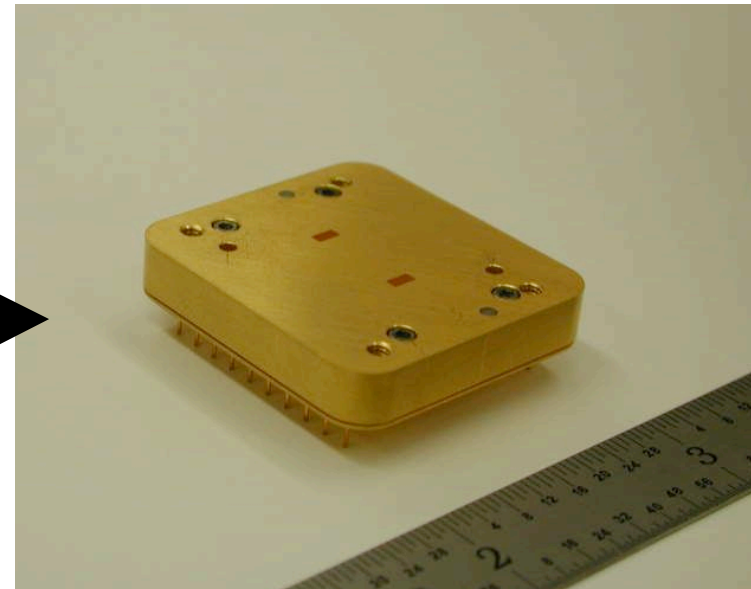
CAPMAP 90 GHz Polarimeter



X-Y Polarizer

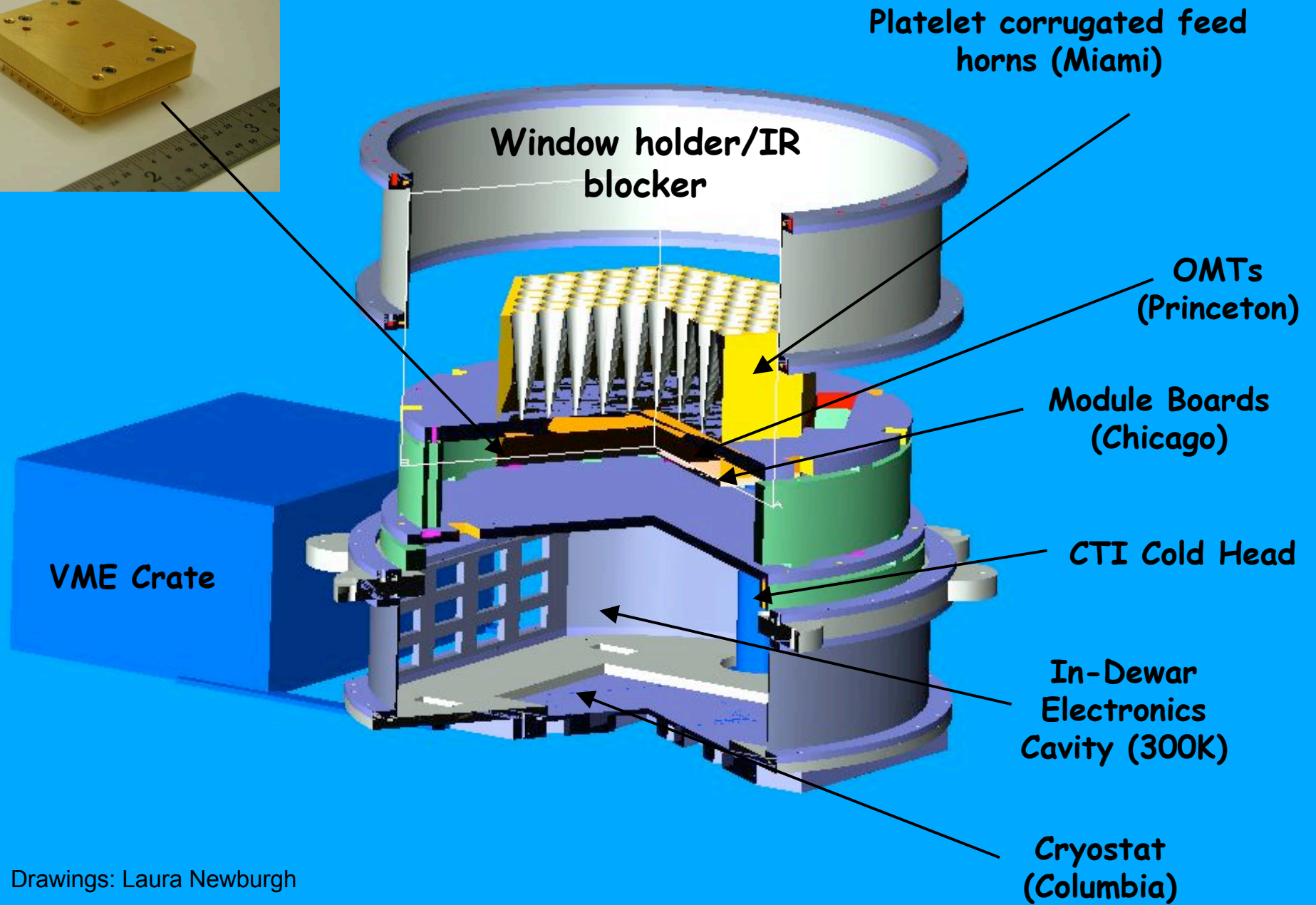
~ \$40K and 50 physicist-hours for checking, characterizing, etc

QUIET Polarimeter IC



~ \$500 and automated assembly and test, completely scalable

QUIET Modules (JPL)



Drawings: Laura Newburgh

contents

- CMB experiments: state of the art
- Open problems : how to attack them with CMB
- Enabling technologies
- High angular resolution CMB anisotropy
- The spectrum of CMB anisotropy
- The polarization of CMB

High Angular Resolution CMB (with spectral capabilities)

- Damping tail (parameters)
- Sunyaev-Zeldovich effect (clusters and nature of dark matter)
- Ostriker Vishniac effect (reionization)
- Metals during reionization
-

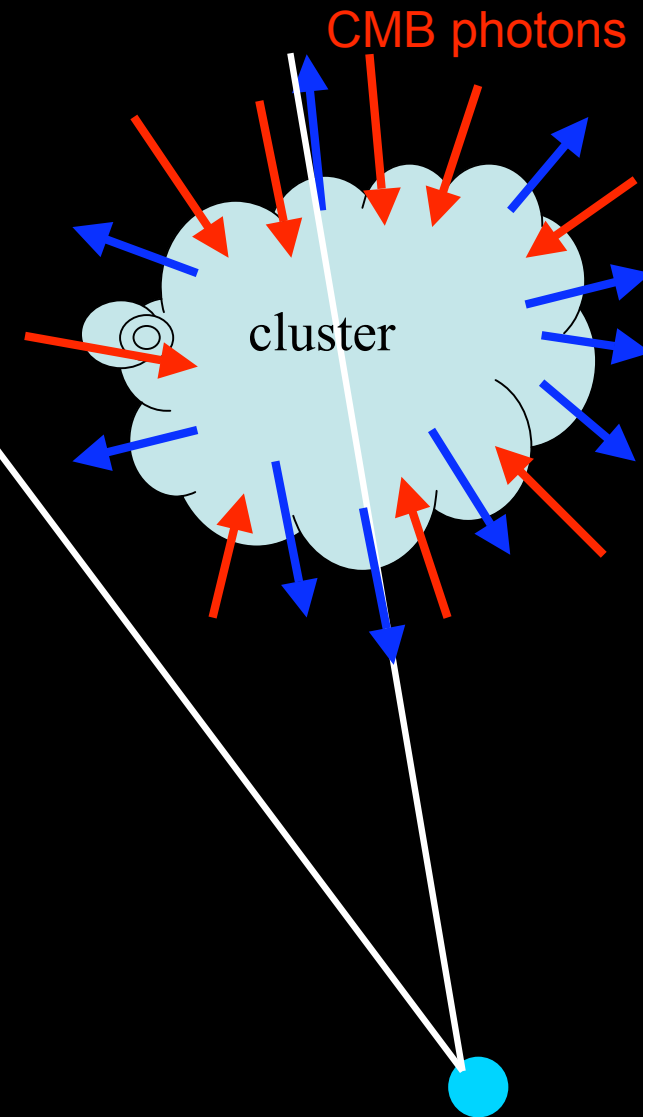
S-Z

- Inverse Compton Effect for CMB photons against charged particles in the hot gas of clusters
- Cluster optical depth: $\tau = n\sigma l$
 - $l = \text{a few Mpc} = 10^{25} \text{ cm}$
 - $n < 10^{-3} \text{ cm}^{-3}$
 - $\sigma = 6.65 \times 10^{-25} \text{ cm}^2$
- So $\tau = n\sigma l < 0.01$: there is a 1% likelihood that a CMB photon crossing the cluster is scattered by an electron
- $E_{\text{electron}} \gg E_{\text{photon}}$, so the electron gives part of his energy to the photon. To first order, the energy gain of the photon is

$$\frac{\Delta\nu}{\nu} = \frac{kT_e}{m_e c^2} \approx \frac{5 \text{ keV}}{500 \text{ keV}} = 0.01$$

- The resulting CMB temperature anisotropy is

$$\frac{\Delta T}{T} \approx \tau \frac{\Delta\nu}{\nu} \approx 0.01 \times 0.01 = 10^{-4}$$



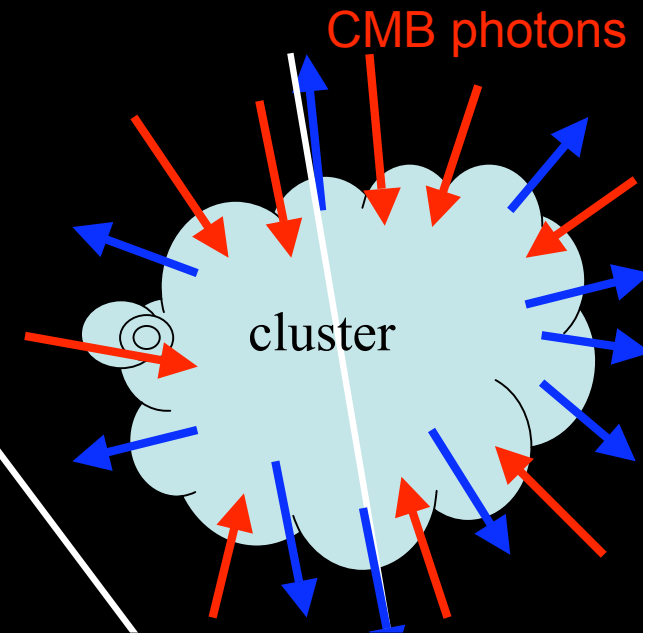
S-Z

- Inverse Compton Effect for CMB photons against charged particles in the hot gas of clusters
- Cluster optical depth: $\tau = n\sigma l$
 $l = \text{a few Mpc} = 10^{25} \text{ cm}$
 $n < 10^{-3} \text{ cm}^{-3}$
 $\sigma = 6.65 \times 10^{-25} \text{ cm}^2$
- So $\tau = n\sigma l < 0.01$: there is a 1% likelihood that a CMB photon crossing the cluster is scattered by an electron
- $E_{\text{electron}} \gg E_{\text{photon}}$, so the electron gives part of his energy to the photon. To first order, the energy gain of the photon is

$$\frac{\Delta\nu}{\nu} = \frac{kT_e}{m_e c^2} \approx \frac{5 \text{ keV}}{500 \text{ keV}} = 0.01$$

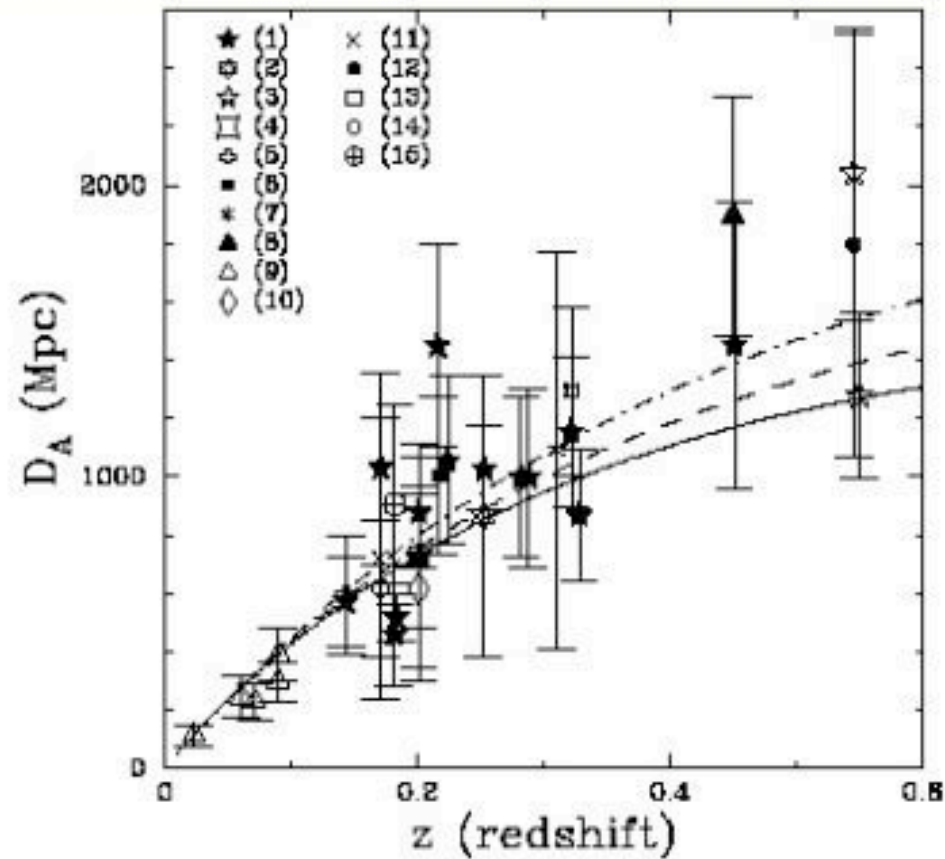
- The resulting CMB temperature anisotropy is

$$\frac{\Delta T}{T} \approx \tau \frac{\Delta\nu}{\nu} \approx 0.01 \times 0.01 = 10^{-4}$$



The ΔT does not depend on the distance of the cluster !

current status of angular diameter distance determinations



H_0
 Λ

Figure 11: SZE determined distances versus redshift. Also plotted is the theoretical angular diameter distance relation for three different cosmologies, assuming $H_0 = 60 \text{ km s}^{-1} \text{ Mpc}^{-1}$. References: (1) [97], (2) [75], (3) [87], (4) [85], (5) [90], (6) [98], (7) [77], (8) [91], (9) [99, 70, 59], (10) [100], (11) [101], (12) [102], (13) [76], (14) [103], and (15) [58].

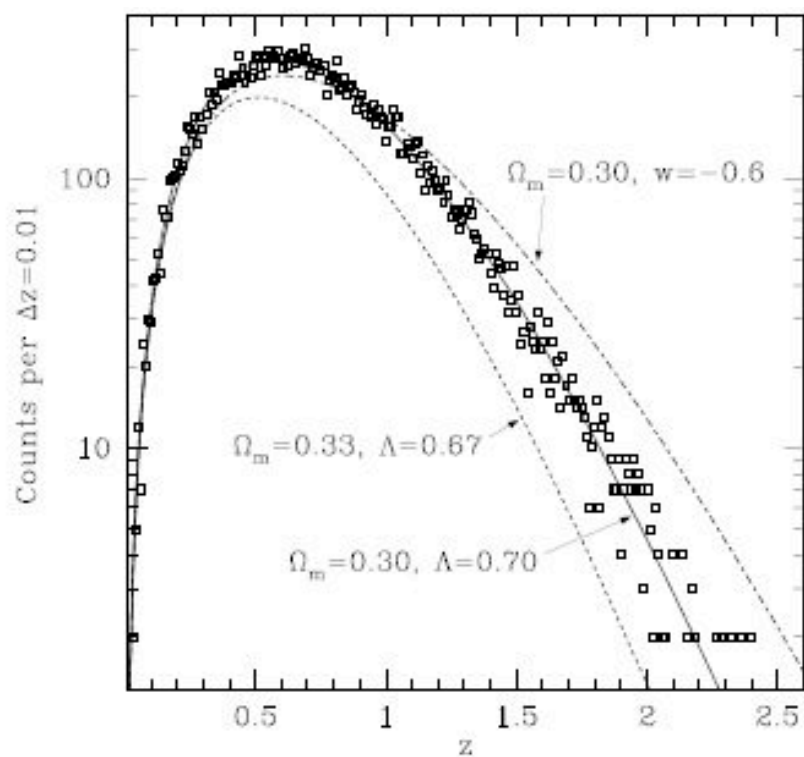


Figure 11. An illustration of the effect of cosmology on the expected number of SZE detected galaxy clusters as a function of redshift. The data points are appropriate for a 4000 square degree SPT survey with idealized sensitivity. The data points and the line passing through them were generated assuming a canonical $\Omega_M = 0.3$, $\Omega_\Lambda = 0.7$, $\sigma_8 = 1$ cosmology. The other two lines show the large effect in the expected cluster counts due to slight changes in the cosmology. The value of σ_8 was adjusted to give the same normalization for the local cluster abundance in each model. The bottom curve is for a model with more matter and correspondingly less dark energy. The top curve at shows the effect of only a change in the equation of state of the dark energy in the canonical model. (Figure courtesy of G. Holder)

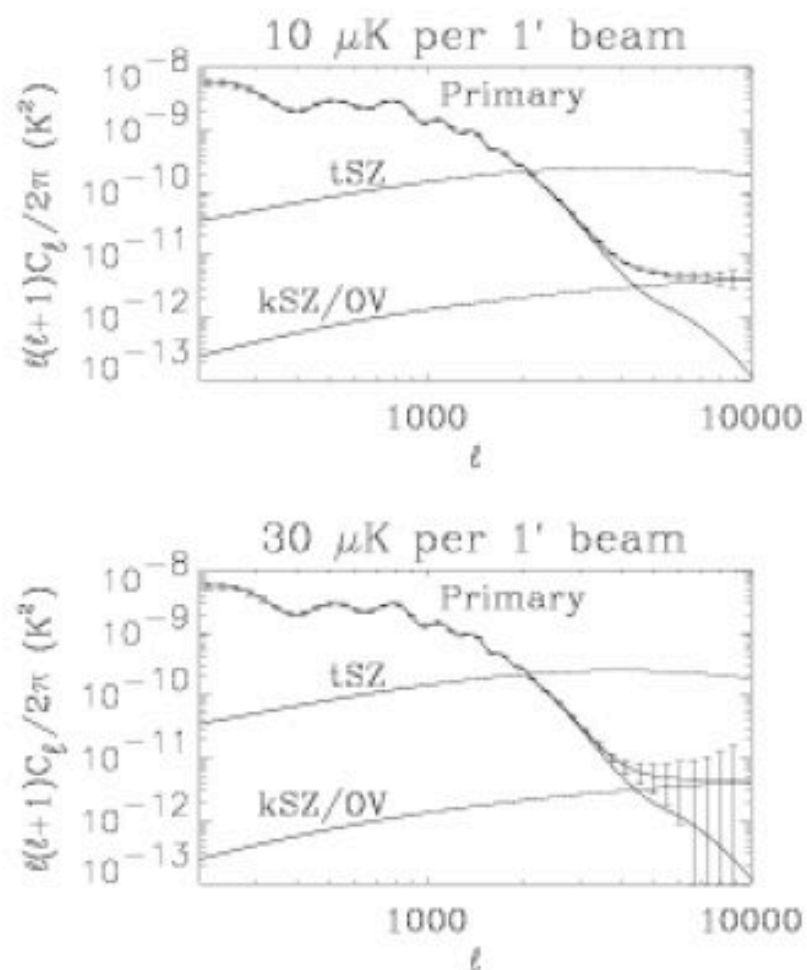
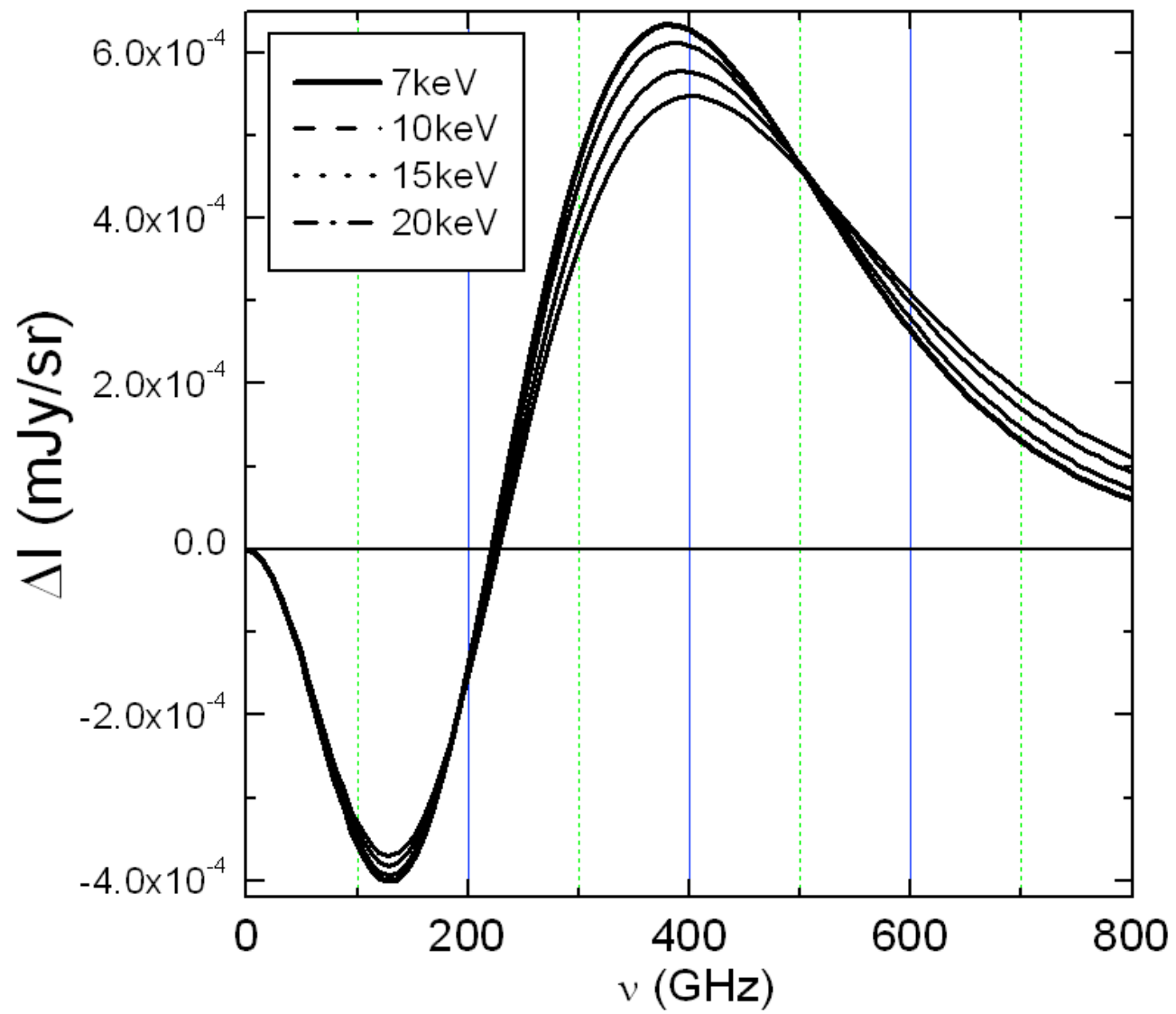
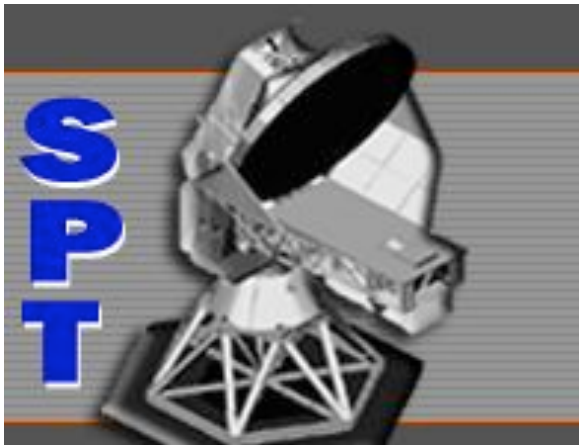


Figure 12. An illustration of the potential of the SPT to measure fine-scale CMB anisotropy. The two panels show statistical errors on the high- ℓ CMB power spectrum from 500 deg^2 of sky measured at two different levels of noise per 1' beam. Both panels assume perfect subtraction of the thermal SZE signal and other astrophysical contaminants; achieving the required accuracy in this subtraction will be a significant challenge. (Spectra courtesy of W. Hu.)





10 m diameter, f/07 primary
90-270 GHz
arcmin resolution
1000 detectors

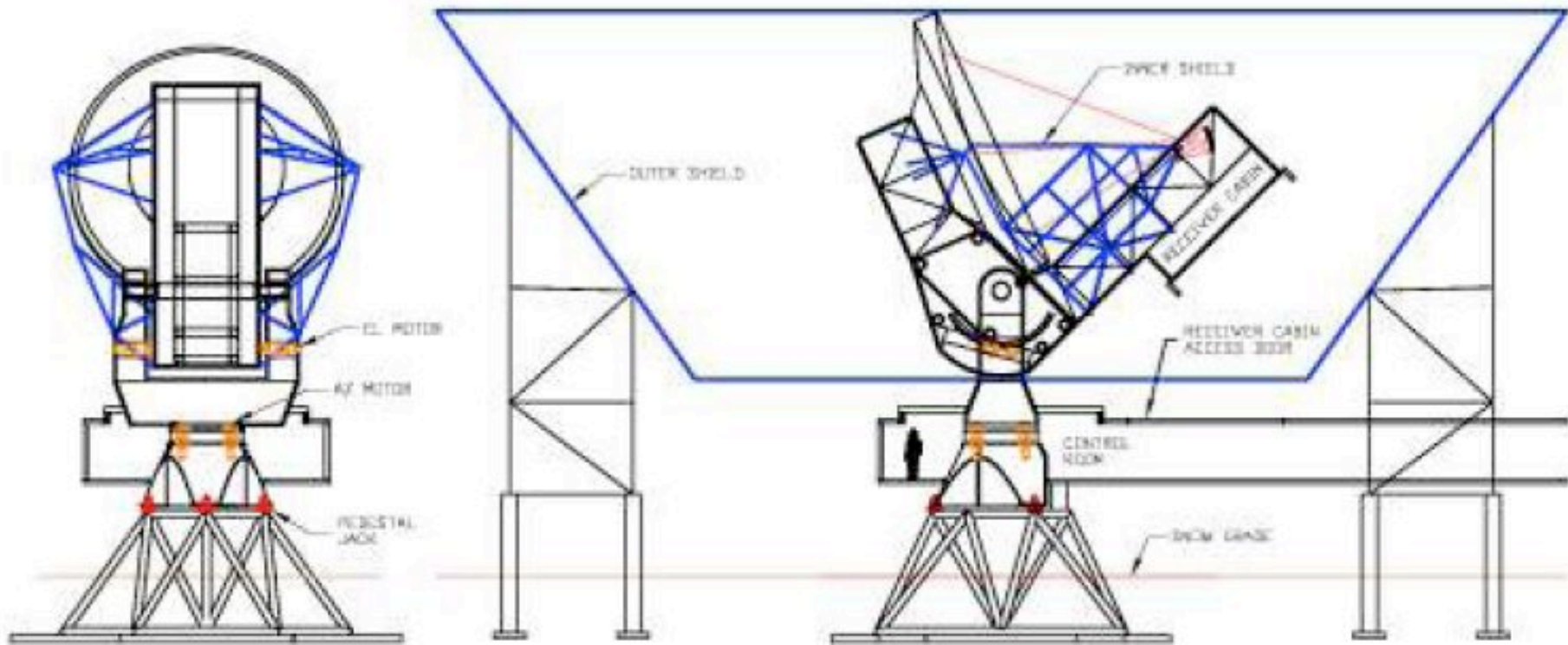
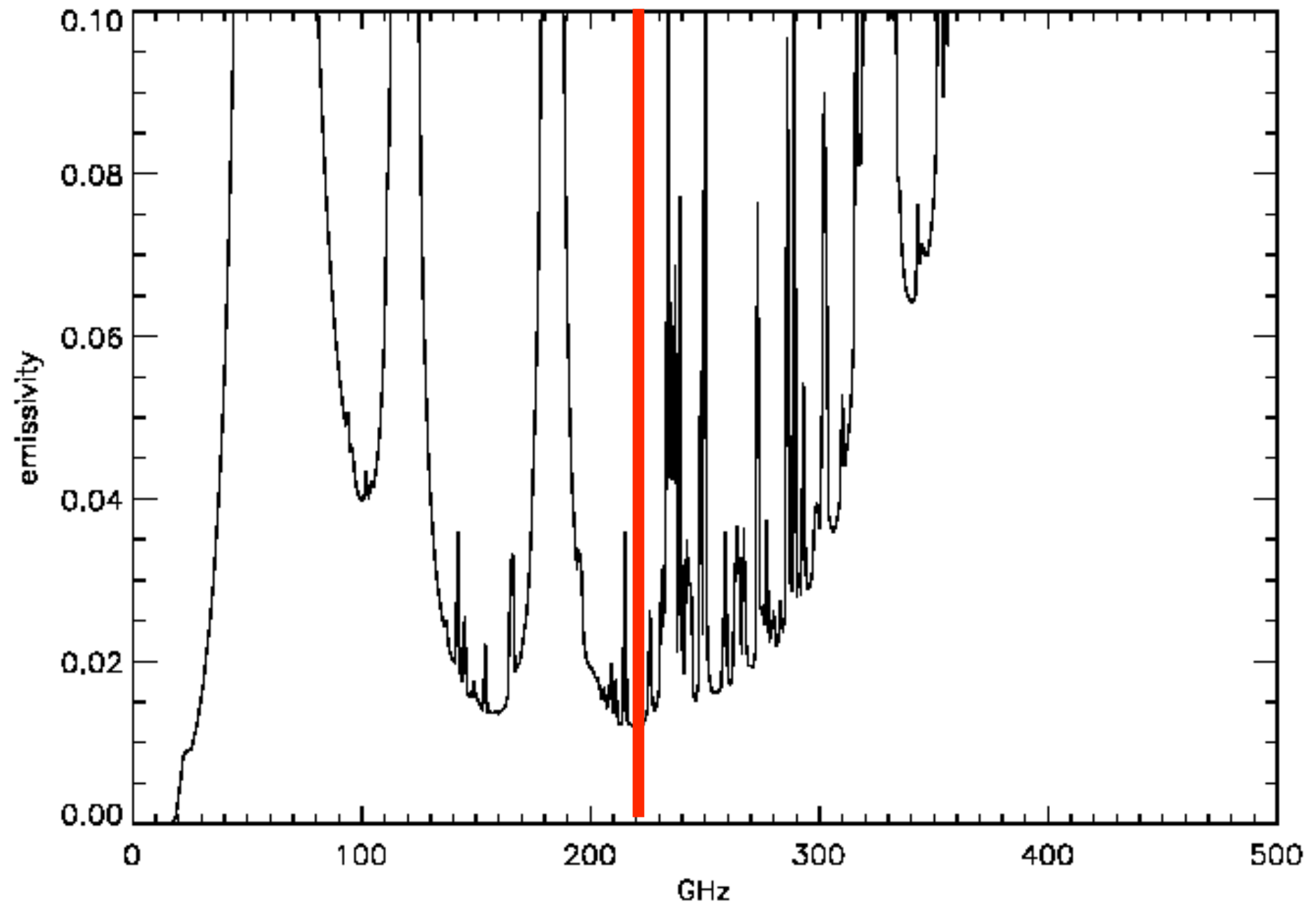


Figure 1. (Left) rear view of the SPT at elevation 0°, and (right) side view at elevation 45° with the outer ground shield.

0.5mm PWV



(<http://oberon.roma1.infn.it/olimpo>)

OLIMPO

**An arcmin-resolution
survey of the sky
at mm and sub-mm
wavelengths**



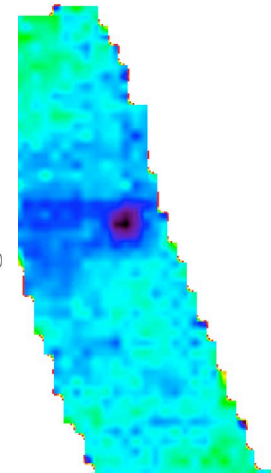
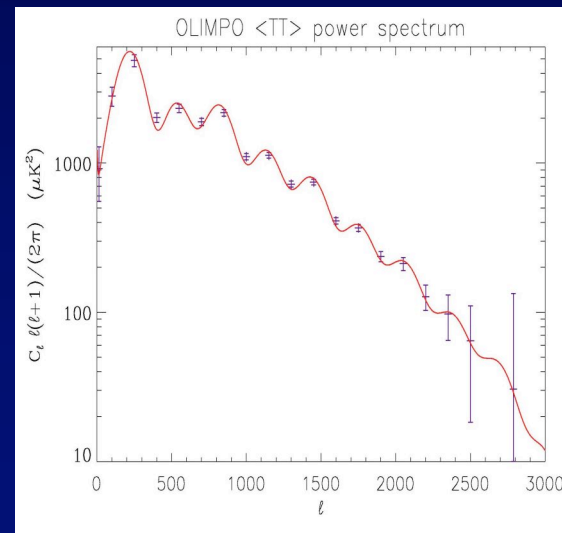
Silvia Masi
Dipartimento di Fisica
La Sapienza, Roma

and

the OLIMPO team

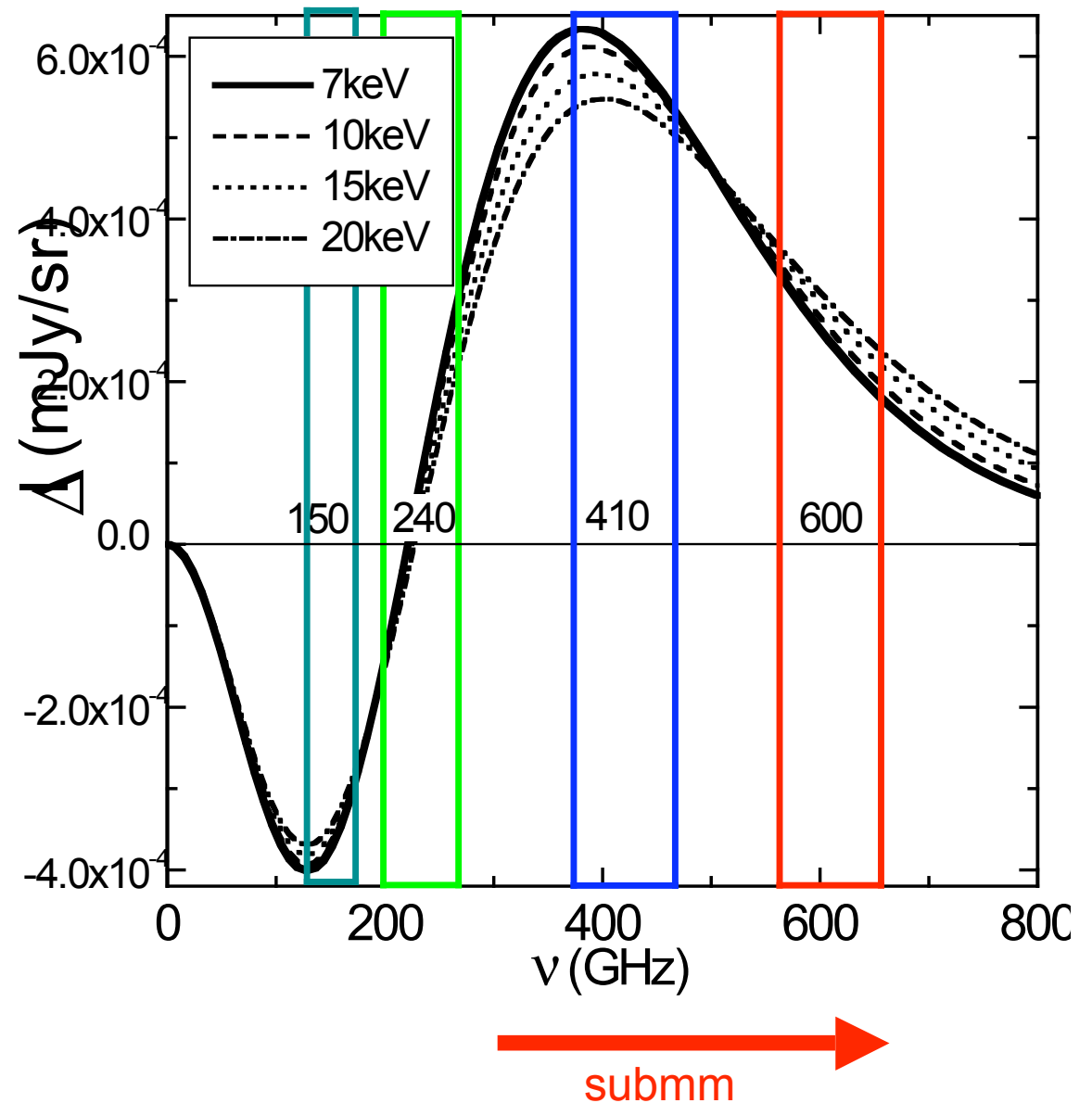
Large Bolometer Arrays

- >400 TES bolometers for the OLIMPO balloon telescope devoted to SZ and CMB anisotropy (Silvia Masi, Roma)



The uniqueness of OLIMPO

- OLIMPO measures in 4 frequency bands simultaneously. These bands optimally sample the spectrum of the SZ effect.
- This allows us to clean the signal from any dust and CMB contamination, and even to measure T_e by means of the relativistic corrections.



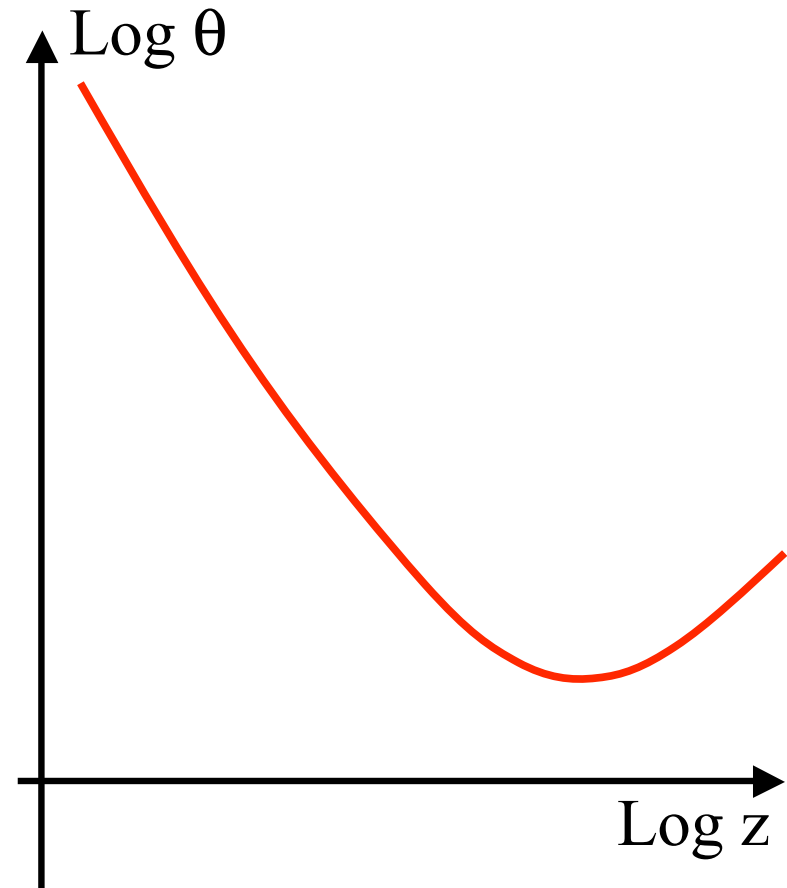
Detailed simulations show that:

- For a
 - $Y=10^{-5}$ cluster,
 - in a dust optical depth of 10^{-5} @ 1 mm,
 - In presence of a 100 μK CMB anisotropy
- In 2 hours of integration over 1 square degree of sky centered on the cluster
 - Y can be determined to $\pm 10^{-6}$,
 - ΔT_{CMB} can be measured to $\pm 10\mu\text{K}$
 - T_e can be measured to $\pm 3\text{keV}$
- OLIMPO WILL MAP 40 OF THESE CLUSTERS, IN A SINGLE, LONG DURATION, POLAR FLIGHT

Angular Diameter Distance

$$D_A = \frac{1}{(1+z)} \frac{c}{H_o} \int_{\frac{1}{(1+z)}}^1 \frac{d\hat{a}}{\hat{a}^2 [\Omega_{Ro} \hat{a}^{-4} + \Omega_{Mo} \hat{a}^{-3} + \Omega_{\Lambda} + (1 - \Omega_o) \hat{a}^{-2}]^{1/2}}$$

- For a 1 Mpc structure, the minimum angular size is 3.8 arcmin
- @ z of the order of 1



Dynamically Relaxed Clusters

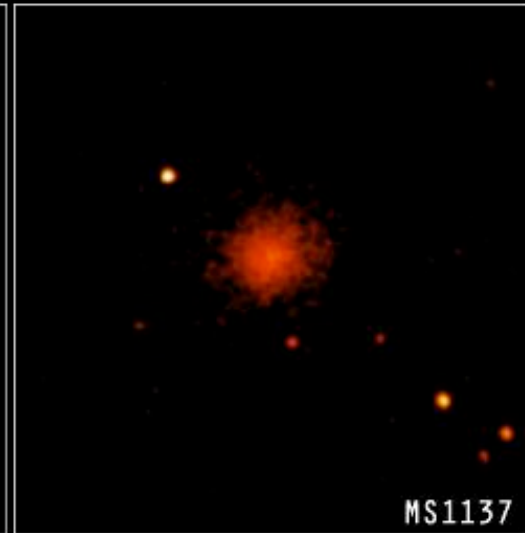
X-ray
Images
(Chandra)



D = 1 GLy

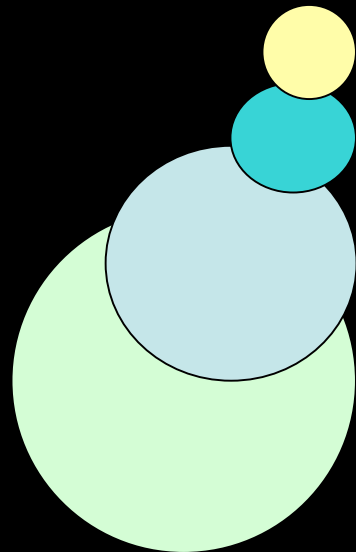


3.5 GLy



6.7 GLy

OLIMPO



0.9' FWHM beam ($\lambda = 0.54$ mm D = 2600 mm)

1.1' FWHM beam ($\lambda = 0.73$ mm D = 2600 mm)

2.2' FWHM beam ($\lambda = 1.4$ mm D = 2600 mm)

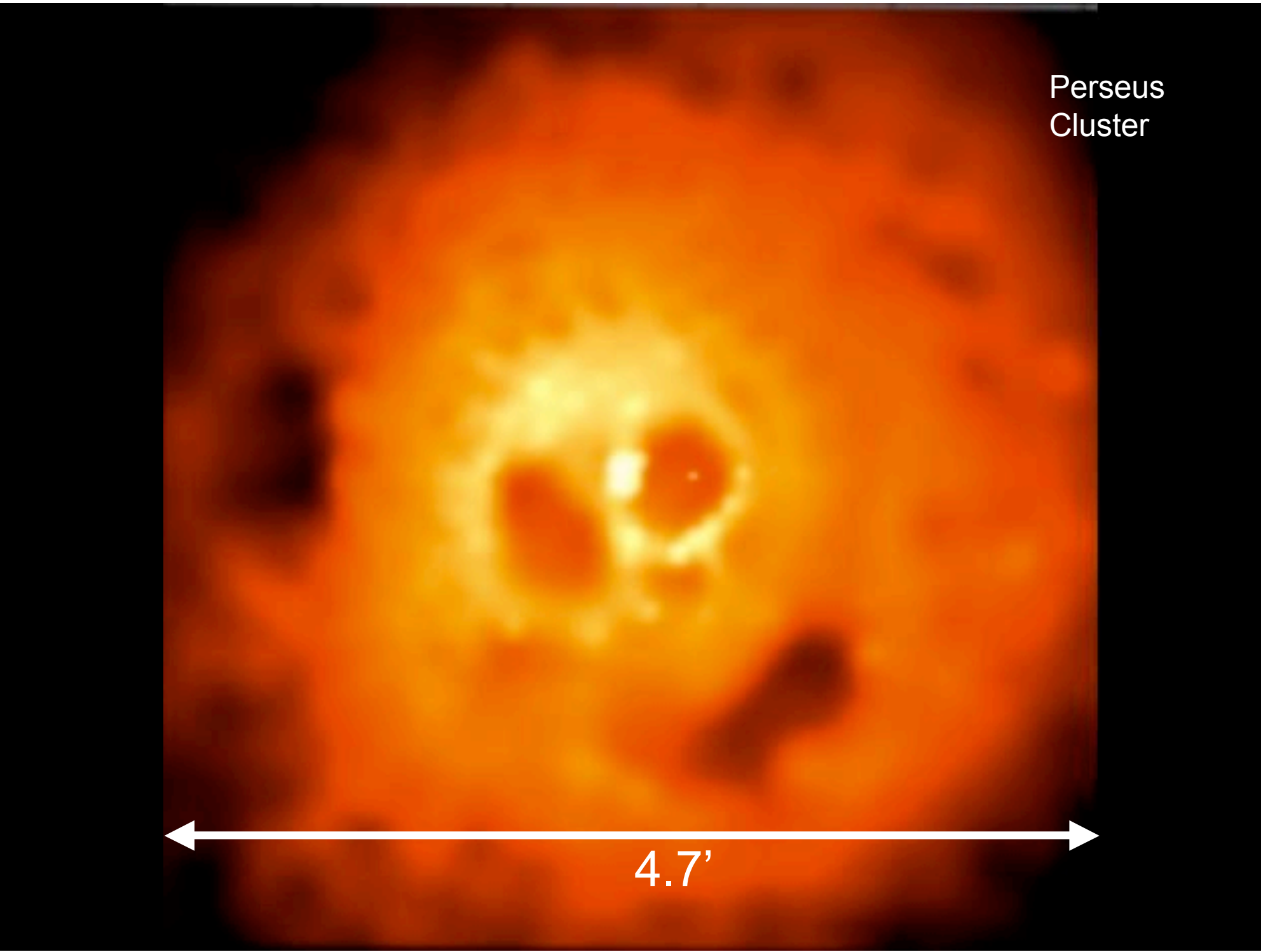
3.1' FWHM beam ($\lambda = 2.0$ mm D = 2600 mm)

EMSS1358



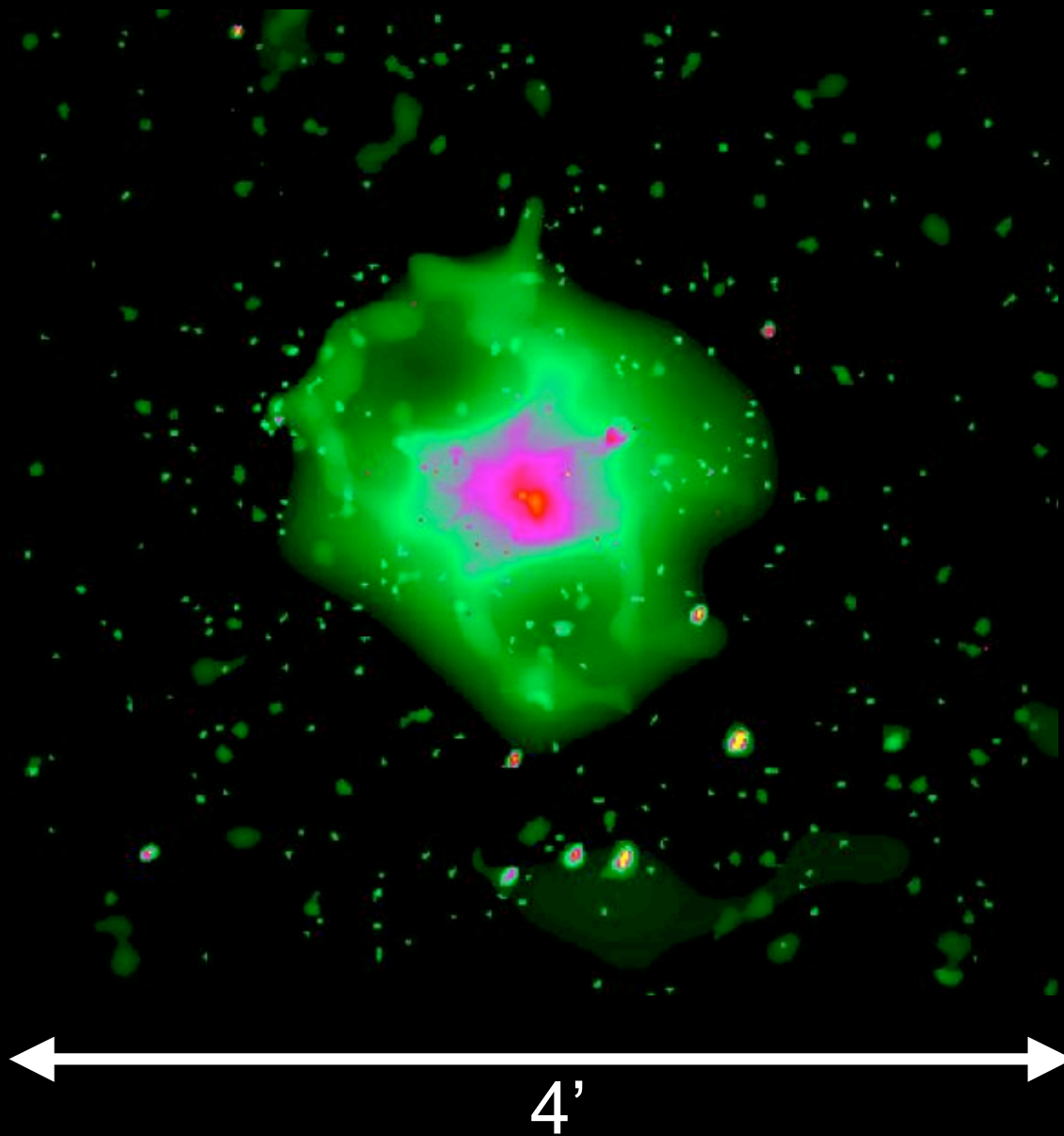
3.8'

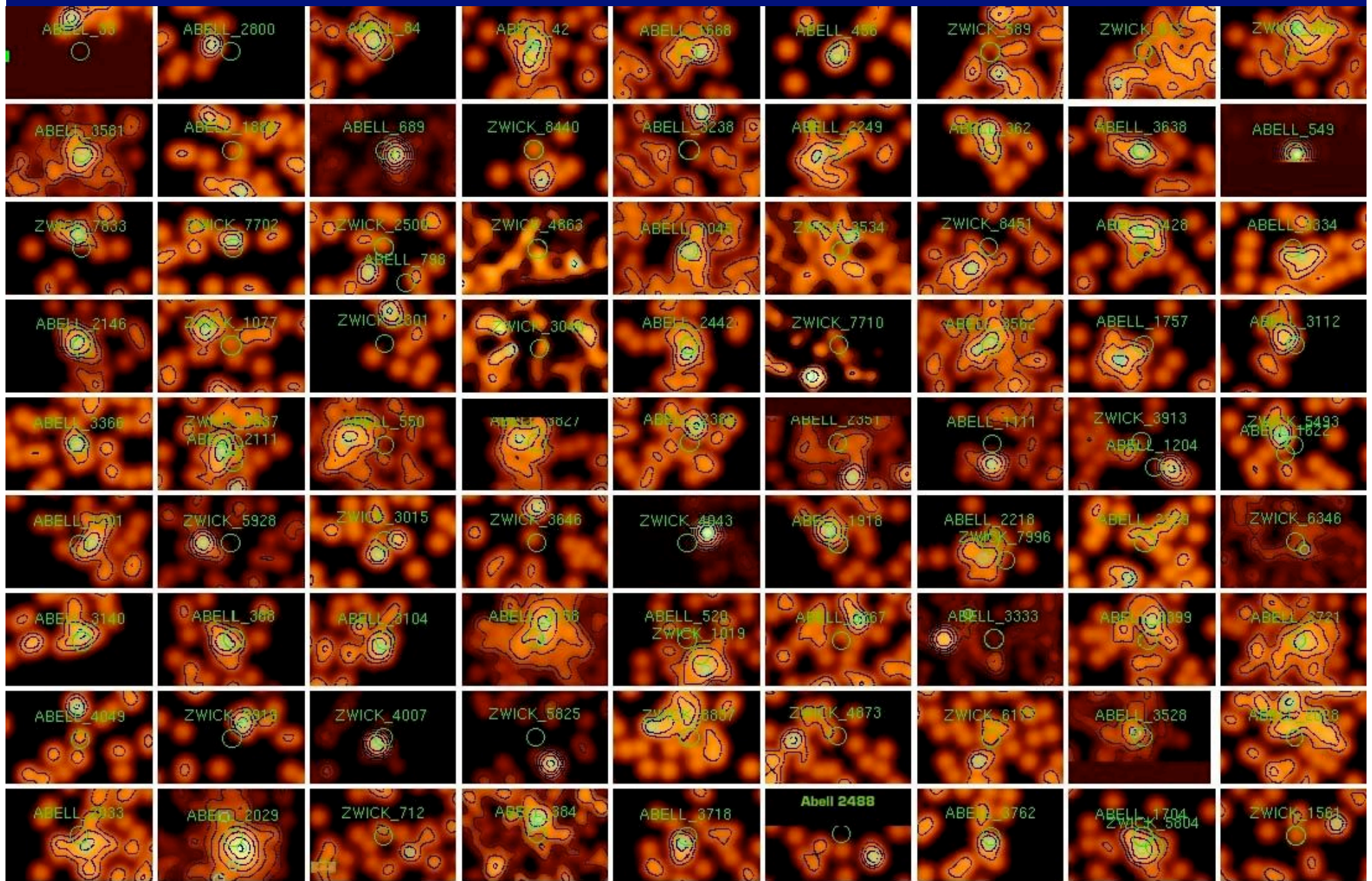
Perseus
Cluster



4.7'

HGC62





- A driver for an even larger telescope !!!
- Other driver : (astro-ph/0309005)

Highlights of Astronomy
ASP Conference Series, Vol. 13, 2003
O. Engvold & M.G. Burton

The Case for a 30m Diameter Submillimeter Telescope on the Antarctic Plateau

Antony A. Stark

*Smithsonian Astrophysical Observatory, 60 Garden St. MS 12,
Cambridge, MA 02138 USA*

Abstract. A large single-dish submillimeter-wave telescope equipped with a focal plane array containing $\sim 10^4$ bolometers and costing about \$120M could locate most protogalaxies in the southern sky within a year of operation.

May be for dome-C or dome-A ?

- Third driver : Study of the nature of dark matter

Dome-C Antarctica (France + Italy)



DARK MATTER

Cosmic
Microwave
Background

Cosmic
Rays

γ rays

Power Spectrum of
CMB anisotropy

Observation of SZ effect
in selected clusters

.....

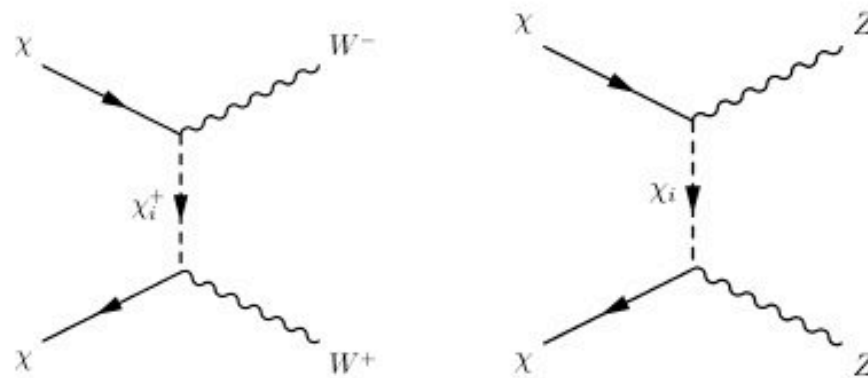
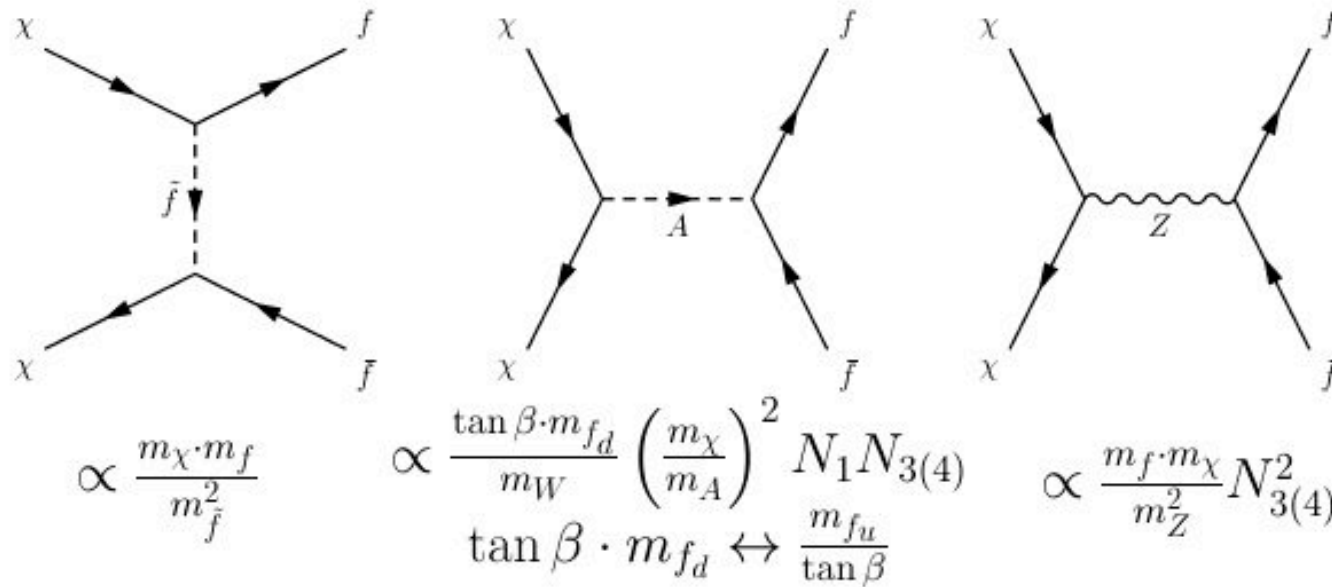
χ - χ annihilation products
in CR spectra

.....

χ - χ annihilation photons
in X and γ -rays spectra

.....

Dark Matter Annihilation Products



$$\propto \frac{1}{1 + (m_{\chi_i^+}/m_\chi)^2 - (m_W/m_\chi)^2}$$

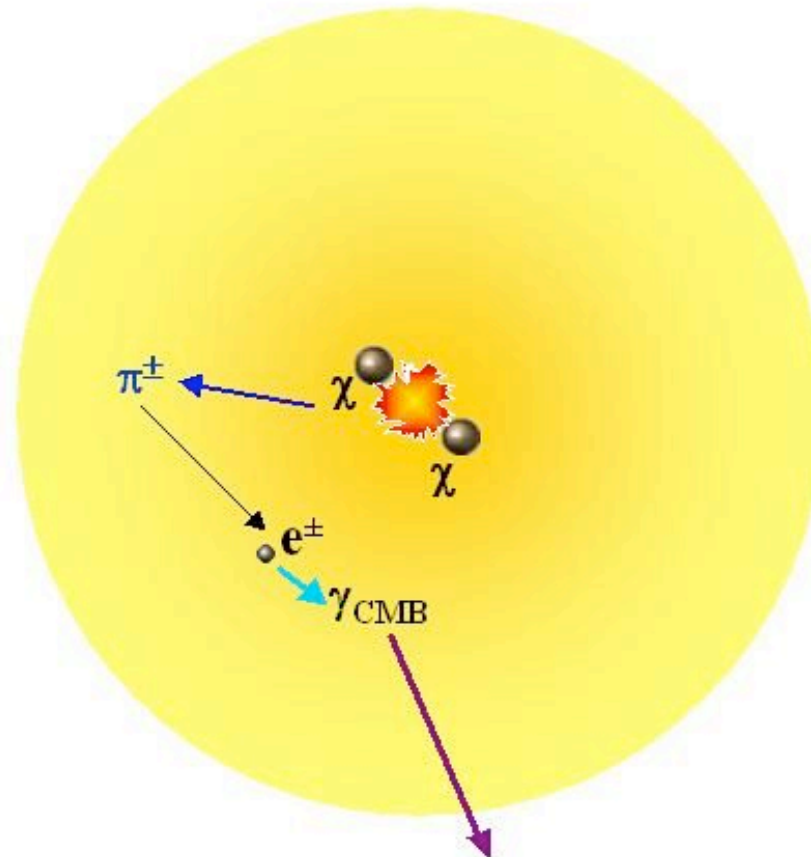
$$(m_{\chi_i^+}, m_W) \leftrightarrow (m_{\chi_i}, m_Z)$$

What is Dark Matter ?

- **Hp**: Weakly Interacting Supersymmetric Particles (WIMPs)
- Lightest one predicted by SUSY : Neutralino χ
- Could be measured by LHC
- χ s tend to cluster in the center of astrophysical structures
- Annihilation of Neutralinos would produce fluxes of
 - Neutral and charged pions
 - Secondary electrons protons
 - Neutrinos
 - etc.
- They produce various effects
- One of them is the SZ from the charged component (see Colafrancesco, 2004)



SZ effect from $\chi\chi$ annihilation



SZ effect
(CS)

What is Dark Matter ?

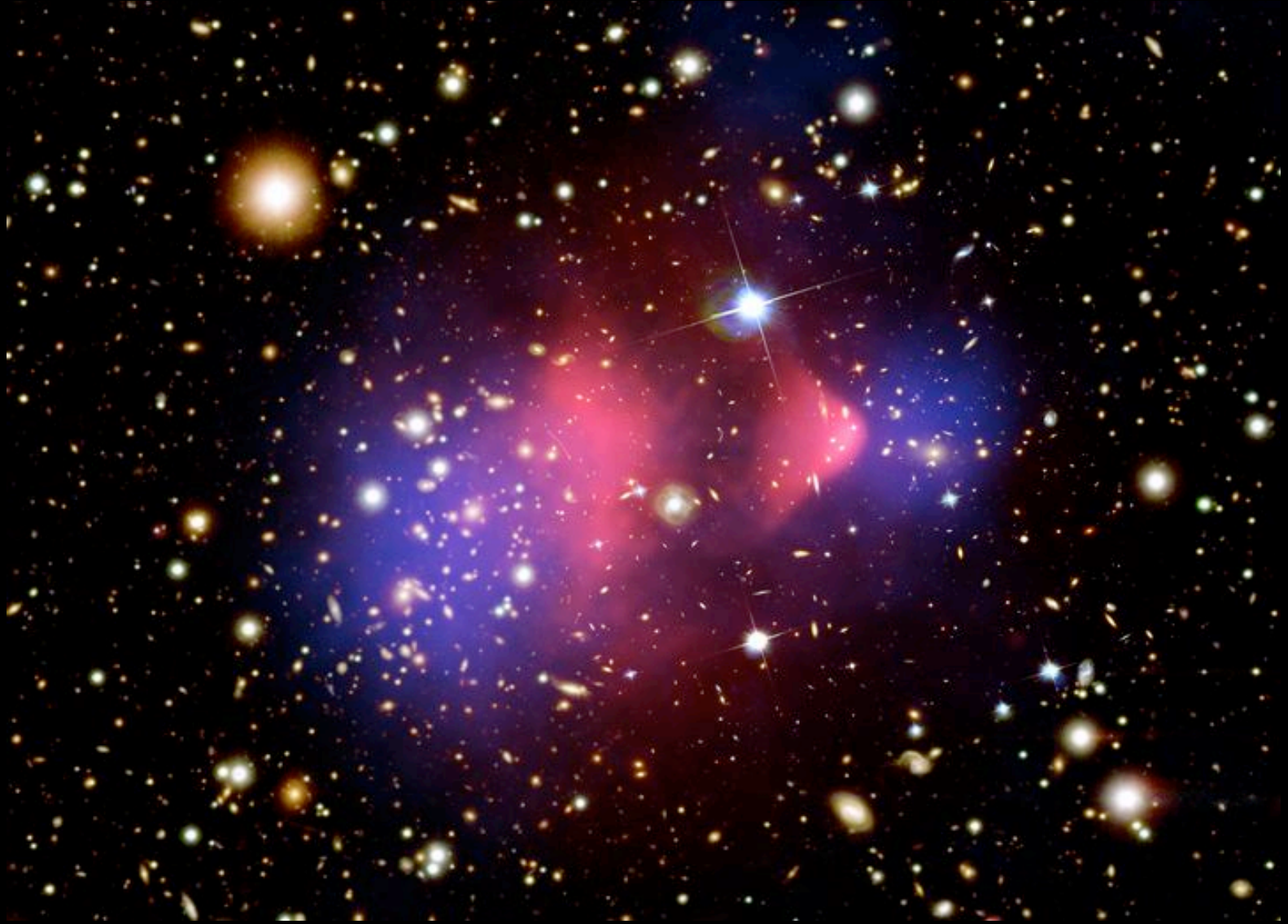
- **Hp**: Weakly Interacting Supersymmetric Particles (WIMPs)
- Lightest one predicted by SUSY : Neutralino χ
- Could be measured by LHC
- χ s tend to cluster in the center of astrophysical structures
- Annihilation of Neutralinos would produce fluxes of
 - Neutral and charged pions
 - Secondary electrons protons
 - Neutrinos
 - etc.
- They produce various effects
- One of them is the SZ from the charged component (see Colafrancesco, 2004)
- Subdominant with respect to SZE from the gas.
- We need clusters where Dark Matter and Baryonic Matter are separated.

1E0657-56



9'

1E0657-56



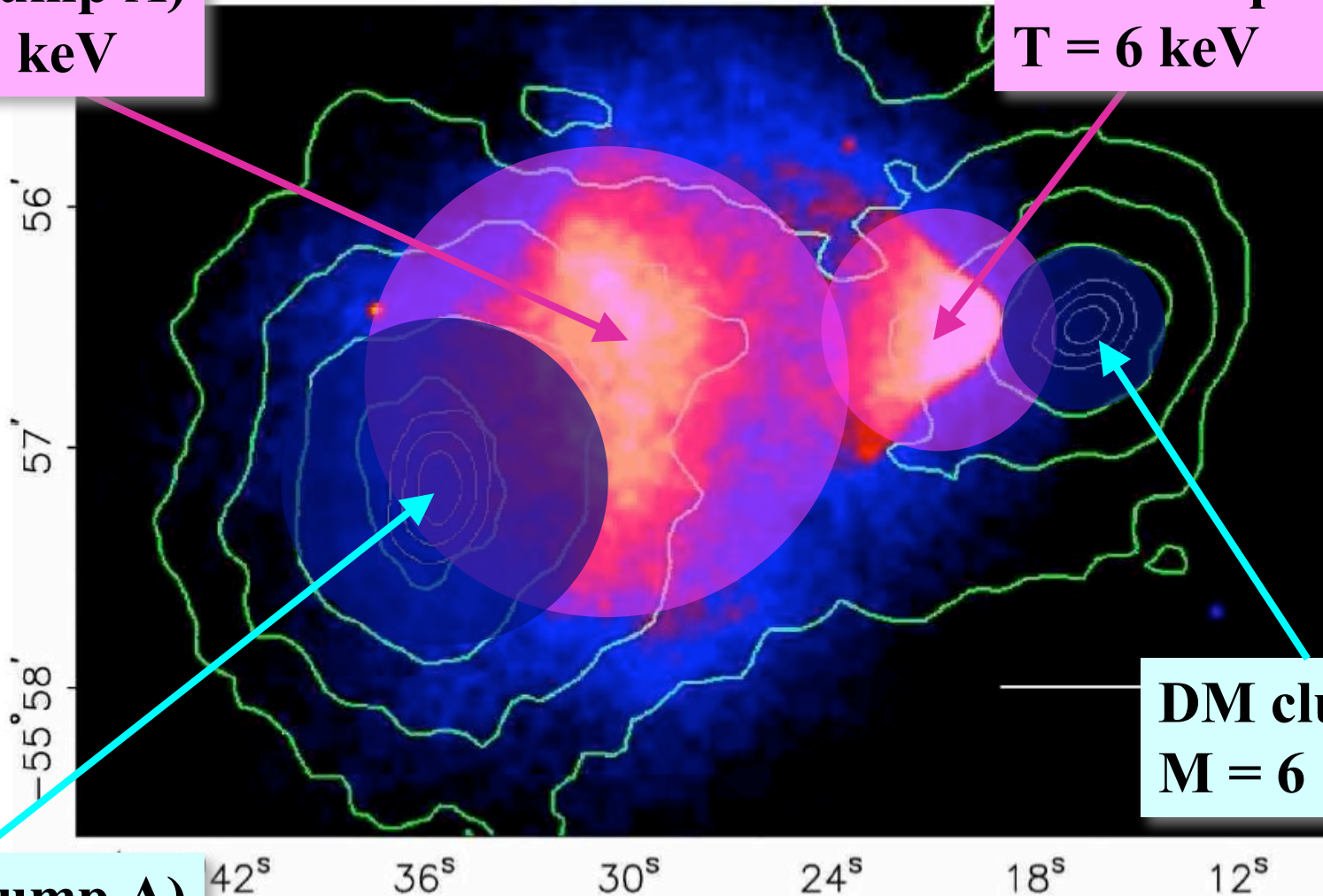
7.5'



1ES0657-556: DM + thermal gas

Gas clump A)
 $T = 14 \text{ keV}$

Gas clump B)
 $T = 6 \text{ keV}$



DM clump A)
 $M = 10^{15} M_{\odot}$

DM clump B)
 $M = 6 \cdot 10^{13} M_{\odot}$

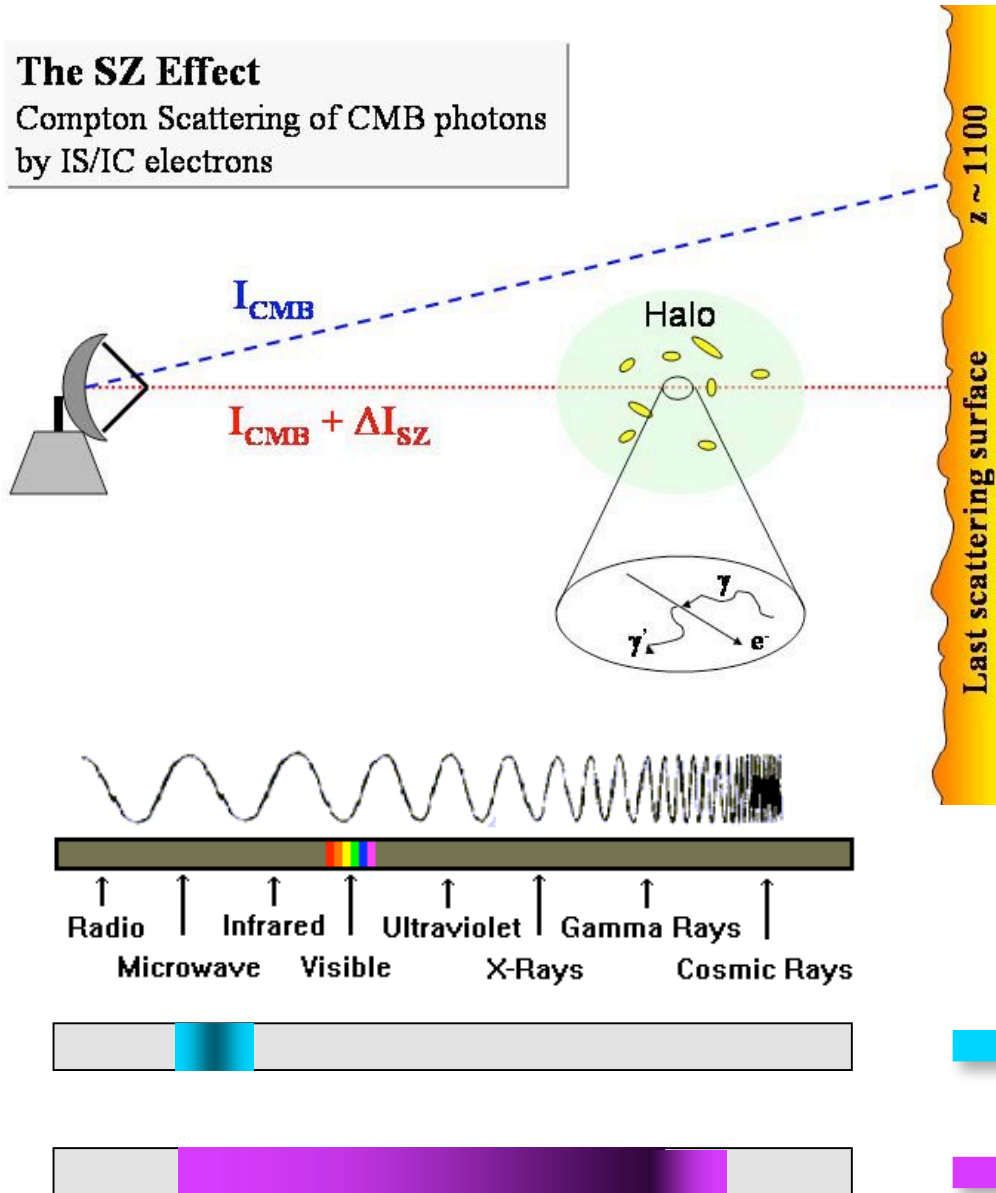
[Clowe et al. 2006, and refs. therein]

SZ effect from DM

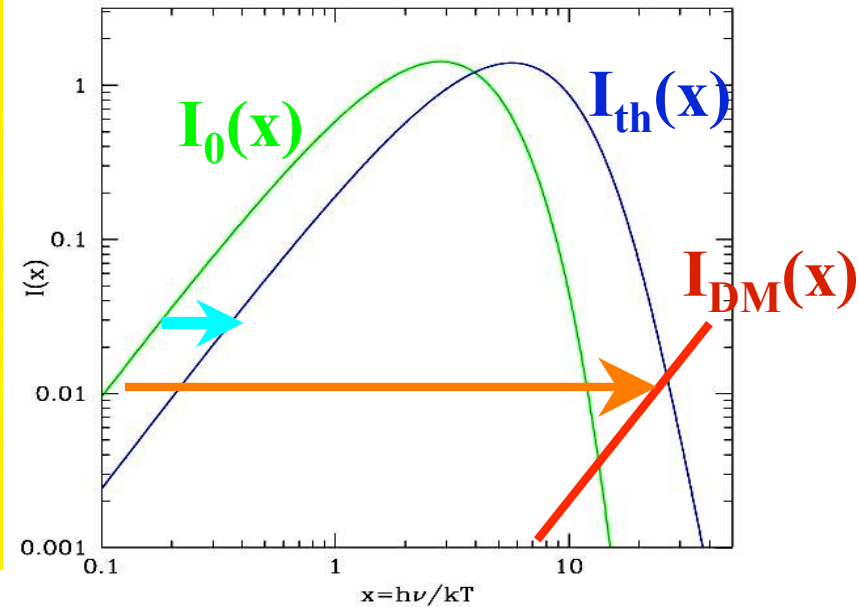
[Colafrancesco 2004 , A&A, 422, L23]

The SZ Effect

Compton Scattering of CMB photons by IS/IC electrons



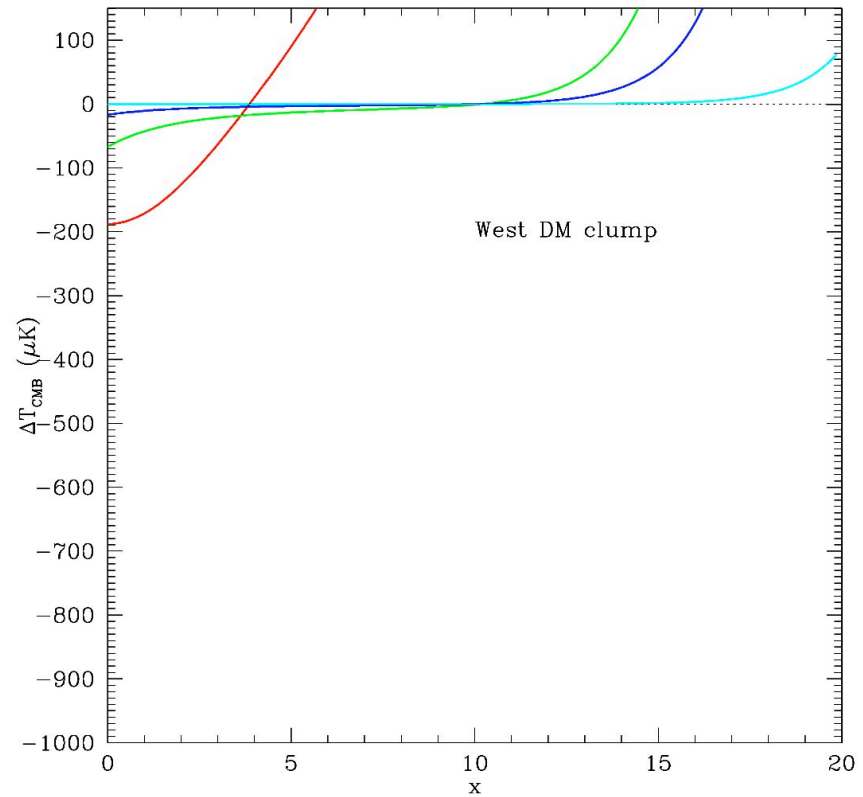
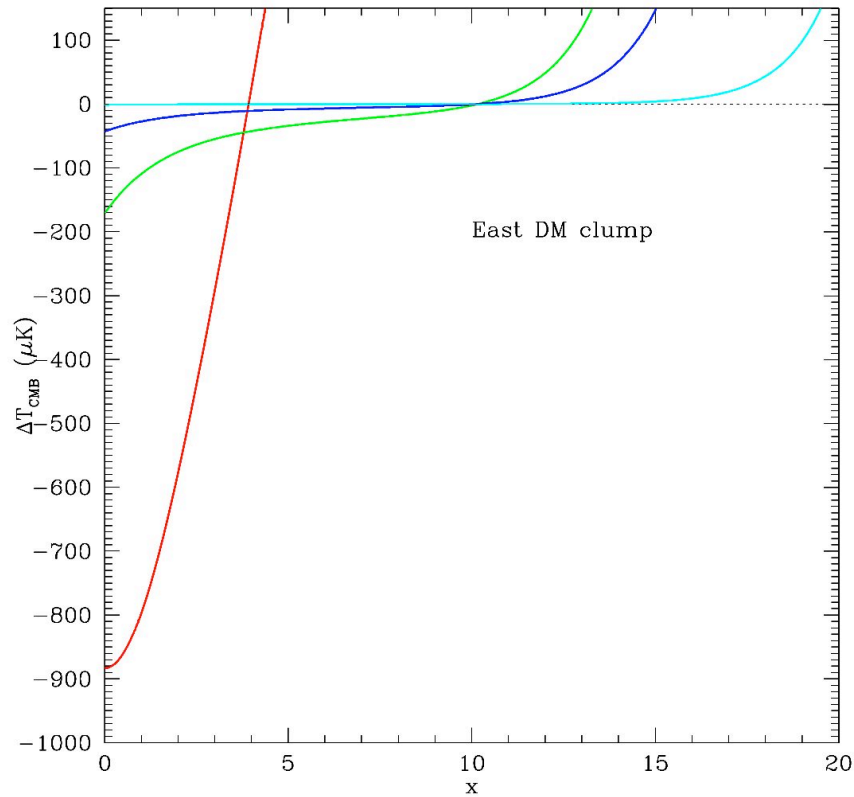
$$\Delta I(x) = I(x) - I_0(x)$$



→ thermal e^- $\frac{\nu'}{\nu} = \frac{4}{3}$
→ relativistic e^- $\frac{\nu'}{\nu} = \frac{4}{3}\gamma^2 - 1$



SZ effect at clump centres



[Colafrancesco, de Bernardis, Masi, Polenta & Ullio 2006]

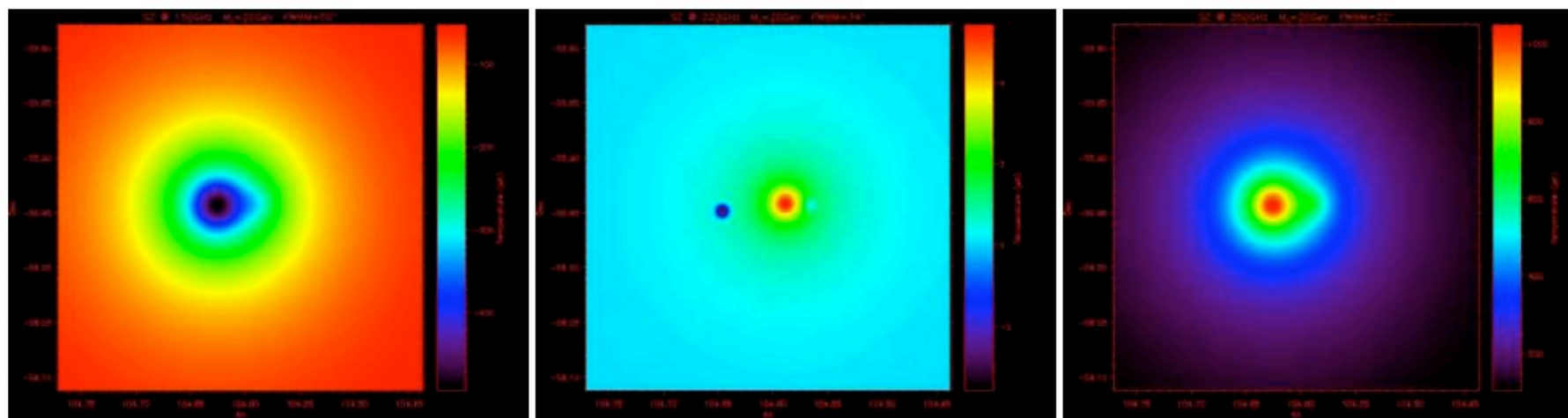


Fig. 2. The simulated SZ maps of the cluster 1ES0657-556 as observable with the SPT telescope at three frequencies: $\nu = 150$ GHz (left panel), $\nu = 223$ GHz (mid panel), $\nu = 350$ GHz (right panel). A neutralino mass of $M_\chi = 20$ GeV has been adopted here. Note that choosing the frequency of 223 GHz where the thermal SZE from the E baryonic clump vanishes maximizes the detectability of the SZ_{DM} effect from the two DM clumps.

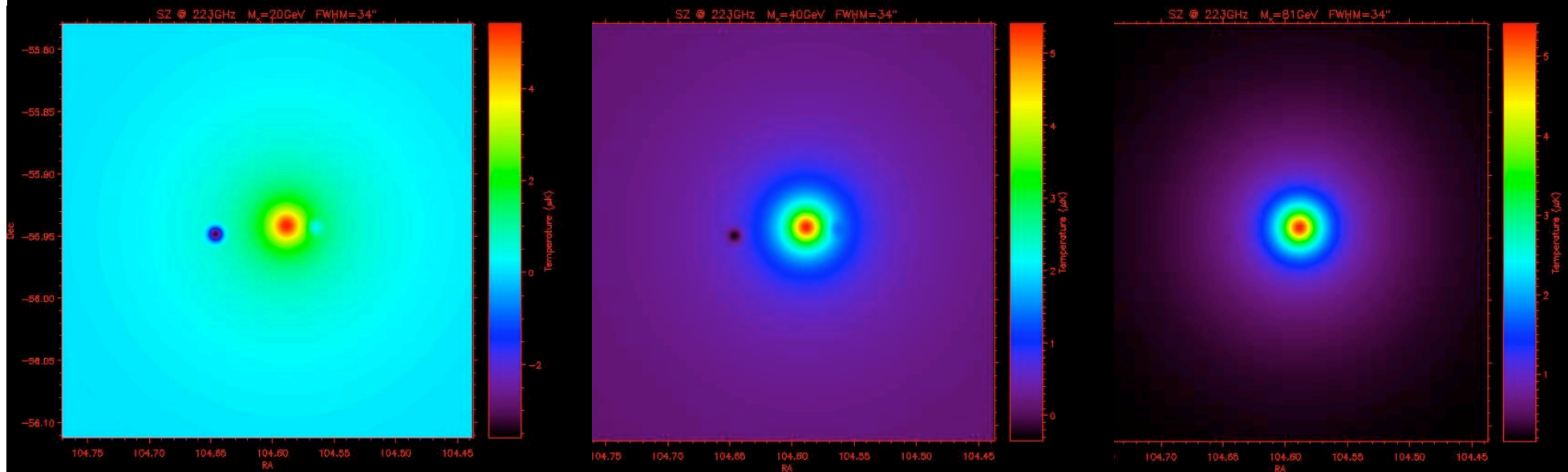
[Colafrancesco, de Bernardis, Masi, Polenta & Ullio 2006]

Isolating SZ_{DM} (at 223 GHz)

$M_\chi = 20 \text{ GeV}$

$M_\chi = 40 \text{ GeV}$

$M_\chi = 80 \text{ GeV}$

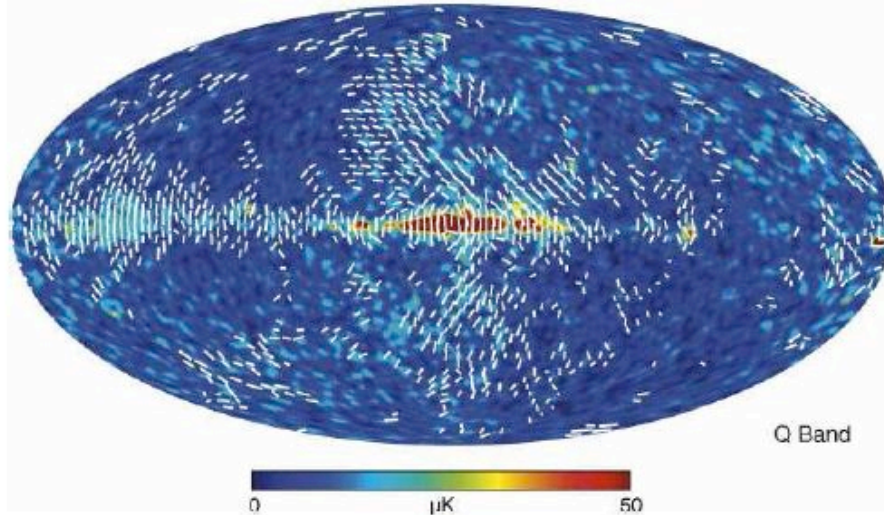
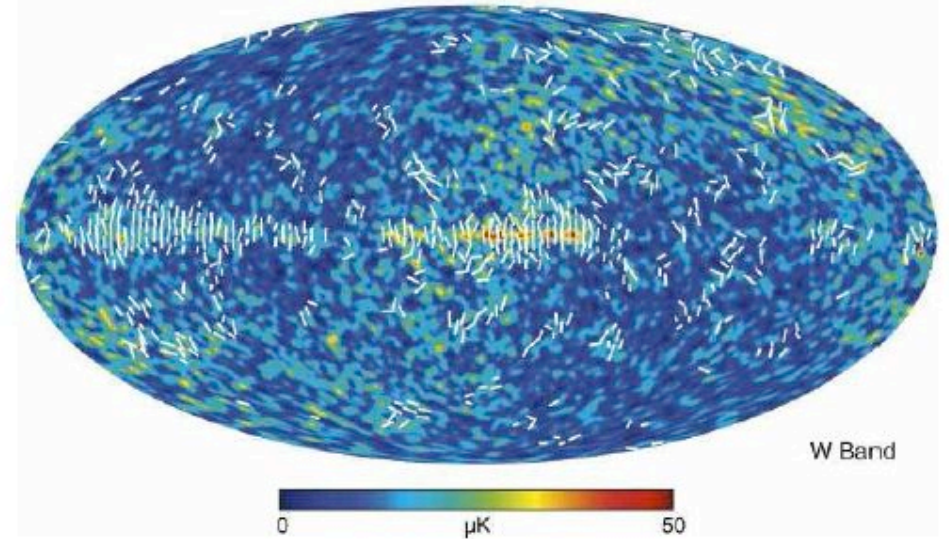
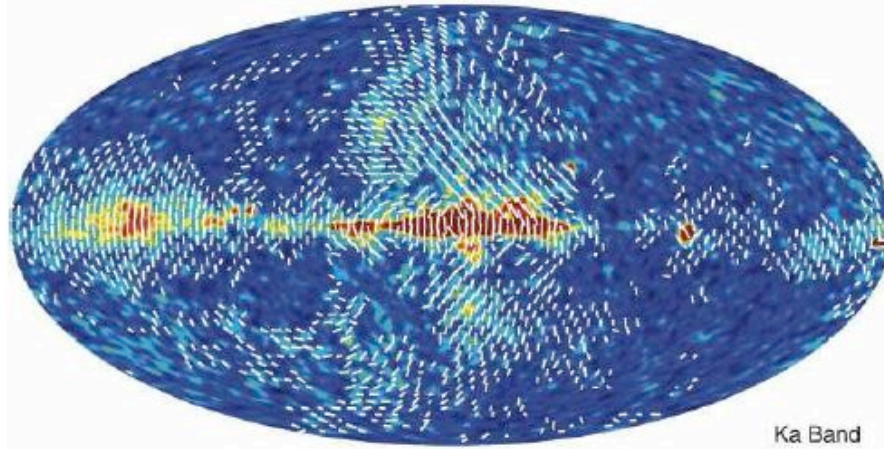
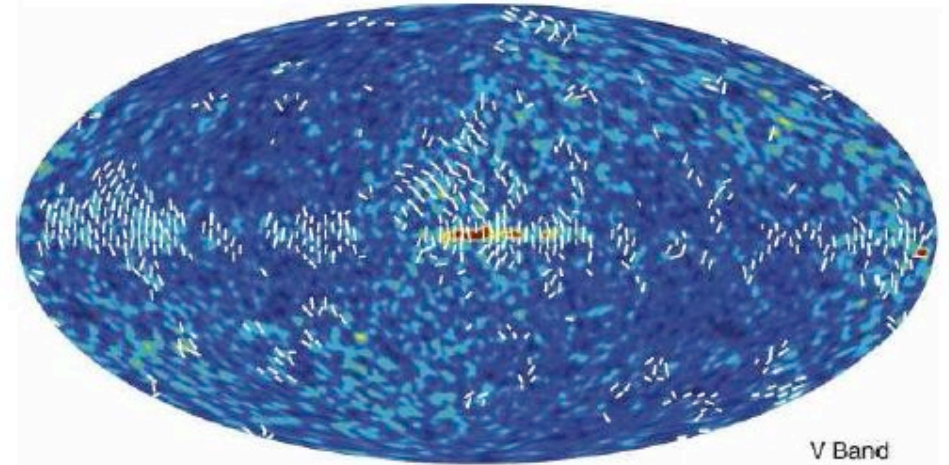
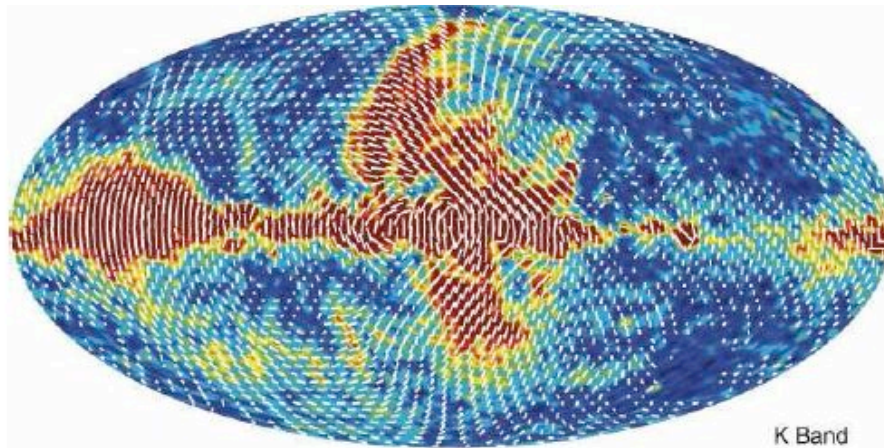


The SZE from the hot gas disappears at $x_{0,\text{th}}$ ($\sim 220\text{-}223 \text{ GHz}$) while the SZ_{DM} expected at the locations of the two DM clumps remains negative and with an amplitude and spectrum which depend on M_χ .

[Colafrancesco, de Bernardis, Masi, Polenta & Ullio 2006]

contents

- CMB experiments: state of the art
- Open problems : how to attack them with CMB
- Enabling technologies
- High angular resolution CMB anisotropy
- The spectrum of CMB anisotropy
- The polarization of CMB



Large-scale Polarization maps from W-MAP 3 years. The detected polarization is mainly due to foregrounds.

- One approach:
 - Focus on the cleanest region of the sky,
 - use extremely sensitive detectors,
 - use frequencies where foreground polarization is lower
- BICEP, QUAD, ... (taking data)
- QUIET, CLOVER, BRAIN, EBEX, ... (funded, will take data in the near future)
- BOOMERanG (polarized foregrounds, funded)

BICEP: A Large Angular Scale CMB Polarimeter

Brian G. Keating^a, Peter A. Ade^b, James J. Bock^c, Eric Hivon^d,
William L. Holzapfel^e, Andrew E. Lange^a, Hien Nguyen^b, Ki Won Yoon^a

^aCalifornia Institute of Technology, Mail Code 59-33, Pasadena, CA, 91125

^bDept. of Physics, Cardiff University, Cardiff CF243YB, Wales, UK.

^cJet Propulsion Laboratory, 4800 Oak Grove Dr., Pasadena, CA 91109

^dIPAC, Mail Code 100-22, Pasadena, CA 91125

^eDept. of Physics, University of California at Berkeley, Berkeley, CA, 94720

ABSTRACT

We describe the design and expected performance of BICEP, a millimeter wave receiver designed to measure the polarization of the cosmic microwave background. BICEP uses an array of polarization sensitive bolometers operating at 100 and 150 GHz to measure polarized signals over a 20° field of view with $\sim 1^\circ$ resolution. BICEP is designed with particular attention to systematic effects which can potentially degrade the polarimetric fidelity of the observations. BICEP is optimized to detect the faint signature of a primordial gravitational wave background which is a generic prediction of inflationary cosmologies.

Keywords: polarization sensitive bolometers, cosmic microwave background – instrumentation, gravitational wave detection

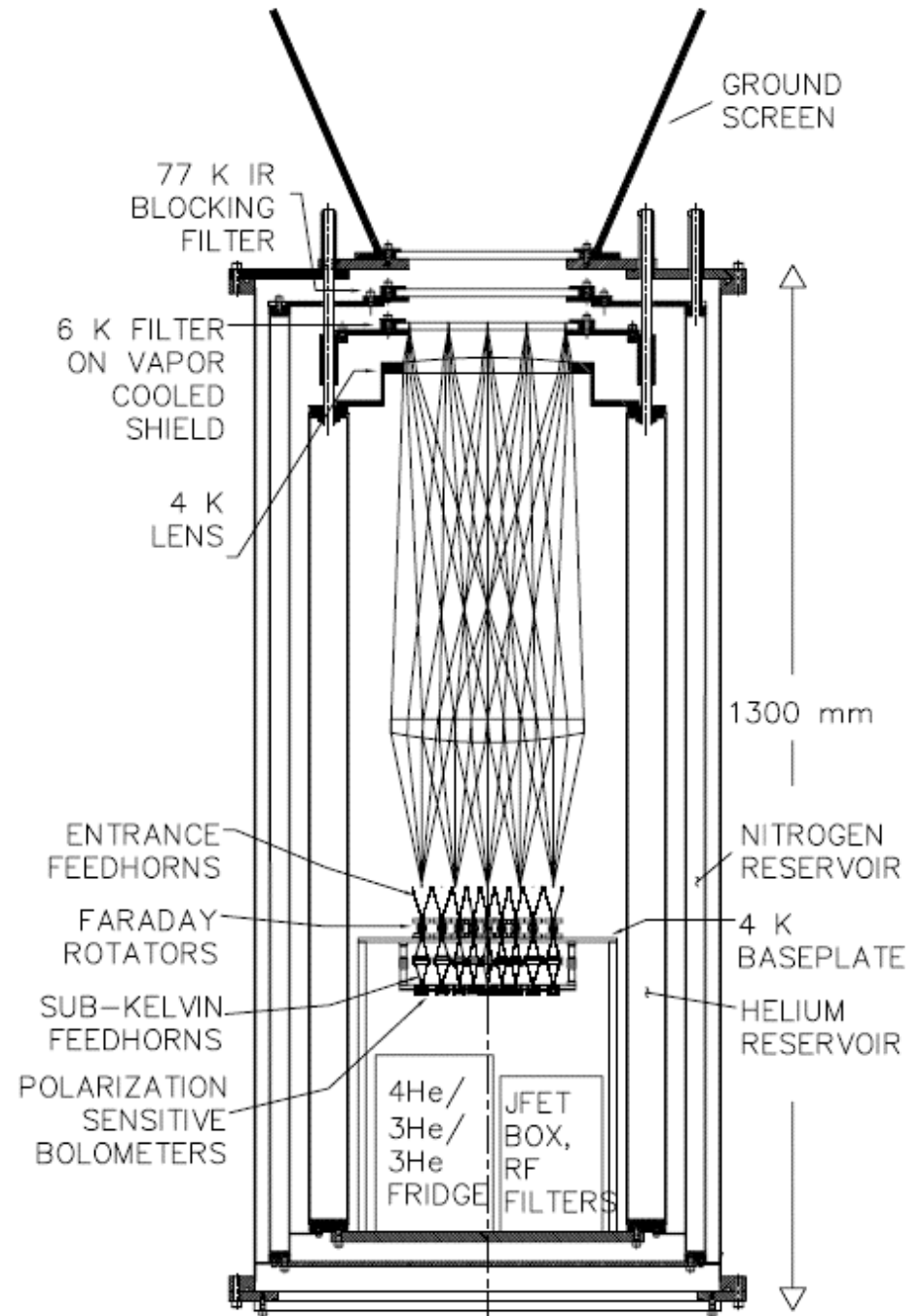
From the Caltech(Lange) web site

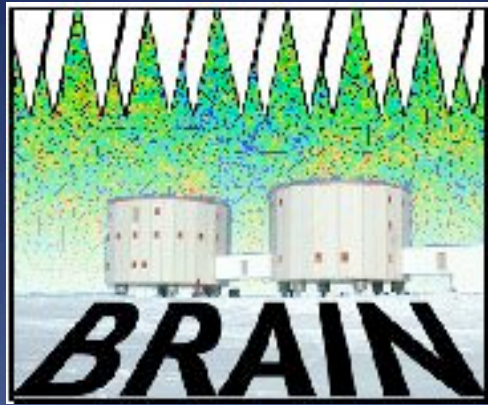


Taking data now from South Pole.

Polarization sensitive detectors
from Caltech/JPL

Main goal: detailed measurement
of CMB polarization spectra (E-
modes)





Background Radiation Interferometer

CARDIFF
UNIVERSITY
PRIFYSGOL
CAERDYDD

Astronomy + 
Instrumentation
Group 



WWW.CESR.FR



TOULOUSE - FRANCE

Orthogonal Technique: combines

- Sensitivity of bolometers
- Cleanliness of interferometers
- Excellence of Dome-C site

Pathfinder experiment installed in summer campaigns. The site is excellent.

Dome-C Concordia Station

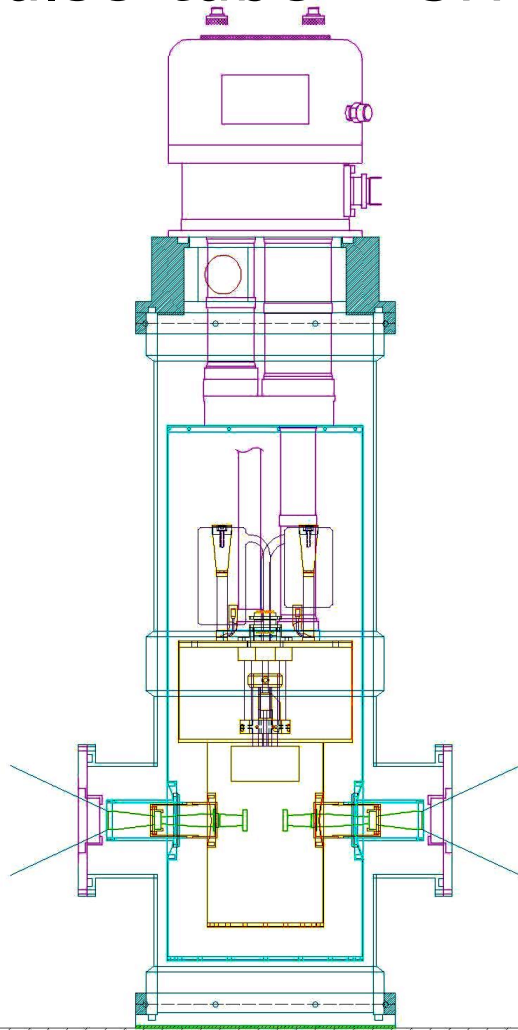
Lat: 75° 06' S Lon: 123° 23' E
Altitude 3230m osl
Main air temperature -50.8 °C
Typical monthly average air temperature in summer -30 °C
Typical monthly average air temperature in winter -60 °C
Mean wind speed 2.8 m/s 5.4 knots
Mean air pressure 645 hPa
Yearly precipitation range (snow) 2-10 cm



BRAIN site

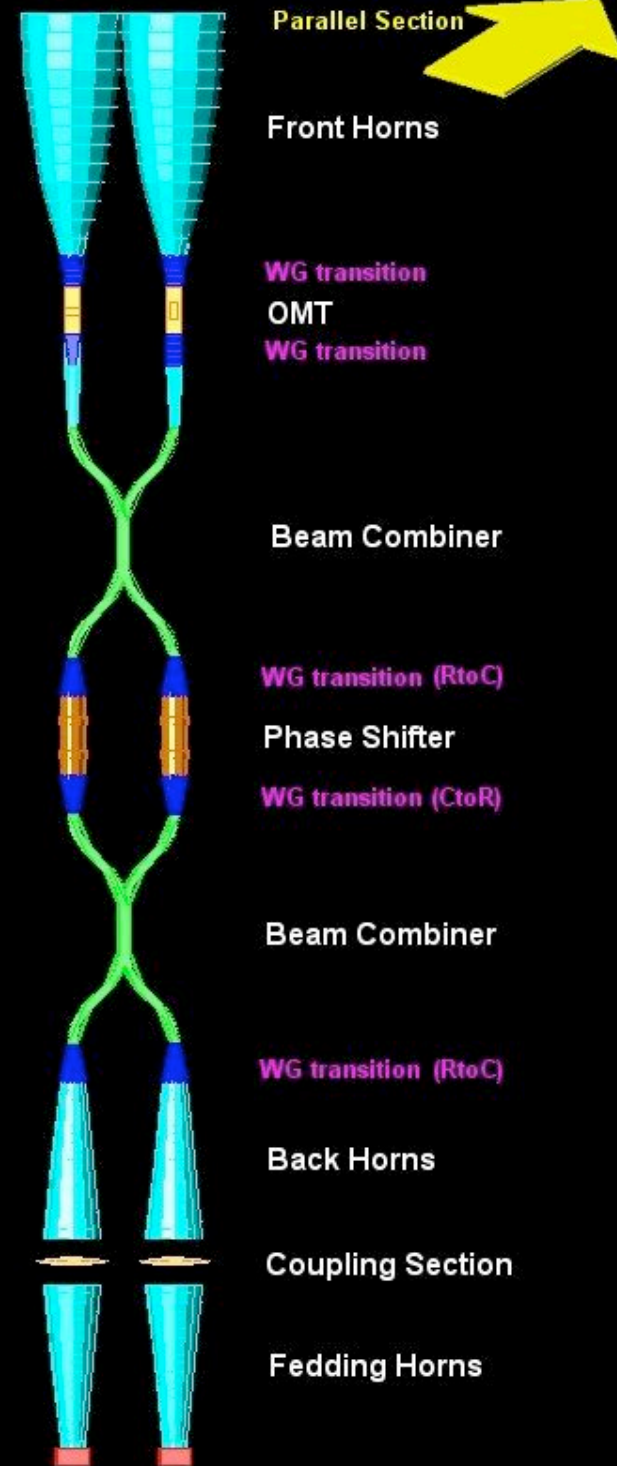
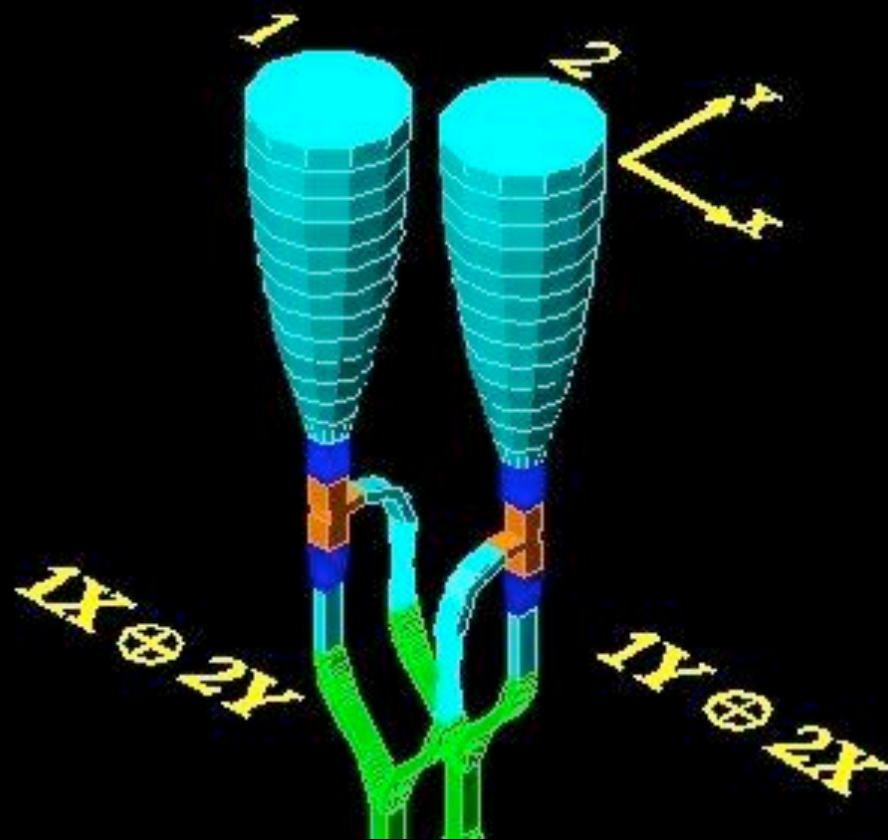
Is Dome-C the best site for B-modes measurements?

- We have already validated on-site (Dome-C) a technique to operate cryogenic detectors without having to use cryogenic liquids.
- Pulse-tube + 3He fridge (0.3 K).



Bolometric Interferometer

Single Baseline



Working principle of ideal Brain components:

$$\begin{matrix}
 90^\circ \text{Hyb} & \text{PhSh} & 90^\circ \text{Hyb} & \text{OMT} & \\
 \left[\frac{1}{\sqrt{2}} \begin{pmatrix} 1 & li \\ li & 1 \end{pmatrix} \right] \cdot \begin{pmatrix} e^{li \cdot f} & 0 \\ 0 & e^{li \cdot g} \end{pmatrix} \cdot \left[\frac{1}{\sqrt{2}} \begin{pmatrix} 1 & li \\ li & 1 \end{pmatrix} \right] \cdot \begin{pmatrix} 1 & 0 \\ 0 & 1 \end{pmatrix} \cdot \begin{pmatrix} E_{1X} \\ E_{2Y} \cdot e^{li \cdot d} \end{pmatrix} \\
 \varphi = f - g \quad (\text{dps - differential phase shift}) & & & & \begin{pmatrix} E_{1Y} \\ E_{2X} \cdot e^{li \cdot d} \end{pmatrix}
 \end{matrix}$$

i.e. the field at the first

detector is:

$$D_1 = \frac{E_{1x}}{2} (e^{i\varphi} - 1) + i \frac{E_{2y} e^{id}}{2} (e^{i\varphi} + 1)$$

And the power $P_i = D_i^* D_i$

using Stokes parameters is:



$$P_1 = \frac{1}{2} (I - Q \cdot \cos \varphi + U \cdot \sin \varphi)$$

$$P_2 = \frac{1}{2} (I + Q \cdot \cos \varphi - U \cdot \sin \varphi)$$

Likewise:

$$P_2 - P_1 = Q \cdot \cos \varphi - U \cdot \sin \varphi$$

If interferometer fringe pattern δ is introduced, V contribution arises:

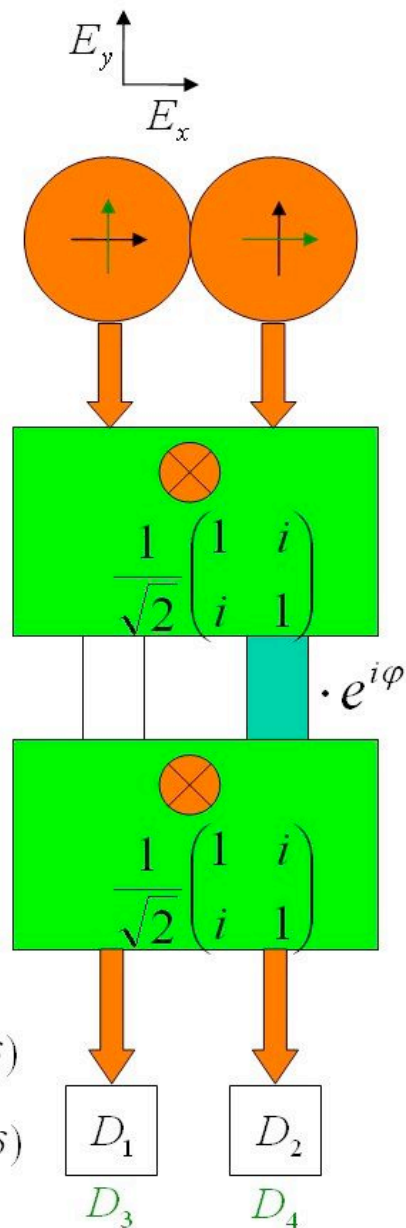


Other two detectors (3 & 4) to combine with (1 & 2) to eliminate V signal and isolate Q and U

$$P_1 = \frac{1}{2} (I - Q \cdot \cos \varphi + U \cdot \sin \varphi \cdot \cos \delta - V \cdot \sin \varphi \cdot \sin \delta)$$

$$P_4 = \frac{1}{2} (I + Q \cdot \cos \varphi - U \cdot \sin \varphi \cdot \cos \delta - V \cdot \sin \varphi \cdot \sin \delta)$$

$$P_4 - P_1 = Q \cdot \cos \varphi - U \cdot \sin \varphi \cdot \cos \delta$$



Brain meeting presentation G.Savini

BRAIN idea:

Frequencies: 90GHz, 150GHz

2x256 horns

2x512 detectors

expected sensitivity per pixel: $1\mu\text{K}$

angular resolution: 1°

cryogenic: Sumitomo Pulse Tube Cooler + 3He - 4He

fridge

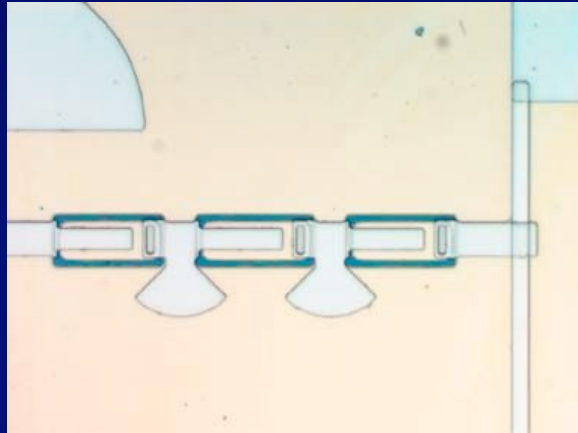
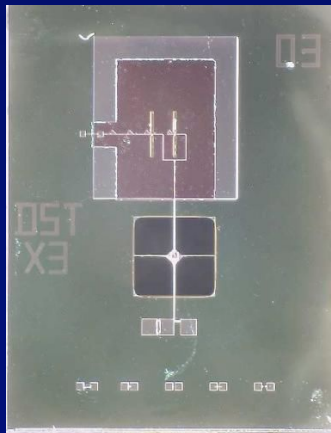
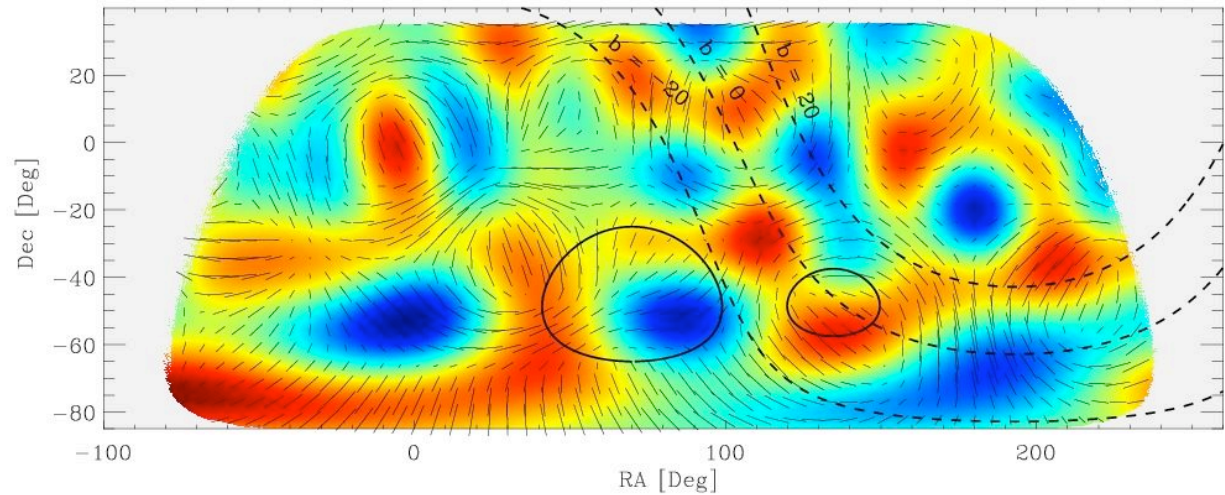
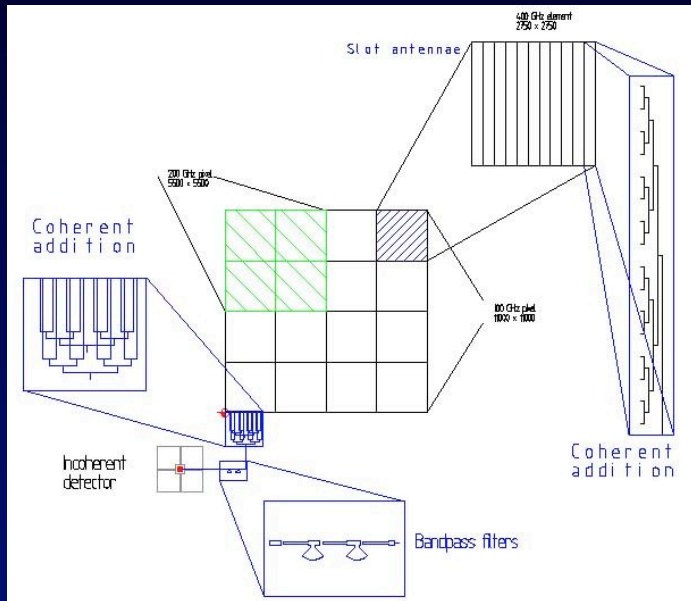
remote control using INMARSAT telemetry system

A full study of the instrument is in progress!

- Another approach:
 - Full sky survey with extremely high precision and wide frequency coverage
 - Go to space
- SPIDER (balloon),
- NASA Beyond Einstein (3 satellite studies)
- BB-Pol (balloon)
- ESA Cosmic Vision (1 satellite study, B-Pol)

Large Bolometer Arrays

- > 1000 TES bolometers for SPIDER a proposed spinning polarimeter on an **ULDB** (Andrew Lange, Caltech) devoted to large scale CMB polarization



Spider Instrument Summary

	40 GHz	90 GHz	145 GHz	220 GHz
Bandwidth [GHz]	10	33	32	40
# Detectors	64	768	512	512
Beam FWHM [arcmin]	145	60	40	26
NET_cmb [uKrt(s)]	16.3	3.8	3.5	6.6

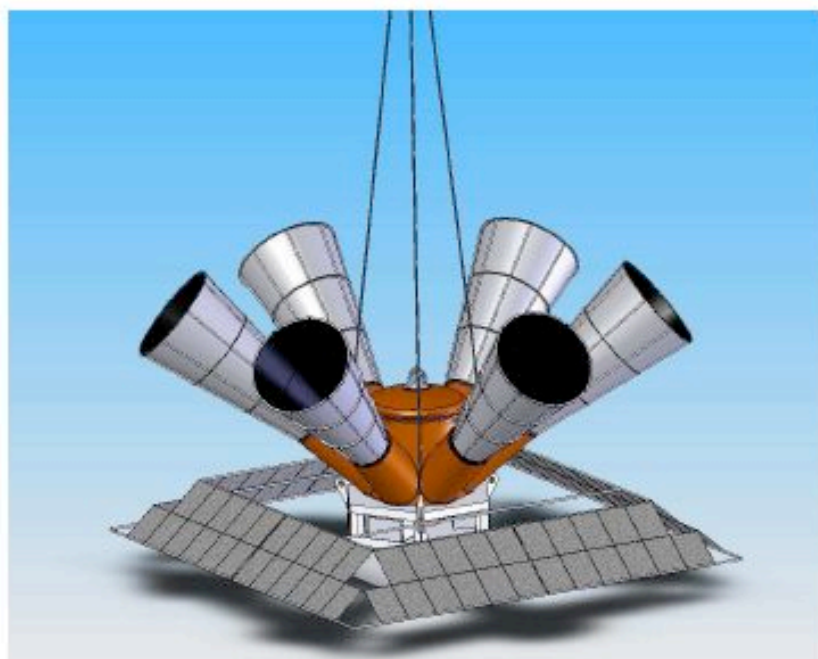


Figure 1: The *SPIDER* payload is designed to obtain maximum sky coverage from a twenty to thirty day mid-latitude balloon flight around the world. The experiment will map out roughly 50% of the sky observing only at night.

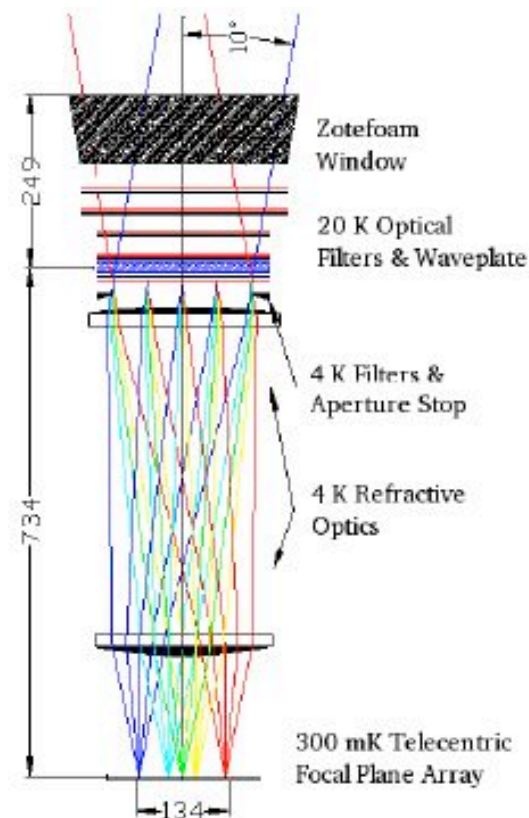


Figure 2: The *SPIDER* optics are based on the BI-CEP design. *SPIDER* will incorporate a rotating half-wave plate to modulate incoming polarization signal.

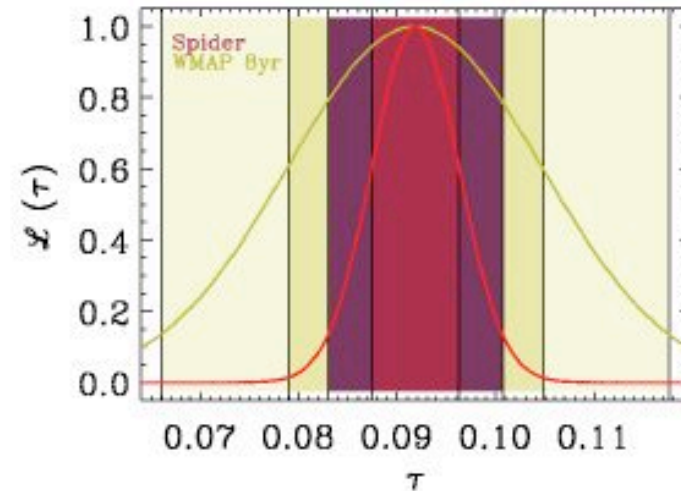
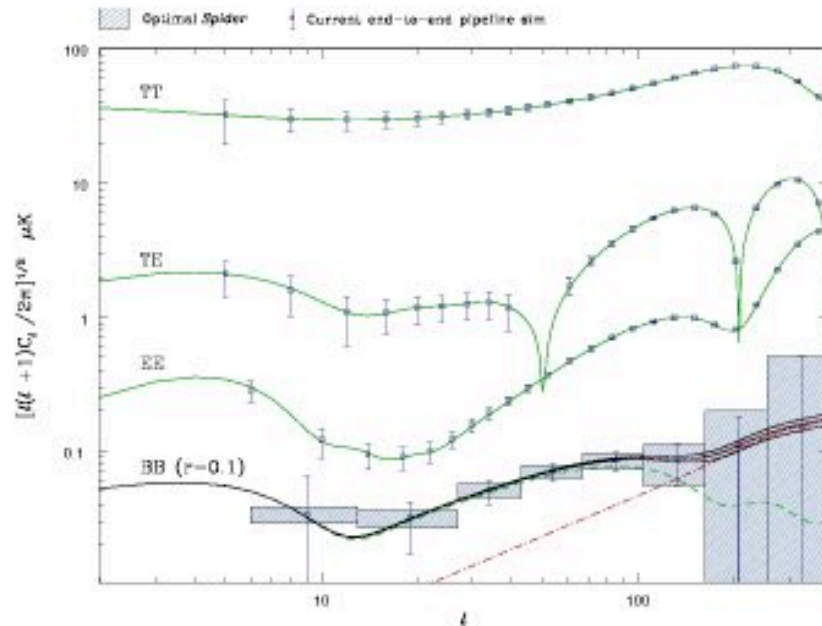
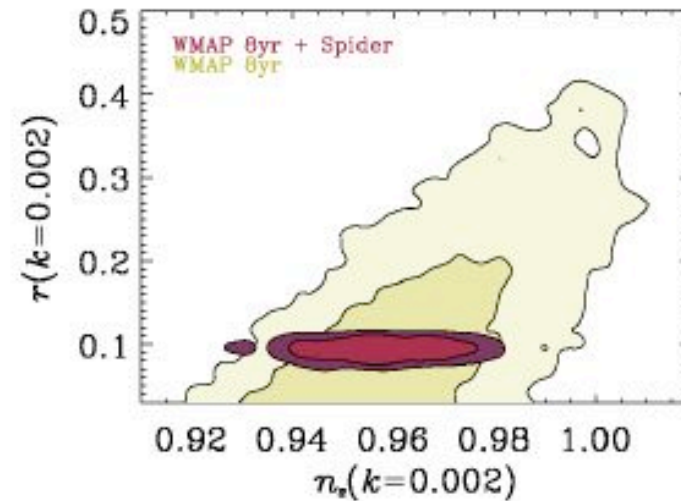
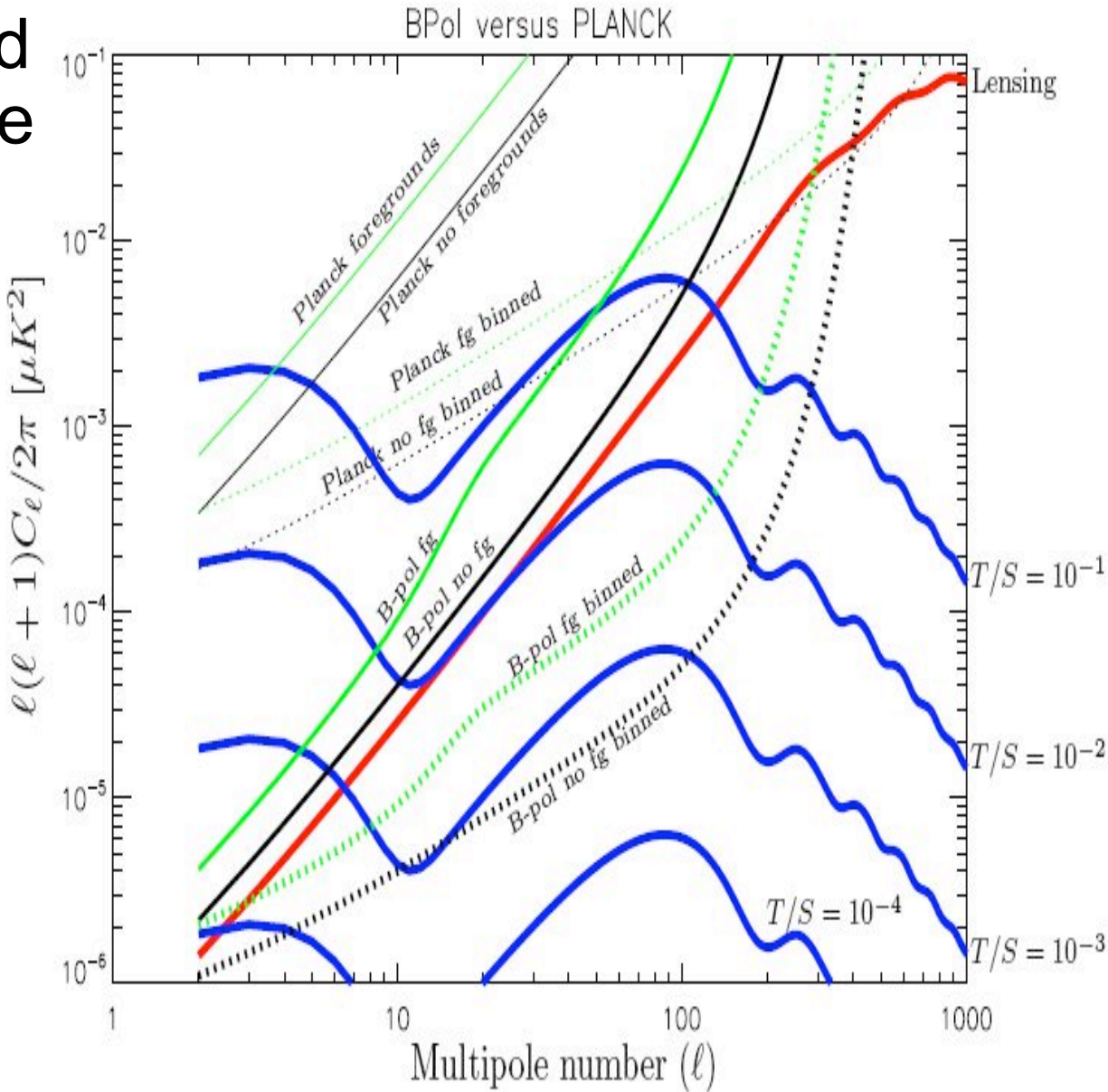


Figure 5: Top left panel: *SPIDER* sensitivity. Data points and errors are derived from end-to-end realizations of a simulated *SPIDER* balloon flight. Minimal modifications to the existing pipeline will result in an improved accuracy of the low multipole BB: the errors will approach the analytical errors (blue boxes) which are fully optimal with respect to the leakage of EE into BB. Top right panel: One-dimensional constraints on τ . Bottom right panel: Two dimensional constraints in the $n_s - r$ plane.



B-Pol

- A mission to study CMB polarization with unprecedented accuracy, at degree angular scales
- Proposed in the framework of ESA Cosmic Vision 2015-2025
- International team (Europe, Canada, USA)
- Able to detect B-modes for T/S down to 10^{-3}



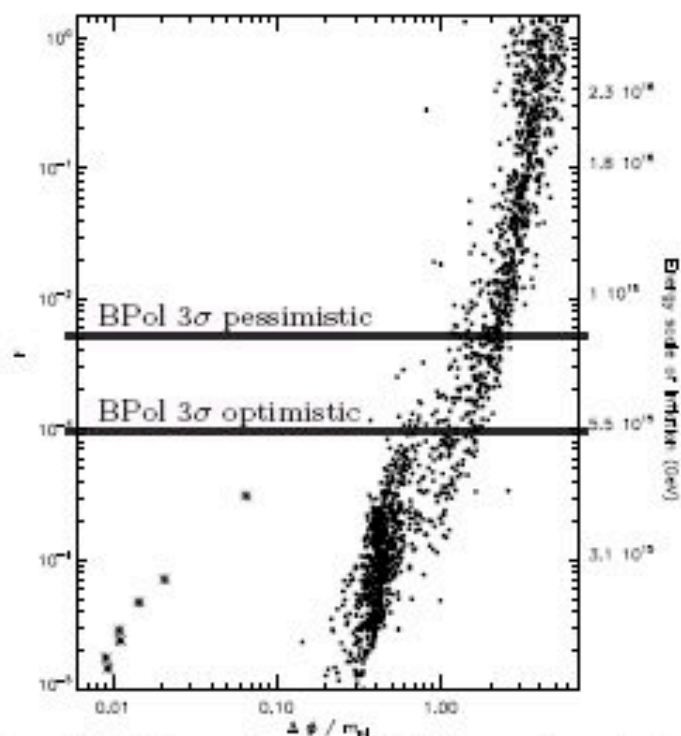


Figure 2: The evolution of ϕ for various inflation models with respect to the energy scale. Dots represent single-field models, which find good agreement with the relation in the text. The crosses represent hybrid models, and due to the sharp features in the potentials of such models, they do not obey the same relation. We show two scenarios for what BPol will accomplish, one with an optimistic and another with a pessimistic projection for the degree to which foregrounds can be removed. We observe that a large range of models will be ruled out, or discovered, by BPol. Figure produced by L. Verde, following closely the method of W. Kinney et al., Phys. Rev. D74, 023502 (2006) (astro-ph/0605338).

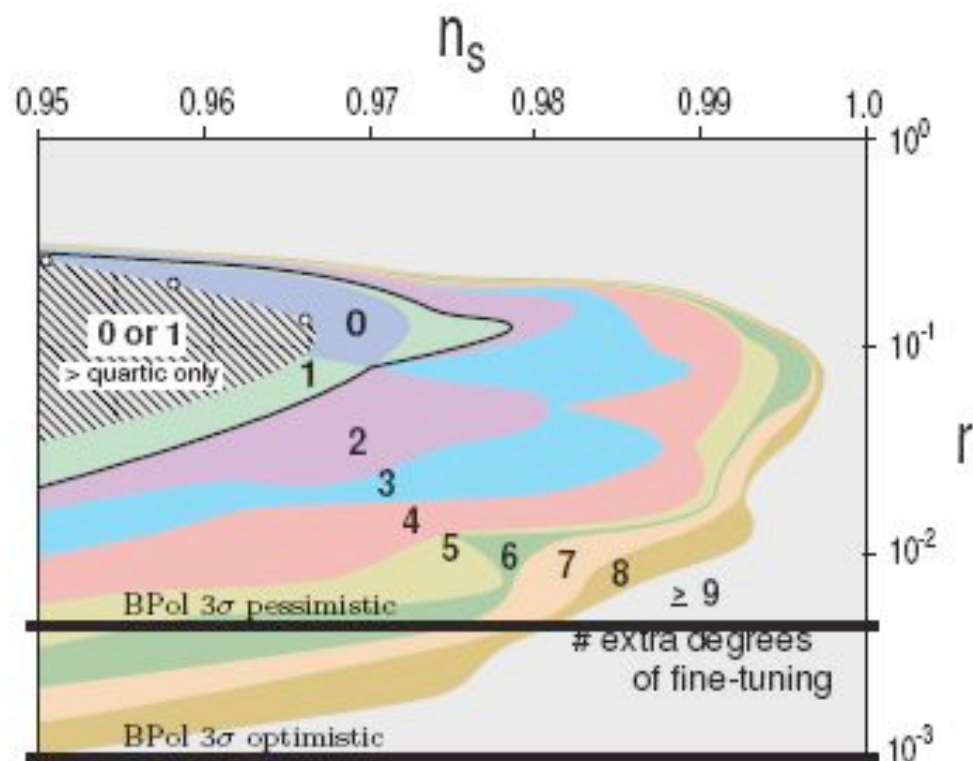
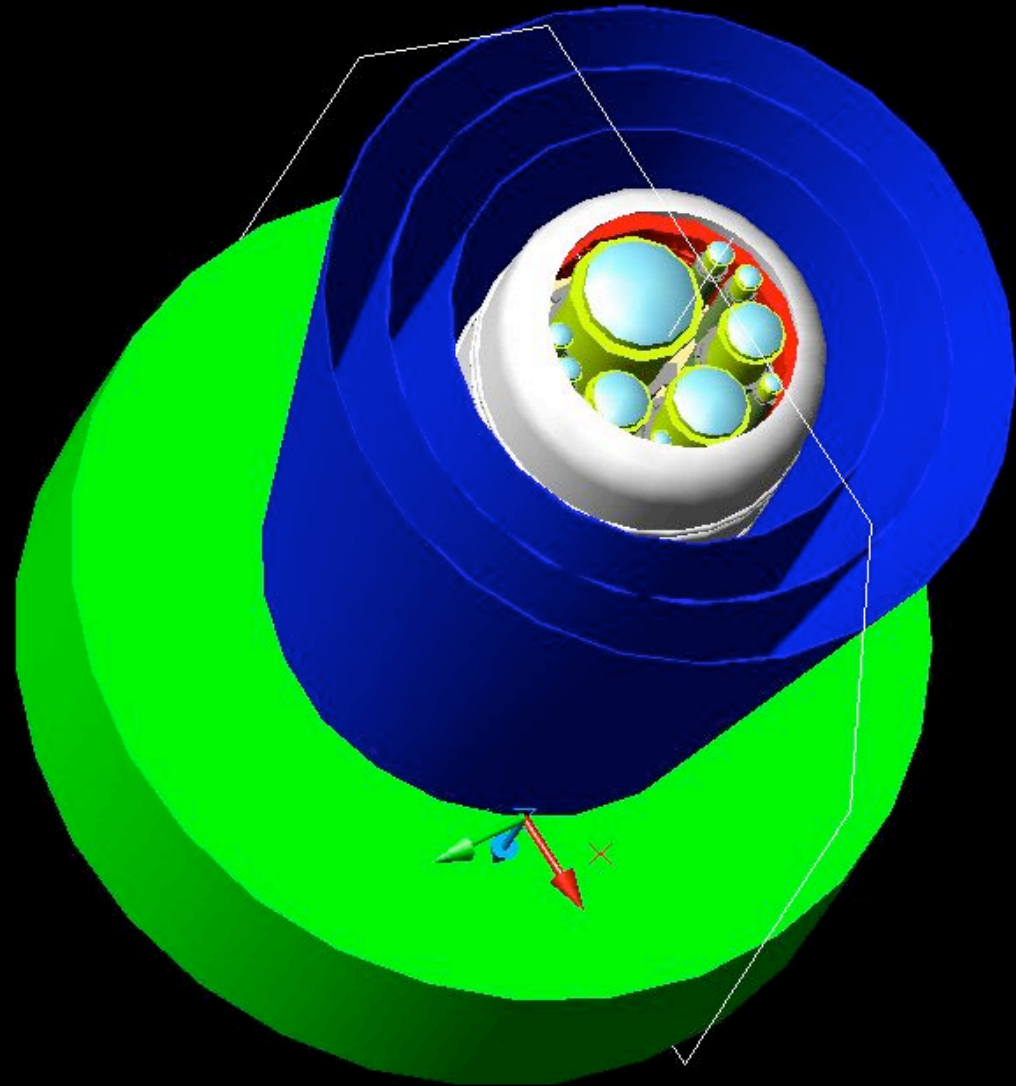


Figure 3: The predictions of general polynomial potentials of increasing order consistent with current observations as a function of degree of 'fine tuning'. This analysis indicates that the most 'natural' potential give values of T/S well within the range of B-Pol. Reprinted from L. Boyle, P.J. Steinhardt and N. Turok, Phys. Rev. Lett. 96, 111301 (2006) (astro-ph/0507455).

B-Pol : how can we get there

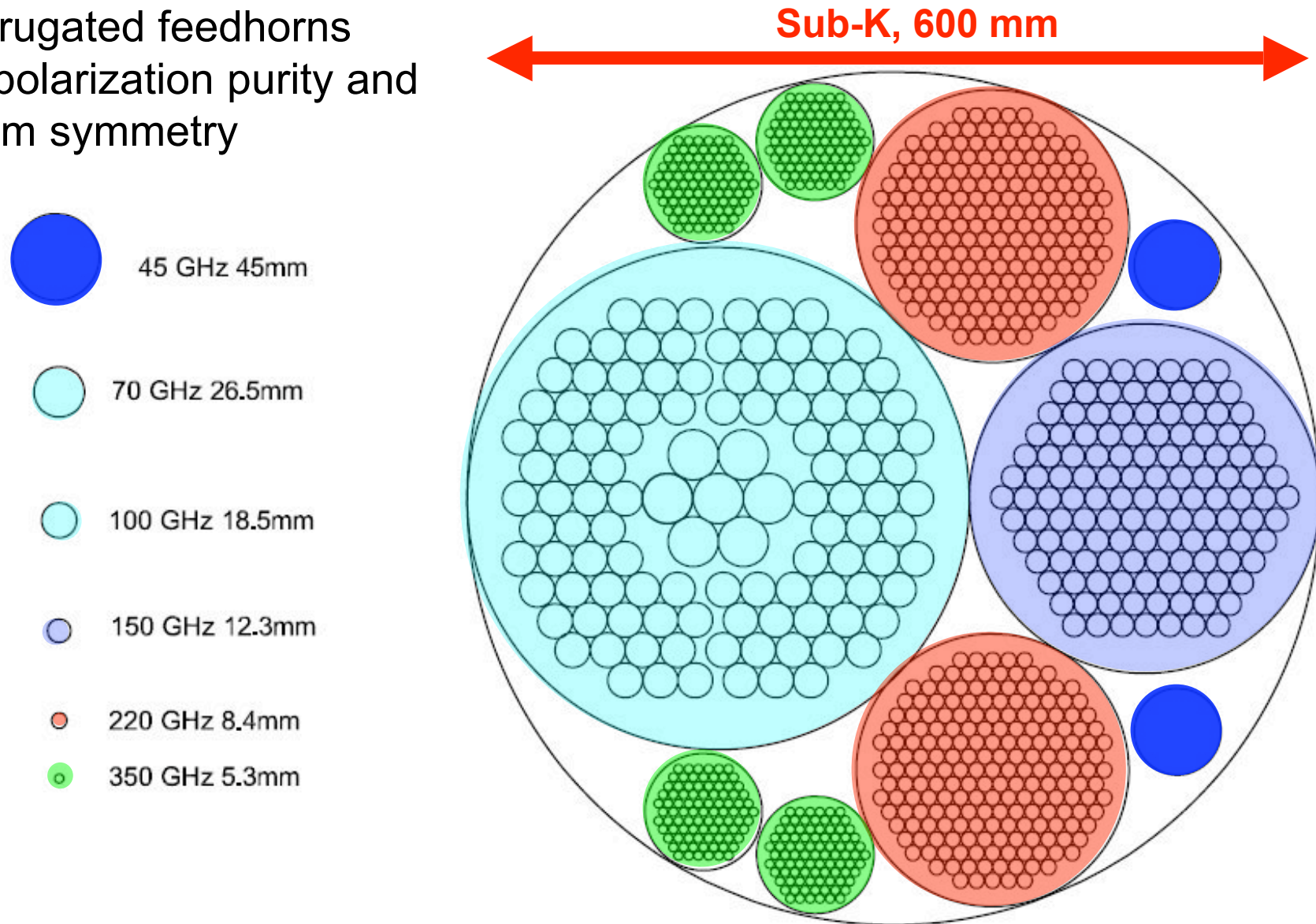
- Soyuz to L2
(sidelobes)
- 70, 100, 140, 240,
340 GHz *(separation
of foregrounds)*
- Total 2012
bolometers with
1006 feedhorns
*(sensitivity,
polarization purity)*
- Internal polarization
modulators
(systematics)
- Fast sky scan
(systematics)

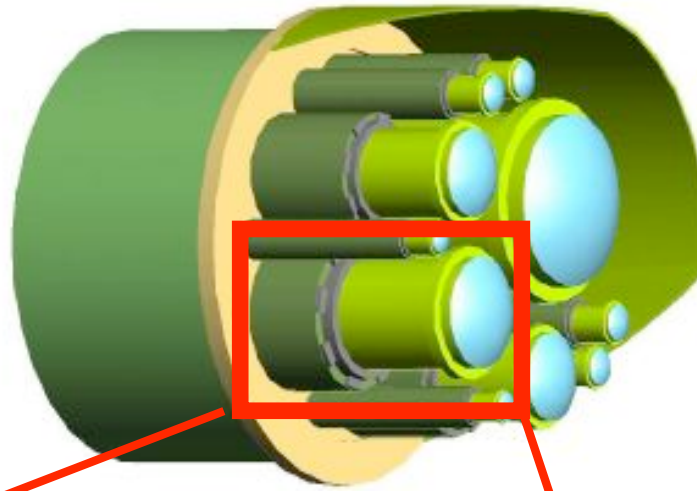


Sensitivity and frequency coverage: the focal plane

- Baseline technology: TES bolometers arrays

Corrugated feedhorns for polarization purity and beam symmetry

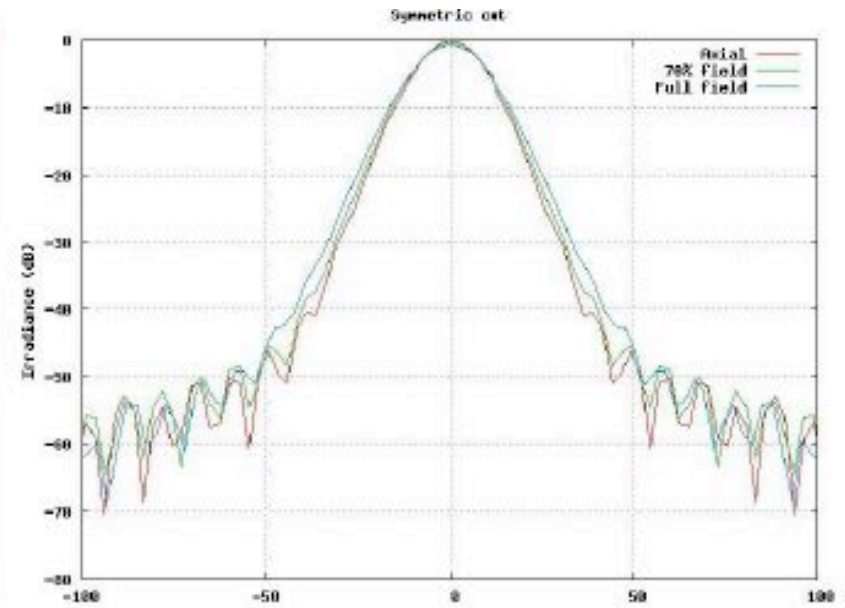
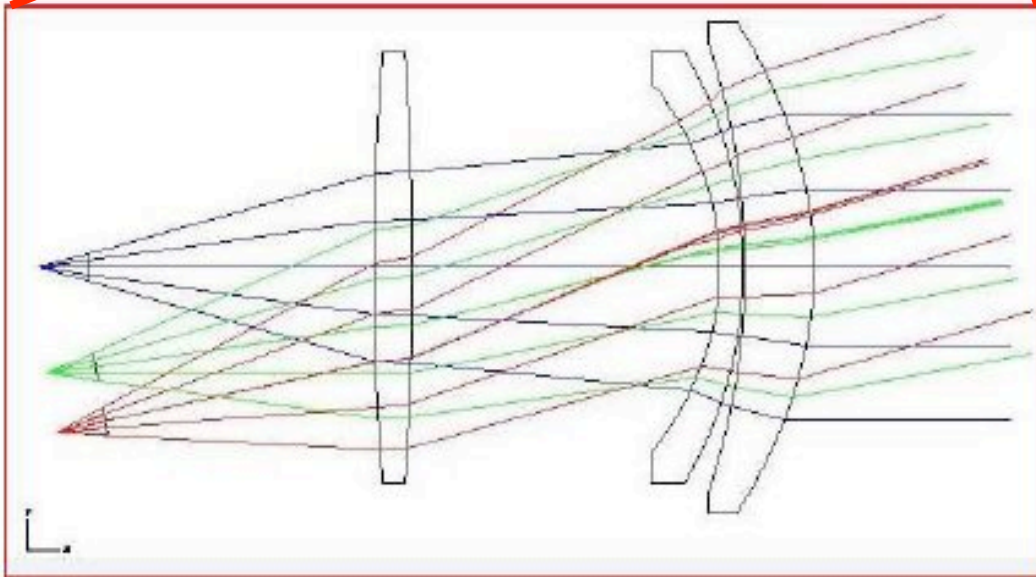




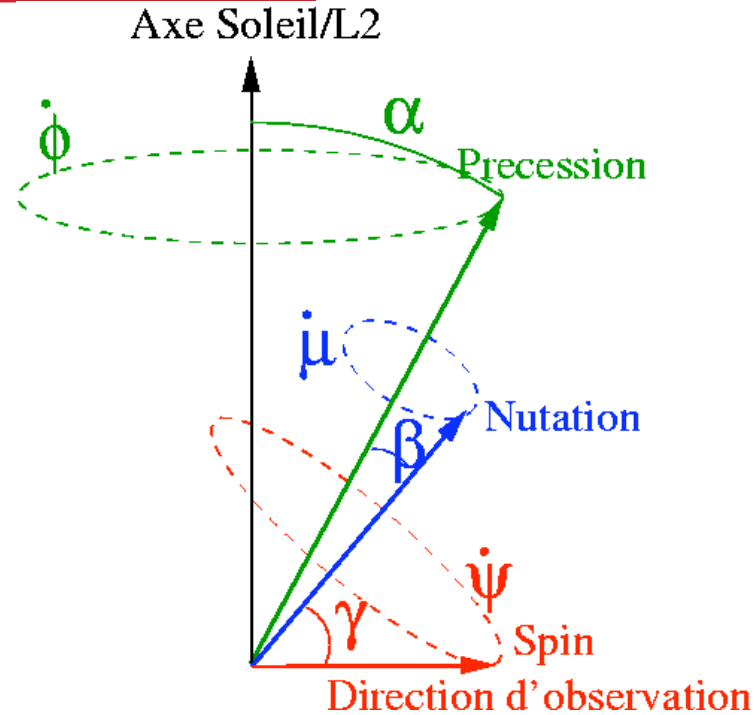
Optical system:

- Wide field,
- low cross-pol,
- low emissivity

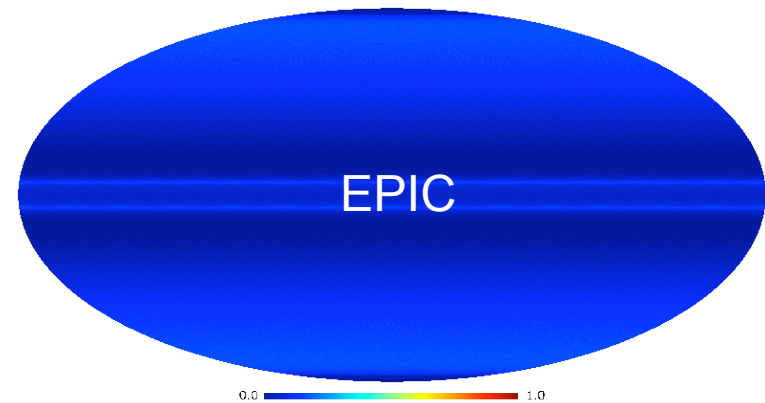
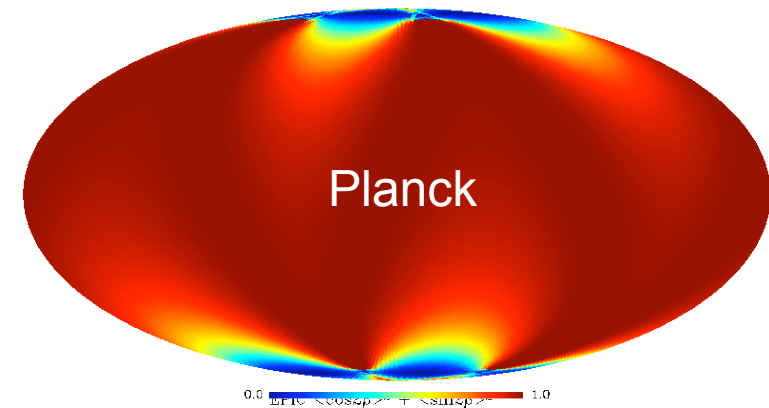
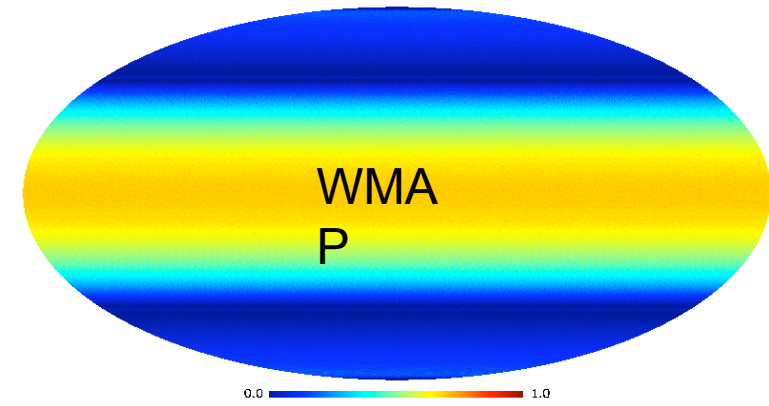
**Possible solution:
modified telecentric
telescope**



Examples:
parameterization



$$\left(\sum_i \cos 2\alpha_i \right)^2 + \left(\sum_i \sin 2\alpha_i \right)^2$$



- **Planck**
 - $\gamma = 85$ deg, $T_{\text{spin}} = 60$ sec
 - $a = 10$ deg, $T_{\text{prec}} = 6$ months
- **EPIC/JPL**
 - $\gamma = 45$ deg, $T_{\text{spin}} = 63$ sec
 - $a = 50$ deg, $T_{\text{prec}} = 3.2$ h

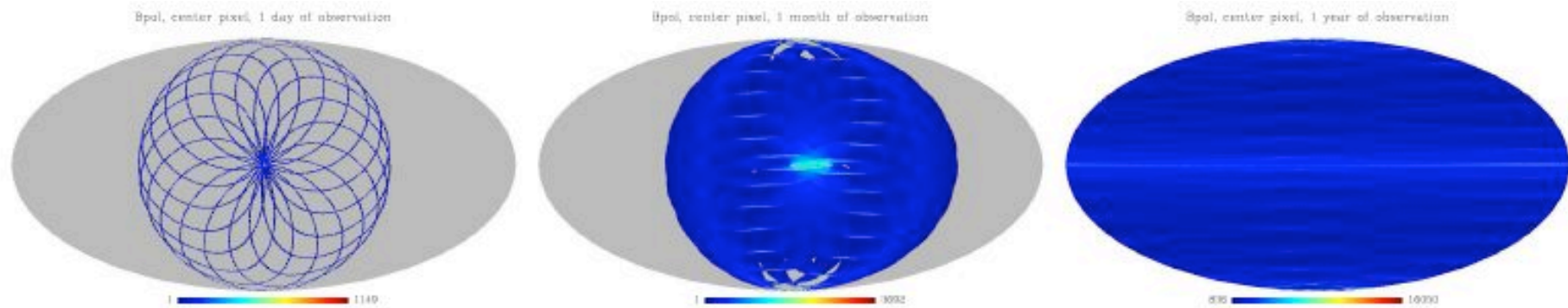


Figure 16: Hit count for a pixel at 1.6 degrees from the center of the B-pol focal plane for observation lasting 1 day (left), 1 month (center) and 1 year (right). The precession and nutation angles are 45 degrees, the precession period is 0.5 days, the nutation period is 40 min. Only one pixel at a fiducial frequency of 10Hz is represented.

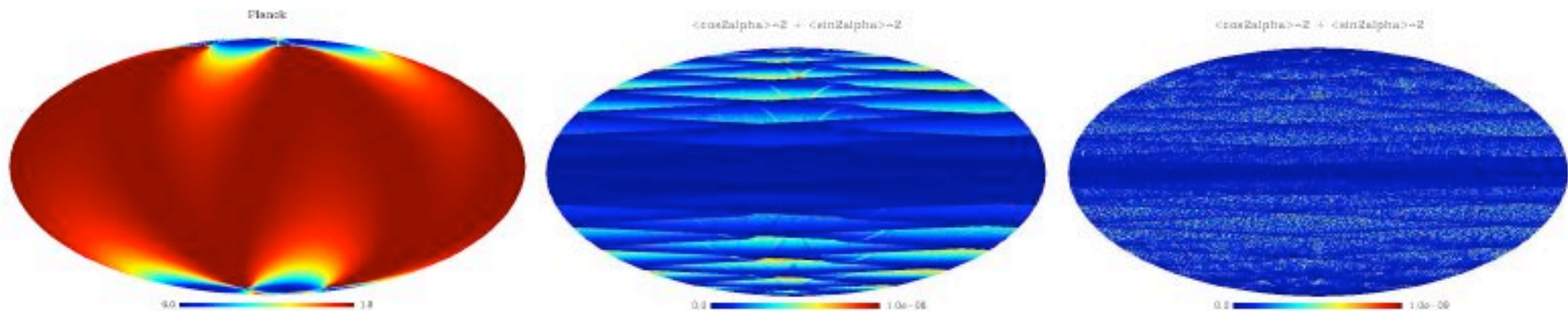
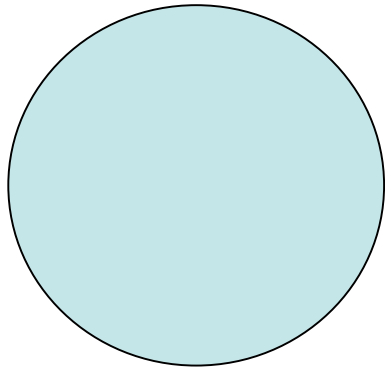


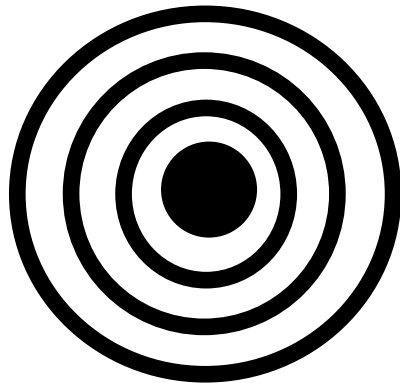
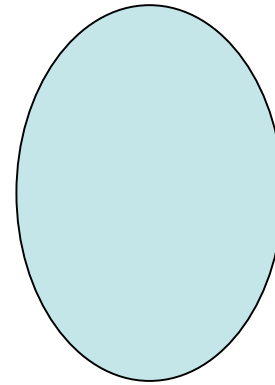
Figure 17: Maps of angular coverage relevant for polarization determination for one year of observation by a pixel at 1.6 degrees from the center of B-pol focal plane. The estimator we chose is $\langle \cos 2\alpha \rangle^{-2} + \langle \sin 2\alpha \rangle^{-2}$, where α is the angle between the main axis of the polarimeter and a reference direction on the sky. The smaller the better (0=ideal, 1=worst). Compared to Planck, (left) B-pol's angular coverage is a factor 10^6 better without an internal modulator (center), and even 10^9 with a rotating Half Wave Plate (5Hz, right)

OPTION 1: NO INTERNAL MODULATORS

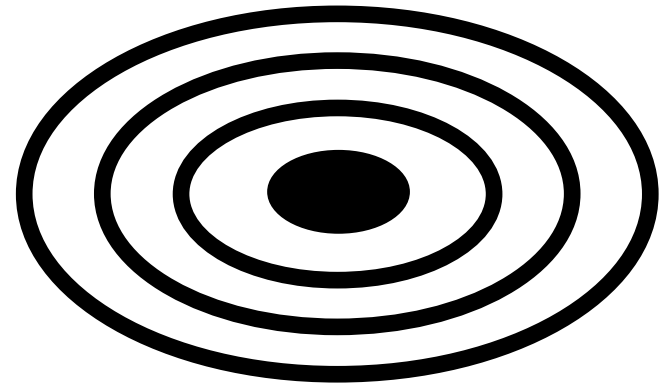
- Interesting option:
 - no cryogenic mechanics / electronics
 - payload spinning is natural
- SAPAN baseline
- However:
 - Adds complexity and cost to the mission, because requires a fast spin (avoid $1/f$) and a fast repointing of the satellite (to fight systematics and drifts).
 - In a real optical system, with a wide focal plane including thousands of detectors, is prone to systematic effects leaking T in Q and U, and Q into U and U into Q, thus contaminating and mixing E-modes and B-modes



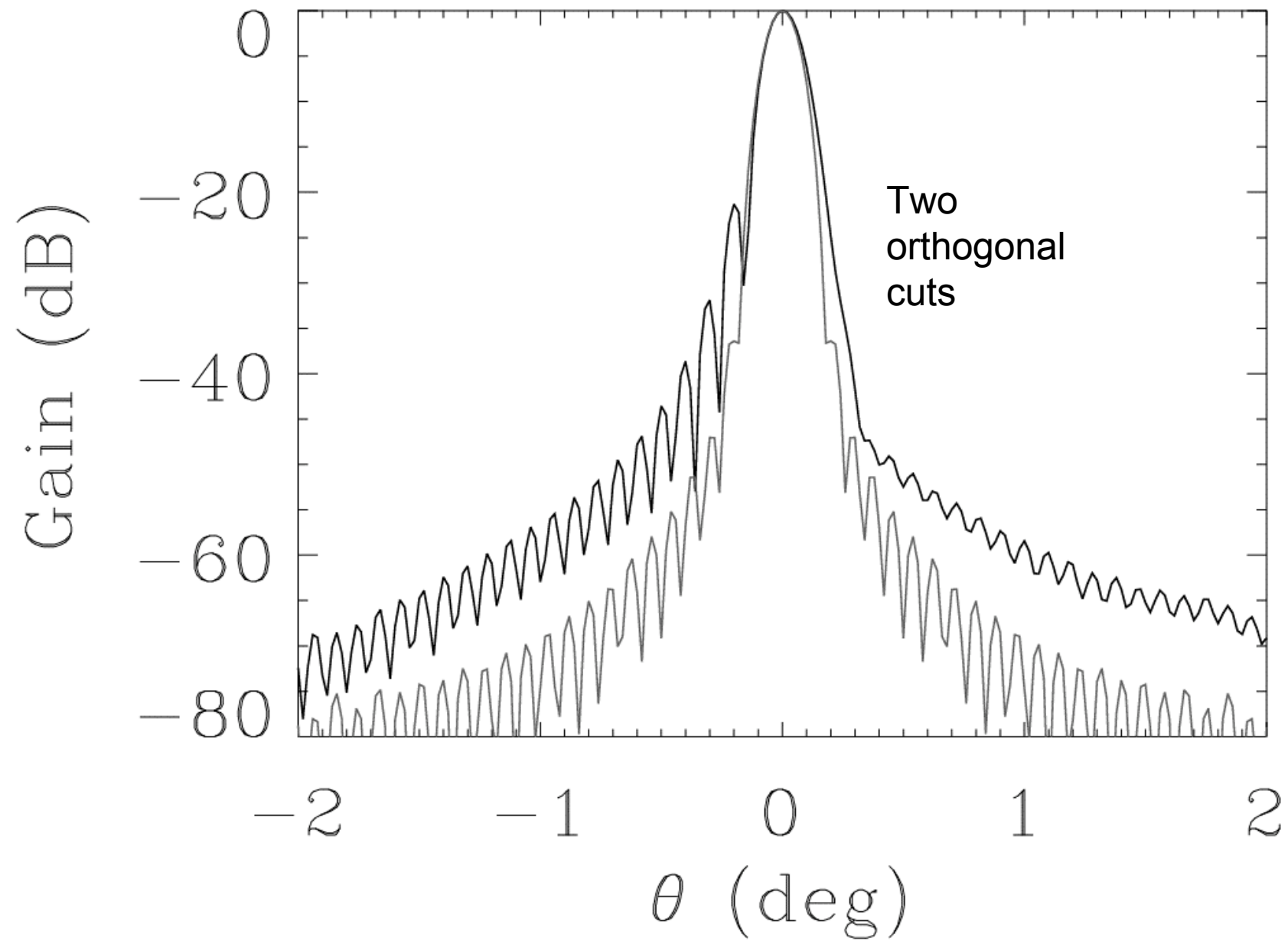
Aperture



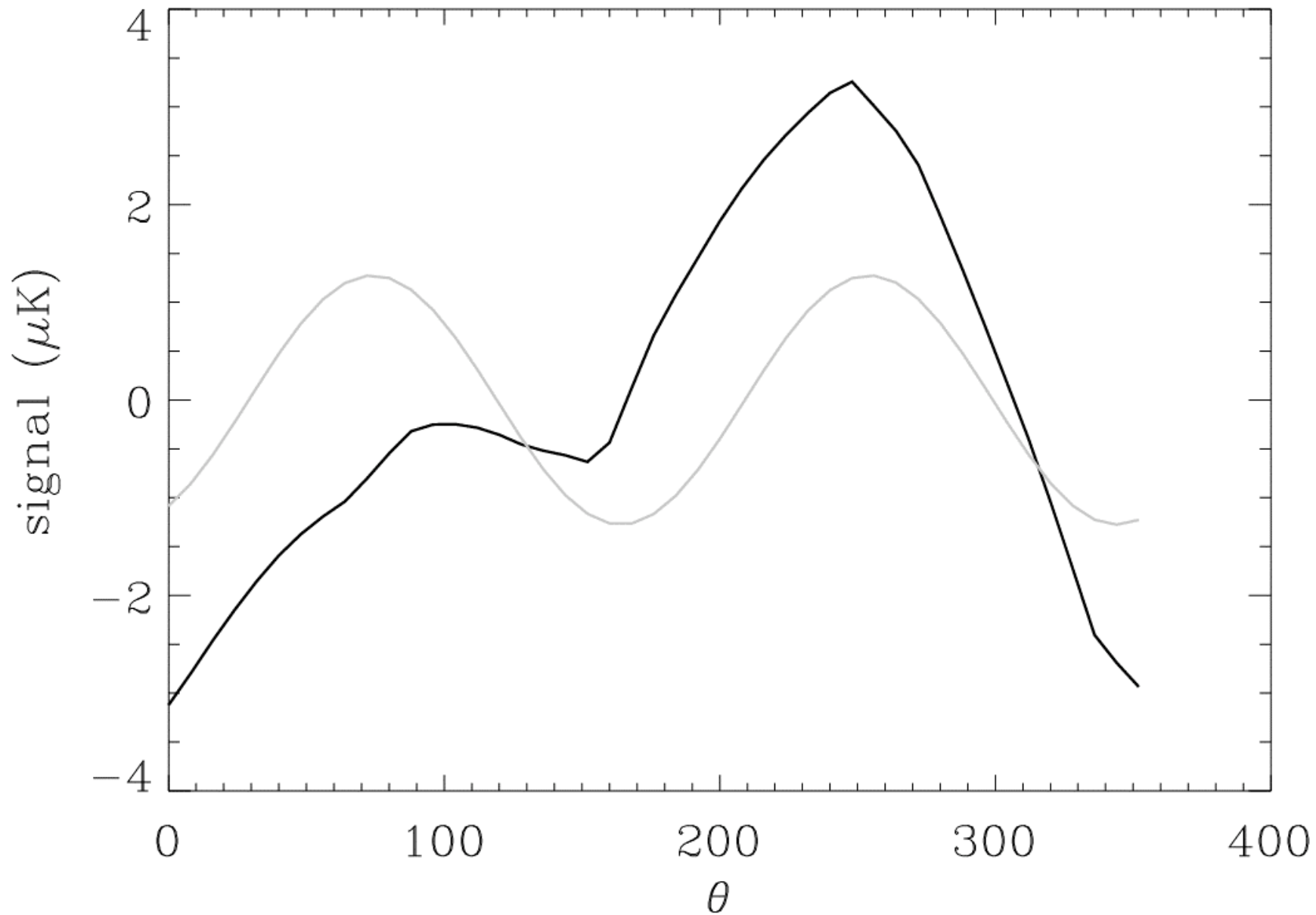
Diffraction
Pattern



CLOVER beam simulation (side pixel) from B. Maffei



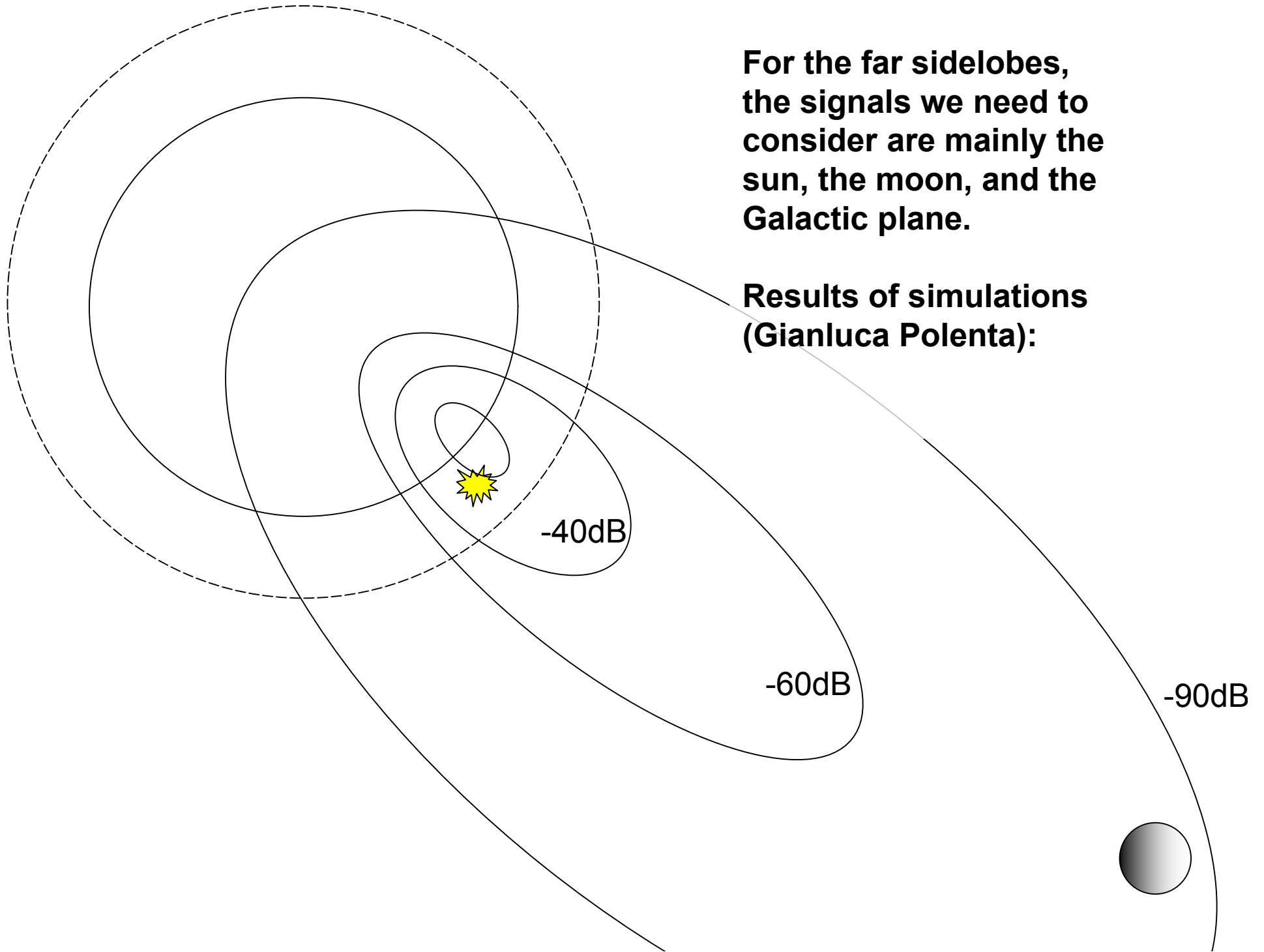
spurious polarization



Simulation by Gianluca Polenta

**For the far sidelobes,
the signals we need to
consider are mainly the
sun, the moon, and the
Galactic plane.**

**Results of simulations
(Gianluca Polenta):**



Far sidelobes must be reduced

- Obvious but not easy
- If you add 40dB of rejection at >30 deg with additional absorbing shields, the signal drops to

D(sun-spin axis) (deg)	2θ component (nK)
90	1.9
120	12
150	1
180	1.9

- Still comparable to 10 nK B-modes...

Lessons:

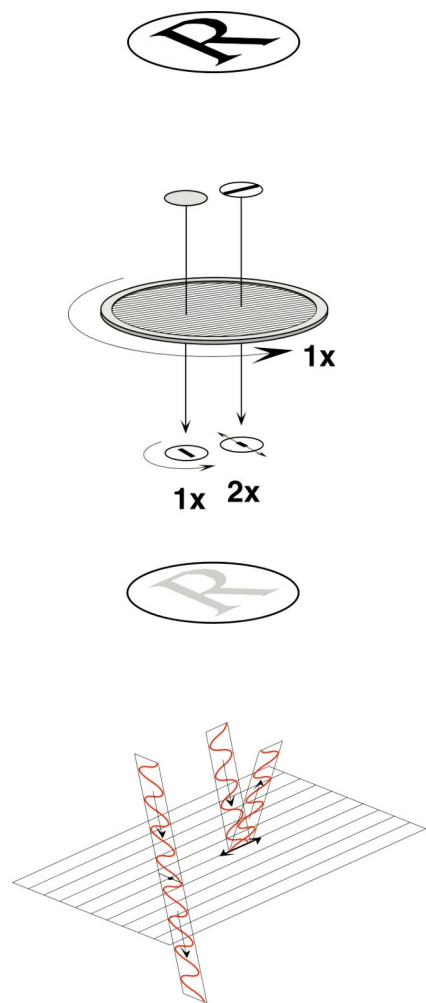
- Whatever configuration we select, we need to analyze this, and set specs for
 - Ellipticity and skewness of main beam
 - Level and symmetry of sidelobes and far sidelobes
- For this, a good help comes from absorbing shields. However, there is a tradeoff with detector loading.

OPTION 2:

INTERNAL MODULATORS

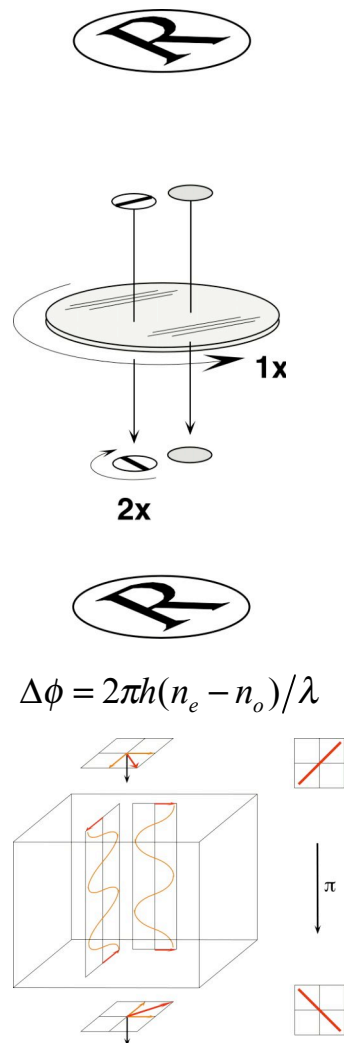
- Allow a fast, controlled modulation of polarization, reducing effects of detector $1/f$ noise
 - Add complexity inside the instrument
 - Relax problems with the satellite (lower cost to ESA, increase cost and risk for Scientists and National Agencies)
 - Introduce small spurious signals, due to their own non-idealities
- Several families:
 - Modulation of polarization in the beam, before antenna
 - Modulation after OMT
 - Correlation systems
 -

Wire-grid polariser



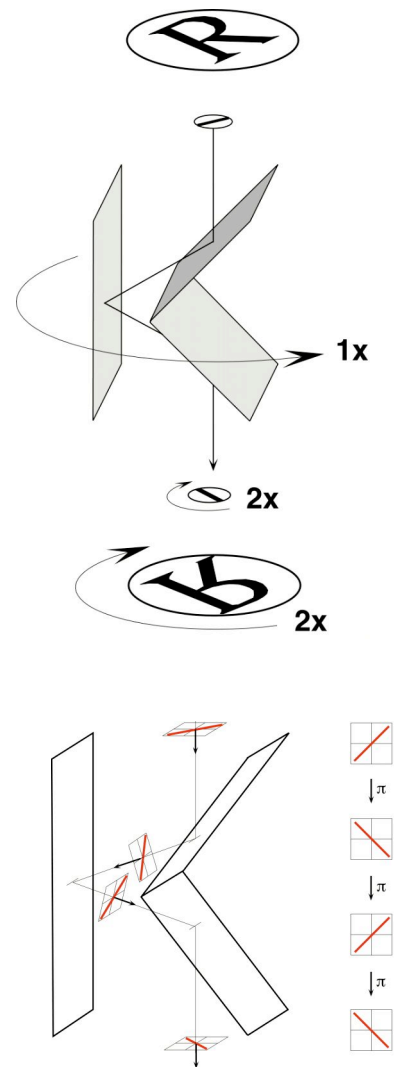
- Achromatic
- Image fixed
- Un-pol light modulated

Half-Wave Plate



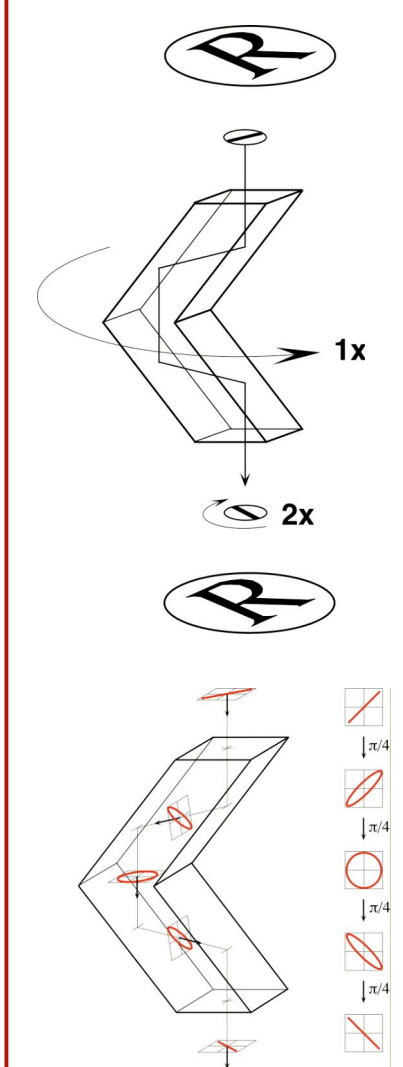
- Monochromatic
- Image fixed
- Un-pol light not modulated

K-Mirror



- Achromatic
- Image rotation
- Un-pol light not modulated

Fresnel double-rhomb

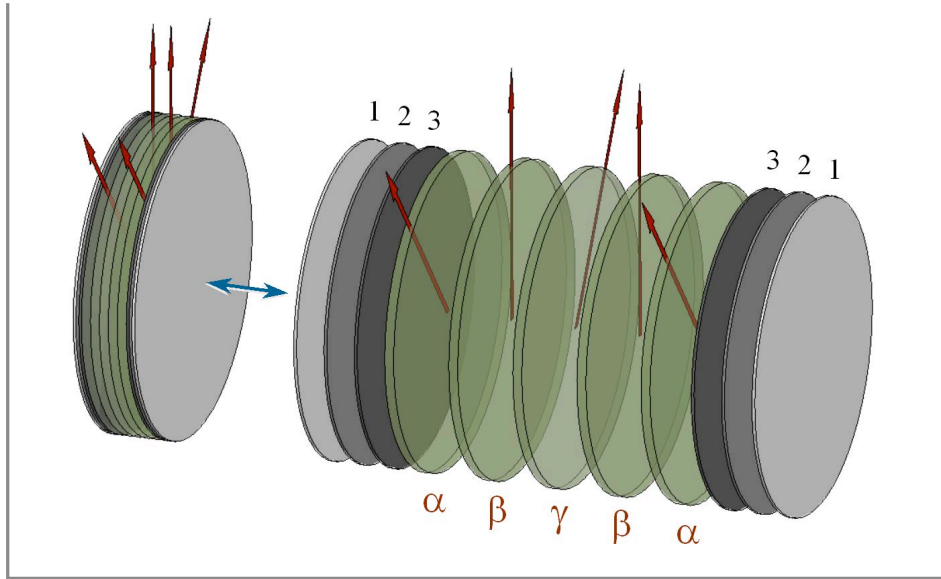


- Achromatic
- Image fixed
- Un-pol light not modulated
- High absorption

Achromatic Sapphire HWP Studies

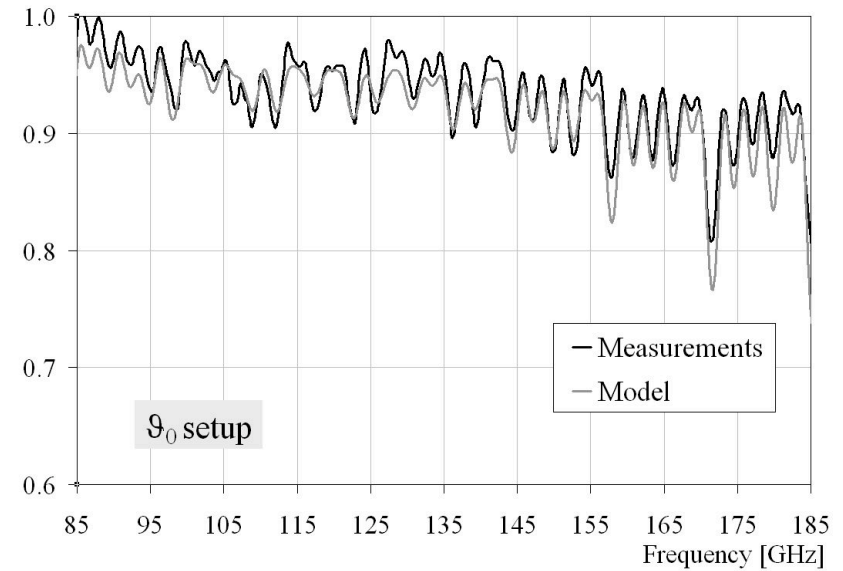
G. Pisano et al., *Applied Optics* v45, n26 (2006)
G. Savini et al., *Applied Optics* v45, n35 (2006)

Model



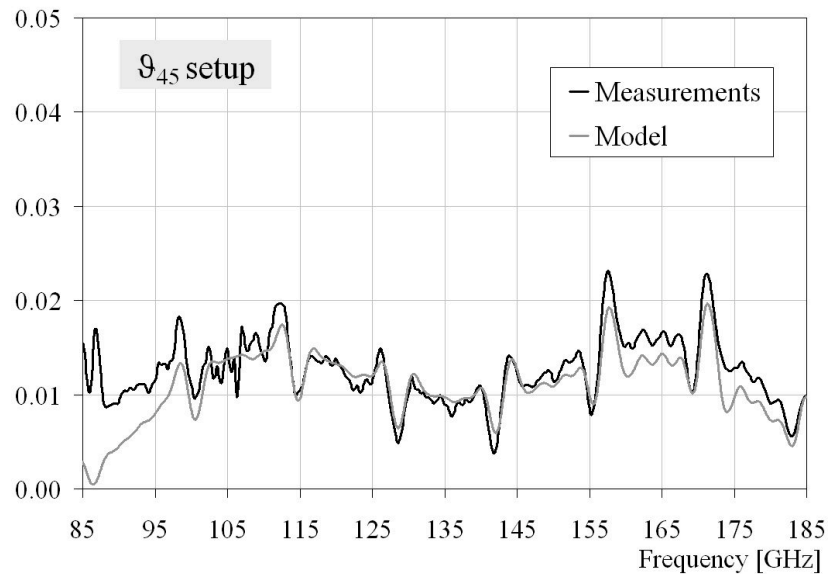
Results

Fast axis Transmission

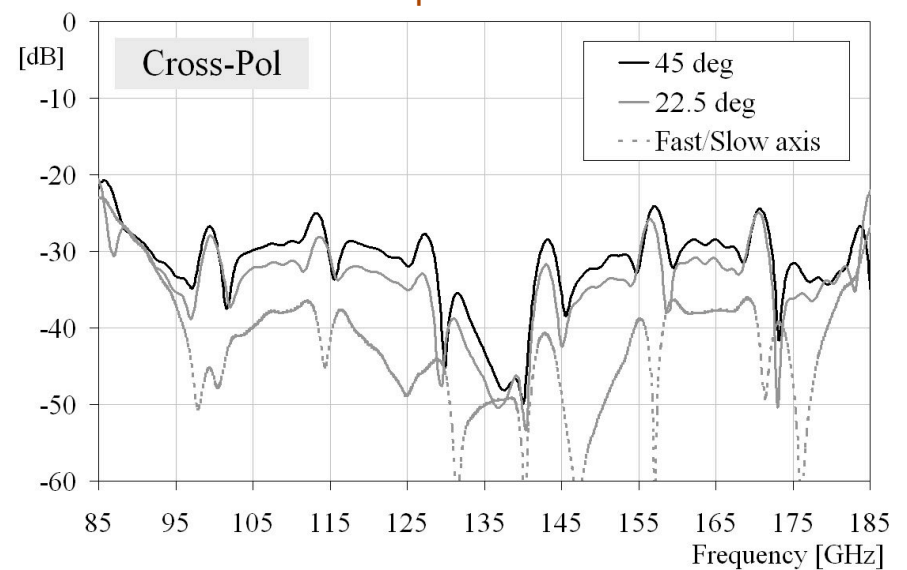


Results

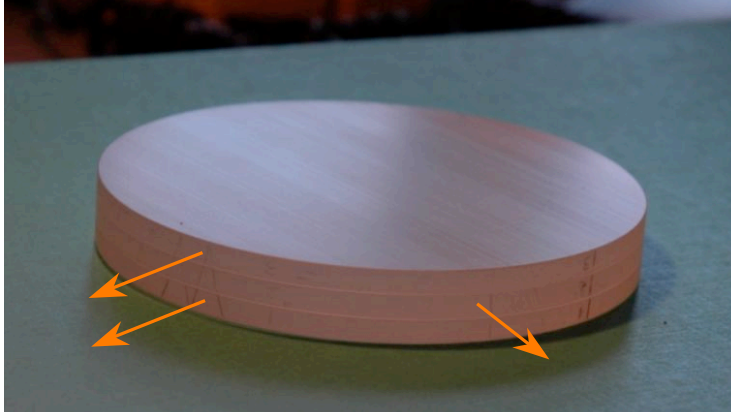
Cross-Polarisation Fit



Extrapolated Cross Polarisation



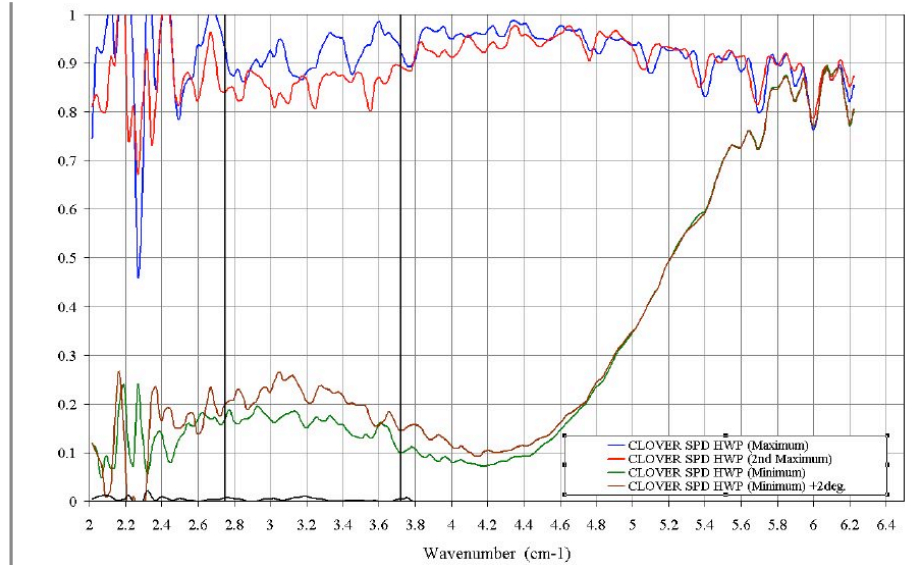
Sapphire HWP Prototype



3-plates Pancharatnam HWP (d=11cm)

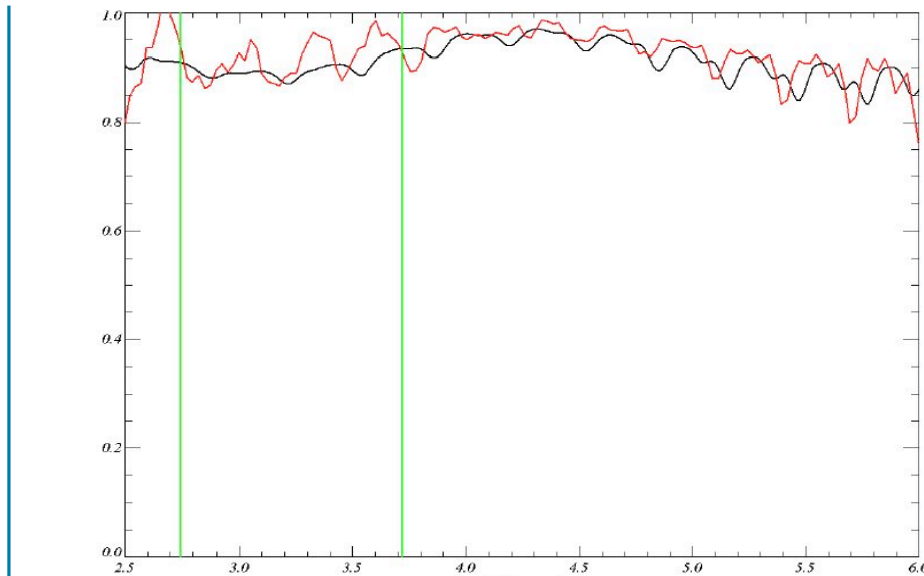
Data

Tx at different angles

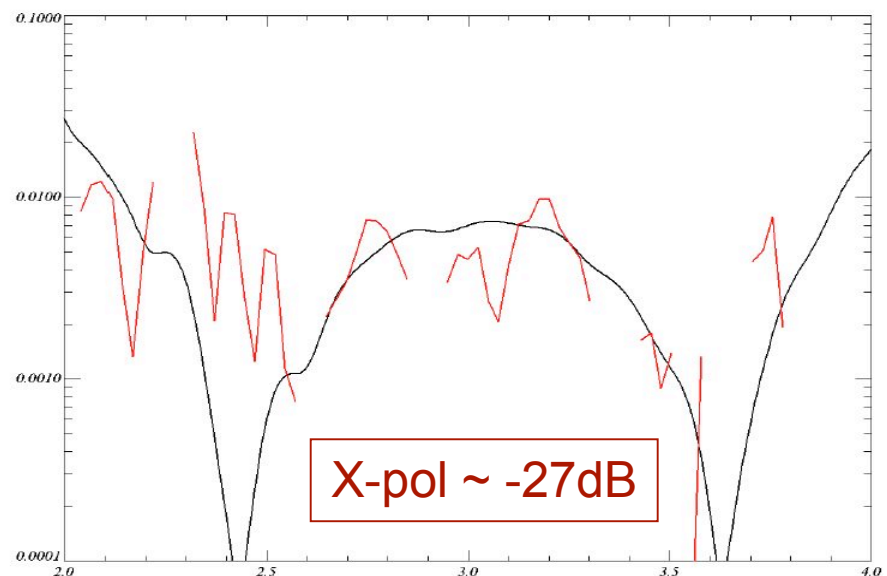


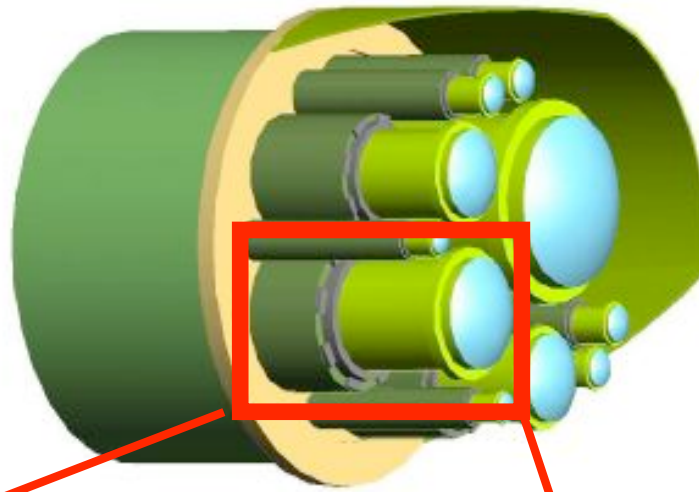
Data & Fits

Fast axis Transmission



Cross Polarisation

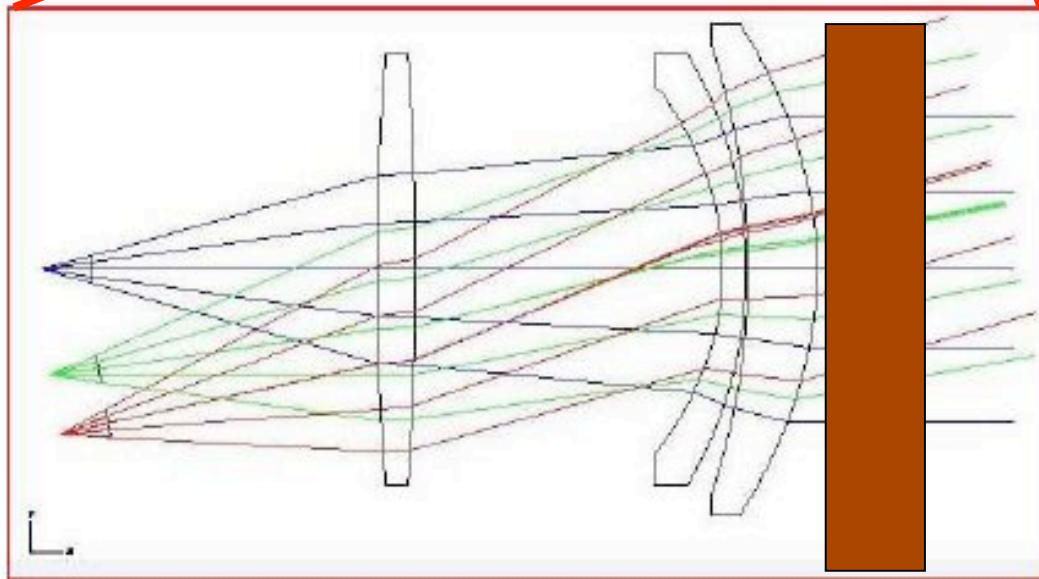




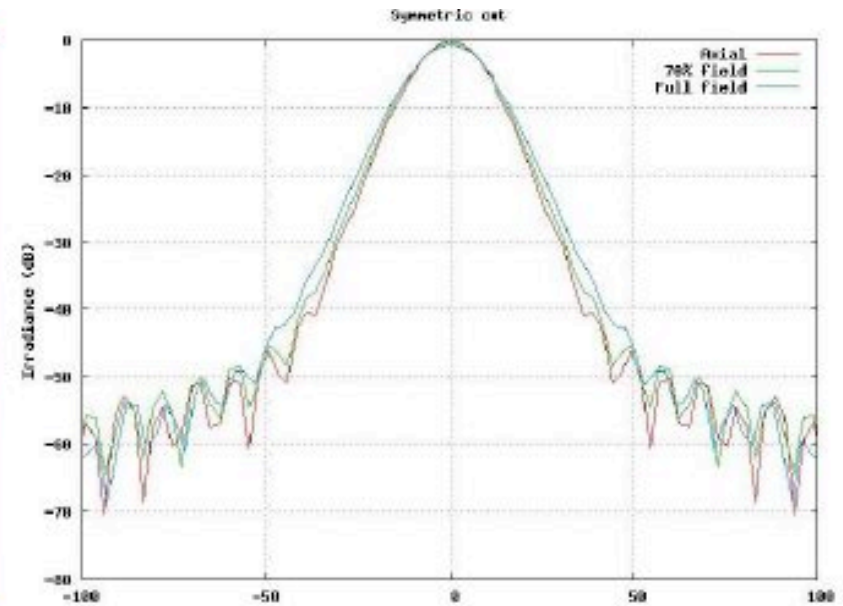
Optical system:

- Wide field,
- low cross-pol,
- low emissivity

Possible solution:
modified telecentric
telescope



HWP



Further studies

- Polarimeters on chip
 - Studies in Cardiff, Chalmers, Manchester, Oxford,

Integrated Phase Modulation

Oxford University, Ghassan Yassin, ...

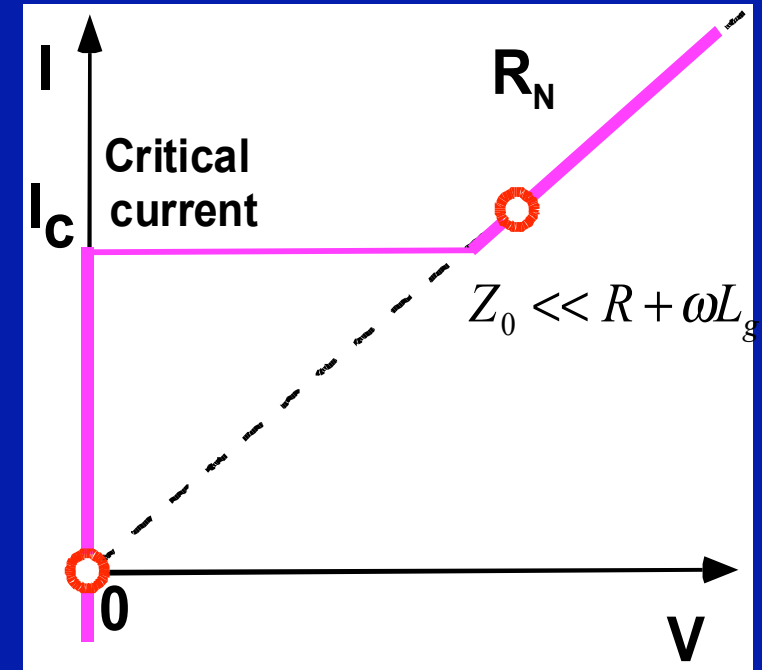
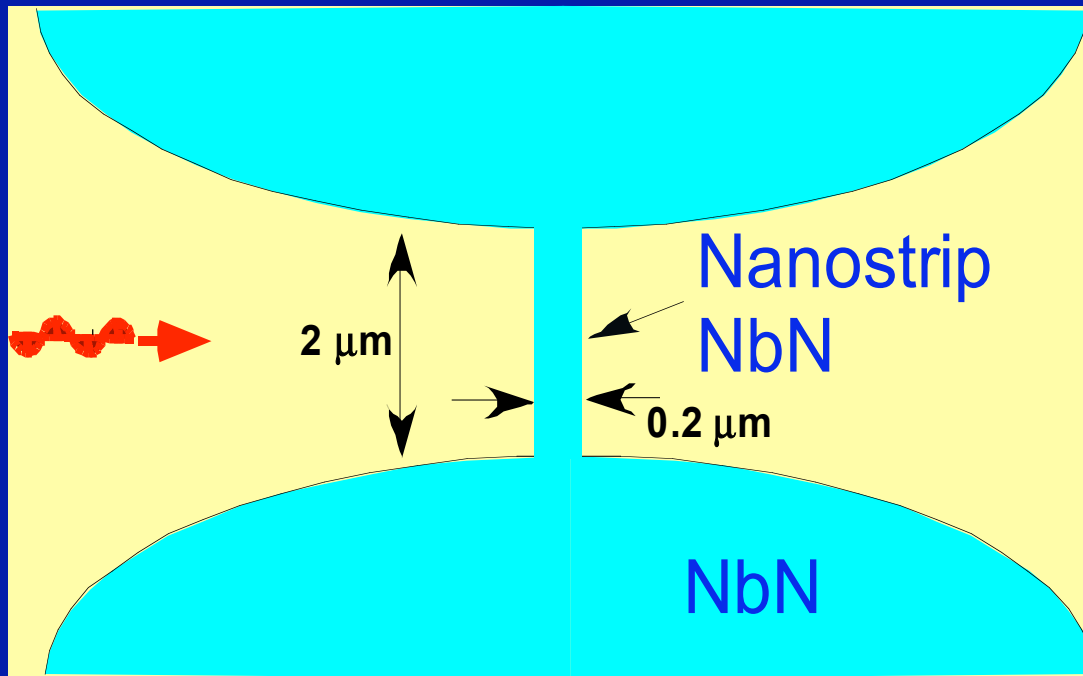
Chalmers University, Leonid Kuzmin, ...

Manchester University, Lucio Piccirillo, ...

- **Superconducting Circuits: Low loss**
- **Lithographic Fabrication: reliable, and mass reproducible**
- **Planar (microstrip): the whole Polarimeter is fabricated in planar structure and integrated in the detector circuits .**

NbN Nanostrip Switch

Kuzmin



$$\omega L_c + \omega L_g \ll Z_0 \ll R$$

$$I_c = j_c * S, \quad L_c = \frac{\hbar}{2eI_c}, \quad R = \rho \frac{l}{S}$$

90, 150, 220 GHz

- *Foregrounds ?*
 - *Tension between covering low frequencies and keeping the cost within the medium mission budget.*
 - *Final configuration to be analyzed in Phase-A*

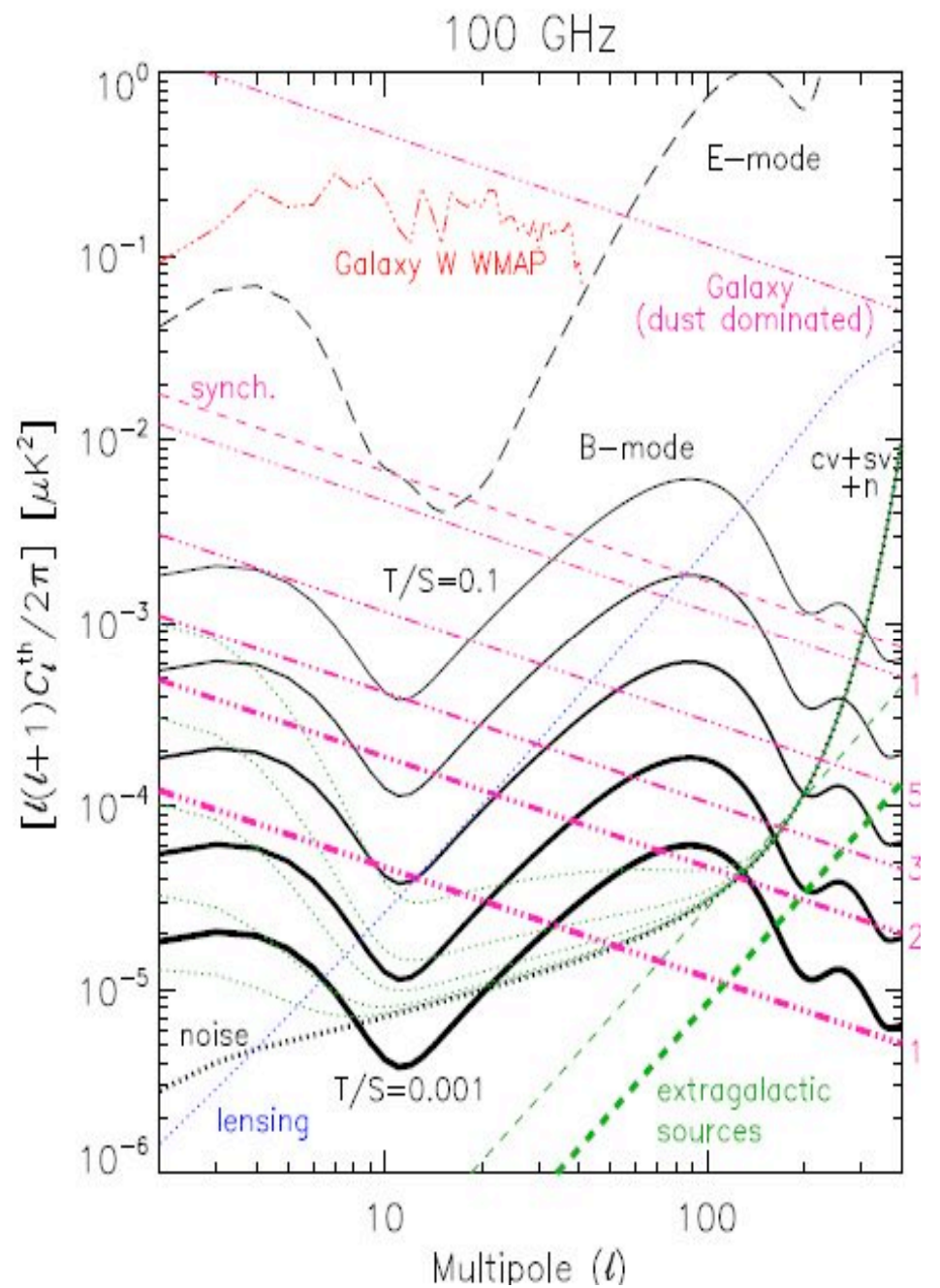
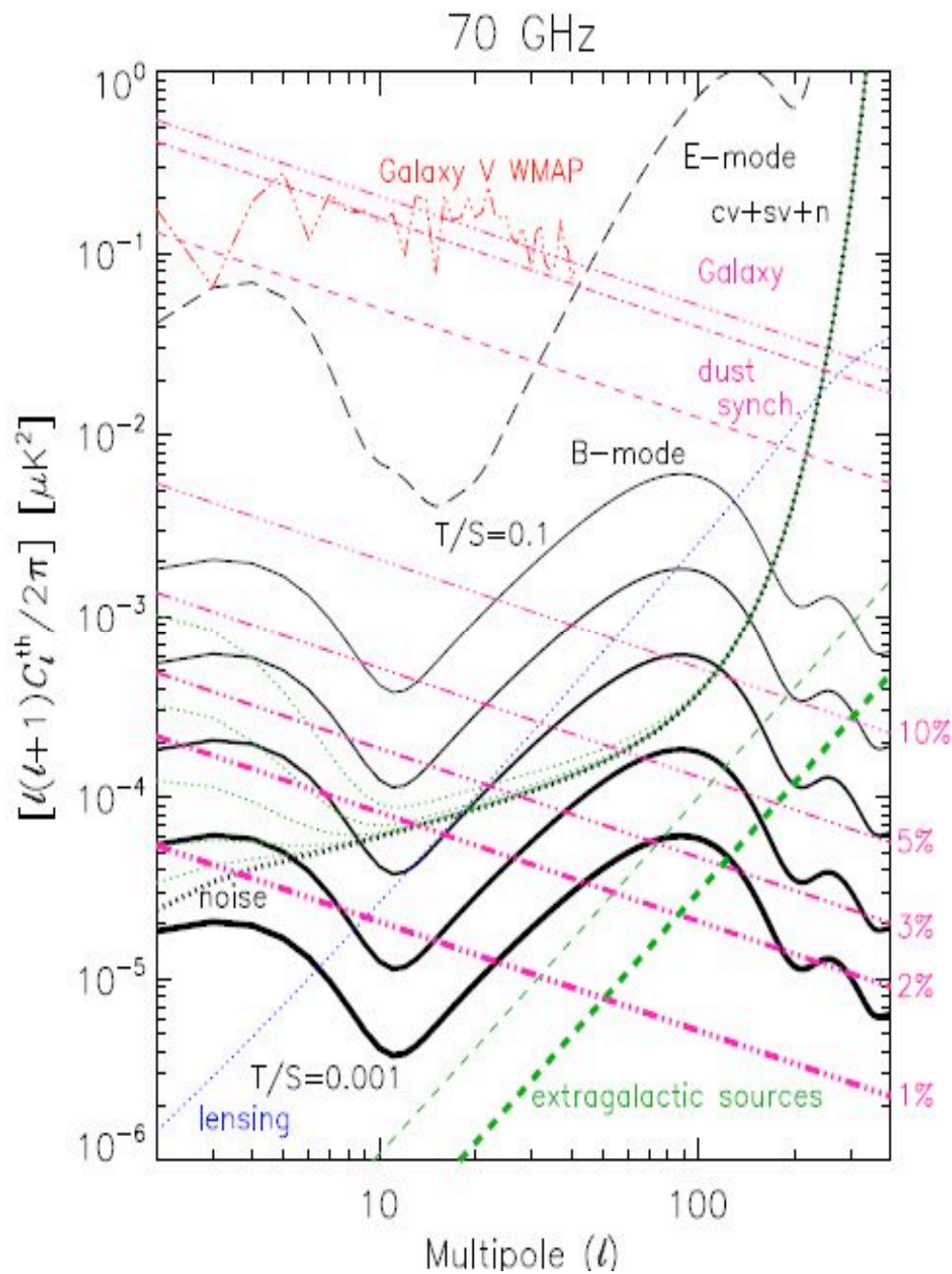


Figure from Carlo Burigana

How to remove the polarized foregrounds ?

- Template fitting methods (Page et al. 2006)
- Wiener Filtering (Bouchet and Gispert 1999)
- Maximum Entropy (Hobson et al. 1998, Stolayrov et al. 2002)
- Blind methods
 - FastICA (see e.g. Stivoli et al. 2006)
 - Spectral Matching ICA (see e.g. Delabrouille et al. 2003)
 - PoEMICA (see e.g. Aumont & Macias-Perez 2007)
 - ..
- Phase methods (see e.g. Coles et al. 2003)
-

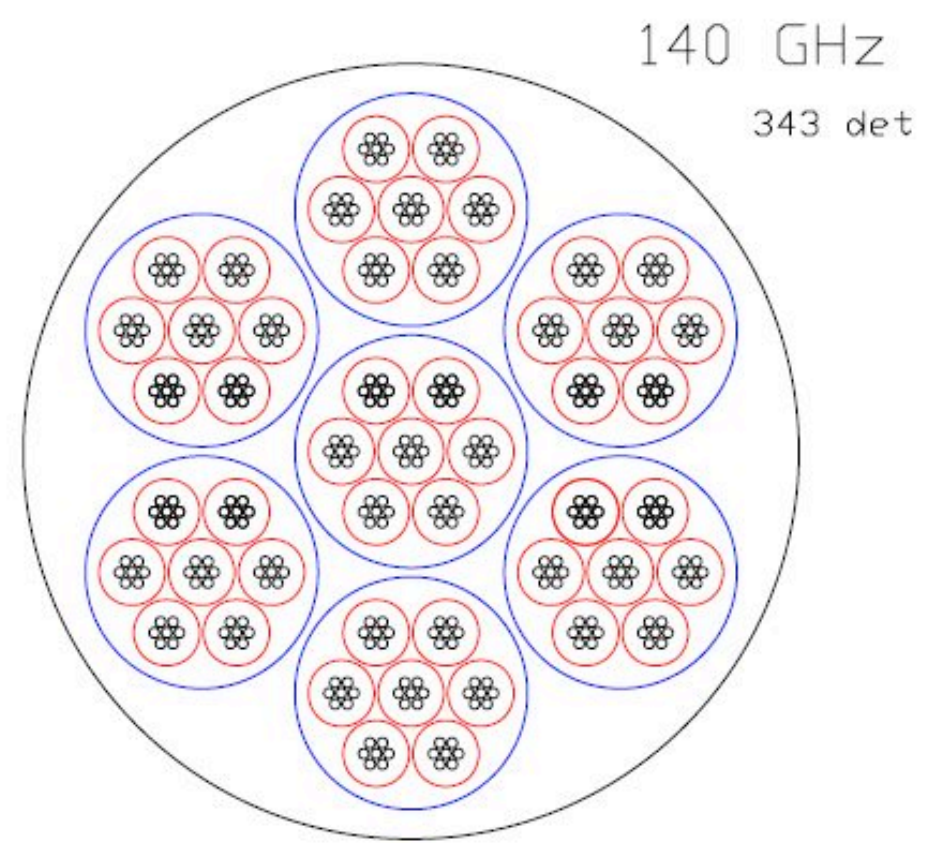
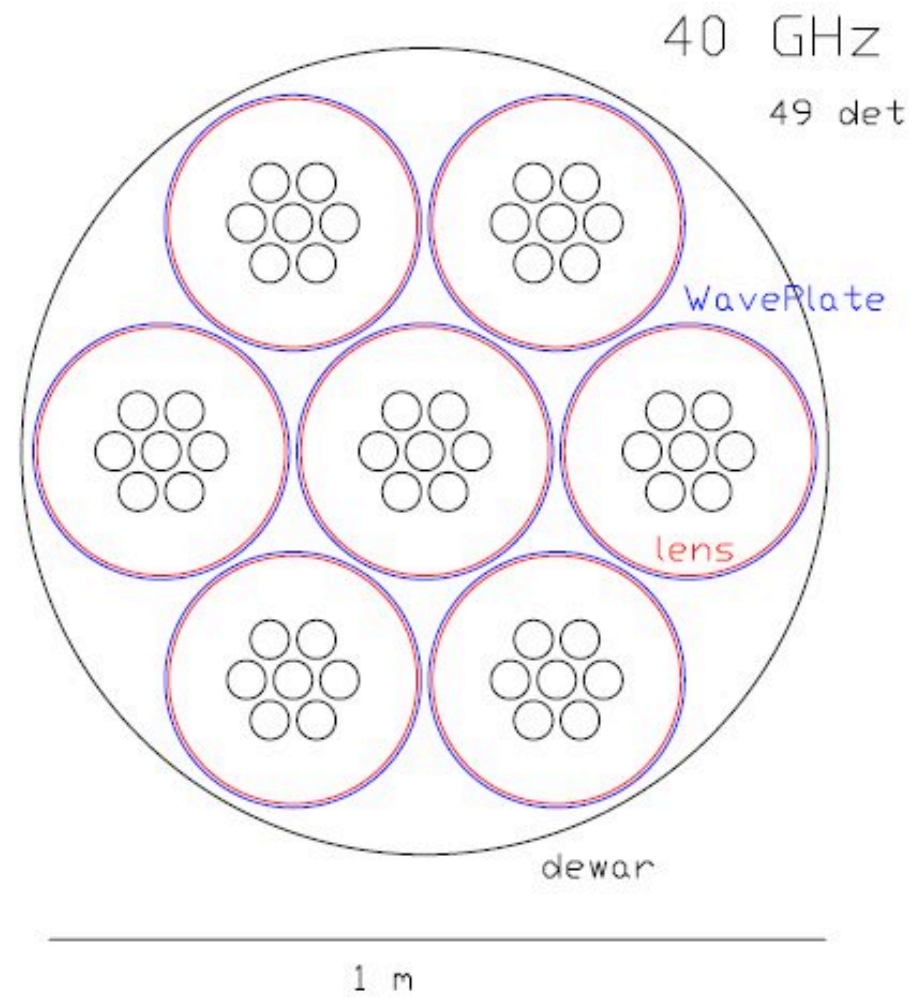
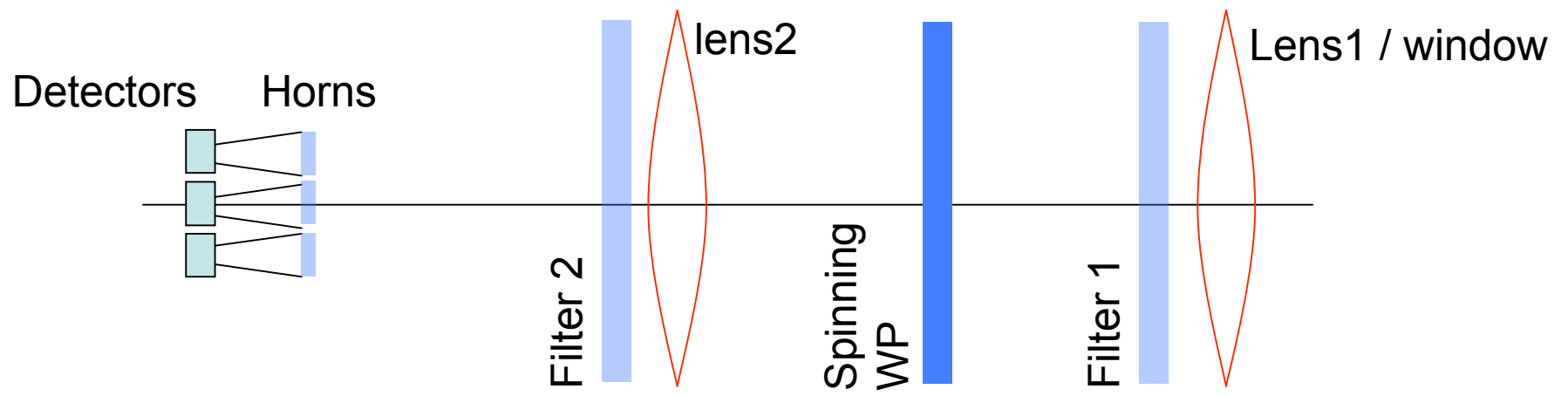
Will this really work at $<1\%$?

Tradeoff coverage/cleanliness ?

*To be studied in phase-A and with
pathfinder experiments (BB-Pol) !*

A clean polarimeter

- Use sensitive (and many) detectors
- Use corrugated feedhorns
- Avoid off-axis positions in the focal plane
- Use a polarization modulator (waveplate)
- Optimize for narrow frequency bands
- Keep it cold
- Cover a wide frequency range
- Cover a wide fraction of the sky to get the reionization peak and the first peak of B-modes
- BB-Pol: scan the sky from a balloon during the arctic night (an azimuth spinning telescope as in Archeops)
- Arctic LDBs in the polar night are possible



- *Will we be able to detect B-modes ?*
 - We do not know for sure.
 - However, it is the only opportunity we have to explore Physics around the Planck scale, where
 - Gravity unifies with the other forces
 - We can test Superstring or M theories
 - ... ? ...
 - When you explore a new continent you always discover something new.